Cationic Rhodium JosiPhos Polymers: Pathway to Highly Reusable Catalysts for
Heterogeneous Asymmetric Hydrogenation

by

Prabin Nepal

A thesis submitted in partial fulfillment of the requirements for the degree of

Master of Science

Department of Chemistry
University of Alberta

Abstract

This thesis discusses a universal strategy to synthesize JosiPhos derivatives with an alt-ROMP active norimido group. Specifically, the alt-ROMP active cationic [Rh(diphosphine)COD]BF_4 (diphosphine = (R)-1-[(S_p)-2-(Diphenylphosphino)-1'-(dimethyl-3'-N-(*cis*-5-norbornene-2,3-dicarboximidopropylsilyl)ferrocenyl]ethyl-di-cyclohexylphosphine) compound was co-polymerized with cyclooctene using the ROMP catalyst $RuCl_2$(=CHPh)$(PCy_3)_2$, and the resulting polycationic polymer adhered via electrostatic attractions to a polyanionic Al_2O_3/Phosphotungstic acid (PTA) support. This heterogenous catalyst was active towards the hydrogenations of methyl-(Z)-α-acetamidocinnamate (MAC) and dimethyl itaconate (DMI). The enantioselective hydrogenation of DMI over this catalyst occurred with excellent activity (100% conversion, 5000 TON) and selectivity (up to 95% *ee*) without significant Rh leaching over 10 reuses.

Preface

The first half of Chapter 1 introduces the history, development, and advancement of asymmetric hydrogenation. The second half explores the relevant immobilization methods of asymmetric hydrogenation catalysts.

Chapter 2 is a part of a manuscript to be written as an article. I was responsible for the synthesis, the characterization of the heterogeneous catalyst and writing the chapter. I carried out all evaluations of catalytic performance, except those identified as being carried out by industrial partners. Together, Suneth Kalapugama and I developed a universal synthetic pathway for alt-ROMP polymers of JosiPhos derivatives. Shuai Xu is currently leading this project. The research was carried out under the supervision of Dr. Bergens.

Chapter 3 summarizes the findings of this research and future directions for the project.

Acknowledgement

Table of Contents

List of Tables

List of Figures

List of Schemes

List of Equations

List of Abbreviations

AAS	Atomic Absorption Spectroscopy
API	Active Pharmaceutical Ingredients
atm	Atmosphere(s)
atl-ROMP	Alternating Ring-Opening Metathesis Polymerization
bar	Bar (Metric unit of pressure)
BINAP	2,2'-bis(diphenylphosphino)-1,1'-binapthyl
BINOL	1,1'-bi-2-naphthol
Br	Broad
CAD ($)	Canadian dollar
CAMP	*o*-anisyl(cyclohexyl)methylphosphine
Cat.	Catalyst
COD	1,5-Cyclooctadiene
COE	Cyclooctene
COSY	Correlation Spectroscopy
Cp	Cyclopentadienyl
Cy	Cyclohexyl
d	Doublet
DABCO	1,4-Diazabicyclo[2.2.2]octane
dd	Doublet of Doublet

DIOP	2,3-*o*-isopropylidene-2,3-dihydroxy-1,4-bis(diphenylphosphino)butane
DIPAMP	1,2-Bis[(2-methoxyphenyl)(phenylphosphino)]ethane
DMI	Dimethyl Itaconate
dpen	1,2-Diphenylethylenediamine
EA	Elemental Analysis
Ee	Enantiomeric excess
Et	Ethyl
Et$_3$N	Triethylamine
ESI MS	Electrospray Ionization Mass Spectrometry
FDA	Food and Drug Administration
g	Gram(s)
GC	Gas Chromatography
GC-MS	Gas Chromatography Mass Spectrometry
GCC	Green Centre Canada
h	Hour(s)
HPLC	High Pressure Liquid Chromatography
Hz	Hertz
ICP-MS	Inductively Coupled Plasma Mass Spectrometry
ICP-AAS	Inductively coupled plasma Atomic Absorption Spectroscopy
JosiPhos	2-(Diphenylphosphino)ferrocenyl] ethyldicyclohexylphosphine

kg	Kilogram(s)
L	Ligand(s)
L-DOPA	*L*-3,4-dihydroxyphenylalanine
m	multiplet
MAA	methyl acetamidoacrylate
MHz	Megahertz
mol	mole(s)
MOM	methoxymethyl
MS	Mass Spectrometry
MAC	methyl(*Z*)-*α*-acetamidocinnamate
Me	methyl
Me-DuPhos	(*R,R*)-1,2-bis(2,5-dimethylphospholano)benzene
Mequiv	mega equivalent
Min	minute(s)
mm	millimeter(s)
mmol	millimol(s)
mL	milliliter
m/z	Mass to charge ratio
NBD	Norbonadiene
NMR	Nuclear Magnetic Resonance
N-BINAP	(*R*)-5,5'-Dinorimido-2,2'-bis(diphenylphosphino)-1,1'-binapthyl

OMIM	1-Methyl-3-octylimidazolium
PEG	Polyethylene Glycol
Pd/C	Palladium on Carbon
PCy$_3$	Tricyclohexylphosphine
Ph	Phenyl
PS	Polystyrene
psi	Pounds per Square Inch
psig	Pounds per Square Inch Gauge Pressure
ppm	Parts per Million
Py	Pyridine
q	Quartet
ROMP	Ring-Opening Metathesis Polymerization
rt	Room Temperature
PNNP	N,N'Bis(R(+)α-methylbenzyl)-N,N'bis(diphenylphosphino)ethylenediamine)
PTA	Phosphotungstic Acid
q	Quartet
s	Singlet
SEM	Scanning Electron Microscope
sol	Solvent
Sub	Substrate

t	Triplet
TEA	Triethylamine
TMEDA	Tetramethylethylenediamine
^{t}Bu	*tert*-butyl
THF	Tetrahydrofuran
TON	Turnover Number
TOF	Turnover Frequency
USA	United States of America
USD ($)	United States dollar
XRD	X-Ray Diffraction
XyliPhos	(*R*)-1-[(*S$_p$*)-2-(Diphenylphosphino)ferrocenyl]ethyldi(3,5-xylyl)phosphine)

Chapter 1 Introduction

1.1 Chirality

Chirality is ubiquitous to life. All naturally occurring amino acids have the *L* absolute configuration and all the naturally occurring sugars (carbohydrates) have *D* absolute configuration.[1] Therefore, it is unsurprising that most physiological phenomena result from chiral interactions between biomolecules. For example, enantiomers of the same molecule often smell and taste differently and have different toxicity, metabolism, pharmacokinetics, etc.[1,2]

(S)-Thalidomide (R)-Thalidomide

Mirror
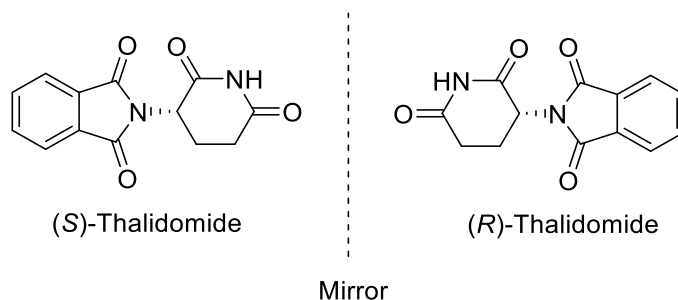
Figure 1.1 *Enantiomers of Thalidomide.*

In 1848, Louis Pasteur helped pioneer the understanding of chirality at the molecular level when he physically separated the chiral crystals of racemic tartaric acid.[3] However, it was not until the tragic deformations of newborns caused by the drug thalidomide in the 1960s that the significance of stereoisomers in biochemistry was appreciated widely.[4] *R*-Thalidomide is a sedative, while the *S*-enantiomer is teratogenic and induces fetal

malformations (Figure 1.1).[4,5] Tragically, racemic thalidomide was prescribed in the 1950s and early 1960s to pregnant women to alleviate morning sickness and led to many deformities and birth defects in newborns.[4] Even the enantiopure form of thalidomide, if consumed, undergoes racemization under physiological conditions.[2] This tragedy was followed by a number of scientific meetings in the late 1980s and early 1990s with academics and industrial regulatory scientists to discuss the significance of chirality in pharmacology and therapeutics.[6]

In 1992, the Food and Drug Administration in the US introduced rigorous guidelines regarding the development and sales of new pharmaceuticals. New drug approval would be based on complete analysis, including pharmacodynamics and pharmacokinetics of all individual stereoisomers, as well as their racemic mixtures.[7] This document directly encouraged the use of clinical drugs consisting of only a single stereoisomer.[7,8] By 2001, worldwide sales of pharmaceutical products consisting of a single enantiomer reached $147 billion.[9] In the agrochemical industry, about 30% of registered pesticide active ingredients contain one or more chiral centres.[10] Because stereoisomers of pesticides and herbicides have different toxicities and degradation lifetimes, using a single stereoisomer increases the potency while significantly reducing environmental damage.[10,11] In addition, since the odour quality, intensity, and taste of many stereoisomers are different, stereoisomer compositions must be taken into consideration in food, flavour additives, and perfumes.[12] Thus, economic, environmental, and pharmacodynamic considerations all drive the development of technologies to selectively synthesize single stereoisomers in the life-science industries.[13]

1.2 Asymmetric Synthesis

Asymmetric synthesis is defined by IUPAC as *a chemical reaction (or reaction sequence) in which one or more new elements of chirality are formed in a substrate molecule and, which produces the stereoisomeric (enantiomeric or diastereoisomeric) products in unequal amounts.*[14] Methods to perform asymmetric synthesis include resolution, chirality transfer, transformations of pre-existing chiral compounds, and chirality multiplication via asymmetric catalysis. The majority of enantiopure compounds are synthesized from the chiral pool or by resolution of racemic mixtures.[2, 15, 16] During 1985–2004, 58 out of the 167 new single enantiomer drugs contained only one stereogenic centre. Of these, 26 were synthesized using optically pure amino acids and glycidol derivatives, while 27 were prepared by resolution of racemates.[16] Kinetic resolution relies upon different rates of reaction between a chiral agent (reagent, catalyst, solvent, etc.) and the enantiomers of a starting material, leading to the formation of intermediates in unequal amounts. The major drawback of resolutions is that the maximum yield is 50%, unless the unwanted enantiomer is racemized and recycled. This often requires extra steps, which increases the amount of waste for the overall process. The availability of specific optically pure natural compounds on a large scale is often limited.[17,18] At present, the pharmaceutical industry produces a high ratio of waste per unit of desired products. There are various metrics to quantify the efficiency of chemical production, including atom economy, Process Mass Intensity (PMI), E factor, and others.[19,20] The E-factor is the ratio of the mass of waste generated per mass of product.[19] The ideal value for a chemical process is 0, i.e., no waste is produced. Table 1.1 lists typical E factors for various sectors of chemical industry.

Table 1.1 *E-Factors for various chemical industries*[19]

Industry	Annual production (ton)	Waste produced (ton)	E-factor
Oil refining	10^6–10^8	10^5–10^7	< 0.1
Bulk chemicals	10^4–10^6	10^4–5×10^6	< 1–5
Fine chemicals	10^2–10^4	5×10^2–5×10^5	5–50
Pharmaceuticals	10–10^3	2.5×10^2–10^5	25–100

The synthesis of pharmaceuticals and fine chemicals, including agrochemicals, cosmetics, insecticides, flavorings, textiles, and fragrances, often require multi-step synthesis and rigorous purification processes to adhere to health and safety standards. Therefore, they operate at high E-factors. The growing adverse environmental impact of chemical production has shifted the interest to sustainable technologies that operate under the core principles of green chemistry. *Green chemistry is the design of chemical products and processes that reduce or eliminate the use or generation of hazardous substances.* [21] Green chemistry is a priority in modern chemistry, and enantioselective catalysis is the most efficient, low waste method to synthesize chiral compounds.[22]

1.3 Asymmetric Catalysis

Asymmetric catalysis is the enantioselective conversion of prochiral substrates into a chiral product with an enantiomerically pure catalyst.[23] The chirality from the catalyst is amplified,

in some cases by the millions, generating large quantities of enantioenriched products. The pioneers that developed catalytic enantioselective hydrogenation, S. Knowles and R. Noyori, and catalytic enantioselective epoxidation, K. B. Sharpless, were awarded the 2001 Chemistry Nobel prize.[24,25]

The efficiency of a catalyst is expressed by the enantiomeric excess (*ee*), enantiomeric ratio (*er*), turnover number (TON), and turnover frequency (TOF). *Ee* is the ratio of excess in one enantiomer over total enantiomers. *Er* is the ratio of major enantiomer to total enantiomers. TON is the number of product molecules generated per molecule of catalyst, and TOF is the TON per unit time.

1.4 Enantioselective Catalytic Hydrogenation

Catalytic hydrogenation of prochiral unsaturated substrates is the most used enantioselective catalytic reaction in industry.[2,13,22,23] A large variety of highly efficient catalysts based on chiral phosphines with transition metal complexes, commonly Rh, Ru, and Ir, have been developed that hydrogenate many prochiral substrates with excellent TONs, TOFs, and high regio-, chemo-, diastereo- and enantioselectivity.[13, 26-28] As well, hydrogenations have very high atom economies because hydrogen gets incorporated fully into the product and generates no waste. A recent review by Blaser and co-workers showed that at least 18 out of the 38 catalytic transformations in the fine chemical and pharmaceutical industries involve asymmetric hydrogenation of C=C, C=0, or C=N functionalities.[28]
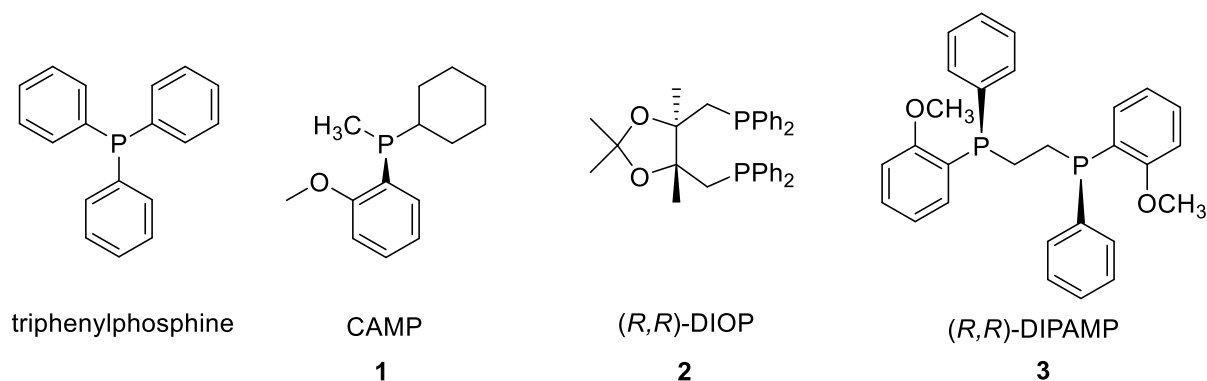
Figure 1.2 *Pioneering chiral phosphine ligands.*

Asymmetric hydrogenation emerged soon after Wilkinson and coworkers discovered that tris(triphenylphosphine)rhodium chloride is an effective catalyst for olefin hydrogenation.[29a] The triphenylphosphine was replaced with a chiral phosphine derivative, and prochiral olefins were hydrogenated. In 1968, Knowles' and Horner's groups independently demonstrated the concept of enantioselective hydrogenation for simple prochiral olefins, such as α-alkylstyrene and α-arylacrylic acids, with optical yields in the range of 8–15%.[29b,c] Knowles then went on to synthesize the new monodentate phosphine, CAMP (**1**, CAMP: *o*-anisyl(cyclohexyl)methylphosphine) (Figure 1.2), and used it to improve the selectivity of hydrogenation.[29d] In 1971, Kagan reported the first bidentate chiral phosphine, DIOP (**2**, DIOP: 2,3-*o*-isopropylidene-2,3-dihydroxy-1,4-bis(diphenylphosphino)butane) (Figure 1.2), and showed that bidentate systems operated with higher enantioselectivity.[29e,f] Knowles then developed the bidentate ligand, DIPAMP (**3**, DIPAMP: 1,2-bis[(2-methoxyphenyl)(phenyl)phosphino]ethane) (Figure 1.2),[29g] which set the foundation for the first industrial application of asymmetric catalytic hydrogenation, the synthesis of L-dopa at Monsanto.[30a-c] Unlike the neurotransmitter dopamine, its precursor,

L-dopa (*L*-3,4-dihydroxyphenylalanine), can pass the blood-barrier. Therefore, L-dopa is used for the treatment of Parkinson's disease, which is a neurodegenerative disorder associated with low dopamine levels in the brain.[30d]

Scheme 1.1
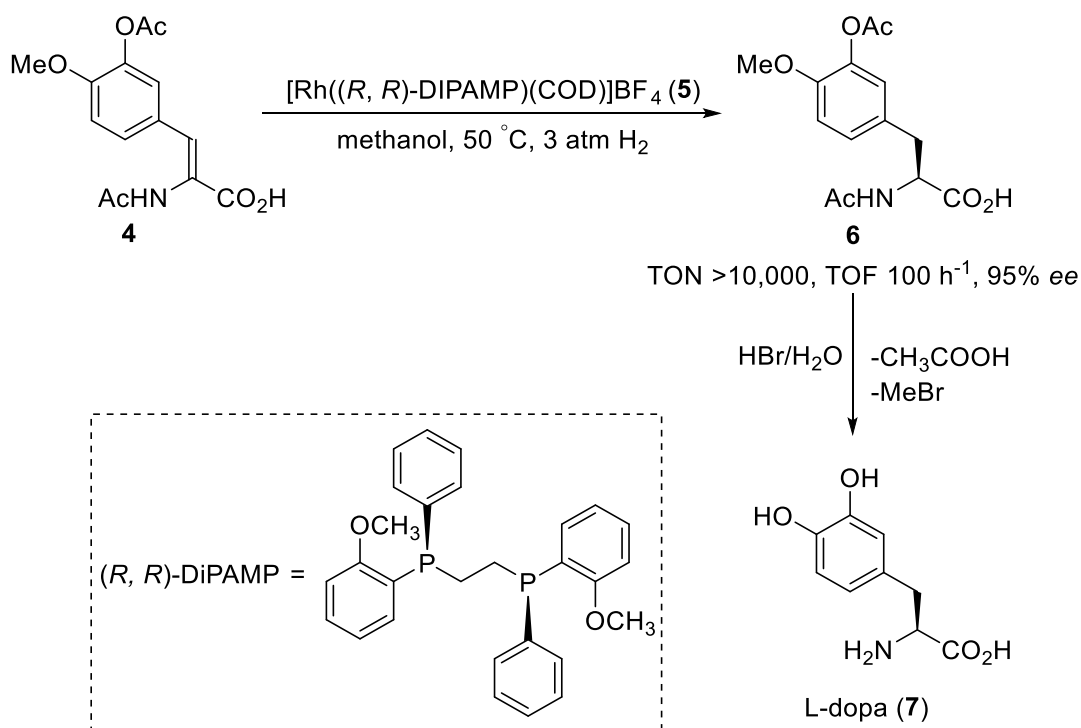
As shown in Scheme 1.1, the key step is the enantioselective hydrogenation of the enamide intermediate **4** using [Rh((*R*,*R*)-DIPAMP)(COD)]BF$_4$ (**5**) (COD: 1, 5-cyclooctadiene) as the catalyst. The reaction is carried out under 3 atm H$_2$ at 50 °C in methanol at 95% *ee* with >10,000 TON.[30c] The product **7** is obtained via acid catalyzed hydrolysis of **6**.[30b] This reaction can be carried out in ethanol, isopropanol, or alcohol-water mixtures at pressures ranging from 1 to 3 atm in 95% *ee* with TONs >20,000 and TOF up to 100 h^{-1}. This efficiency is remarkable, even by present standards.[30a-c] L-DOPA is still synthesized in ton scales using this pioneering method.[30d]

Scheme 1.2

cis-Hedione®
(fruity/jasmine odour)

trans-Hedione®
(fatty odour)
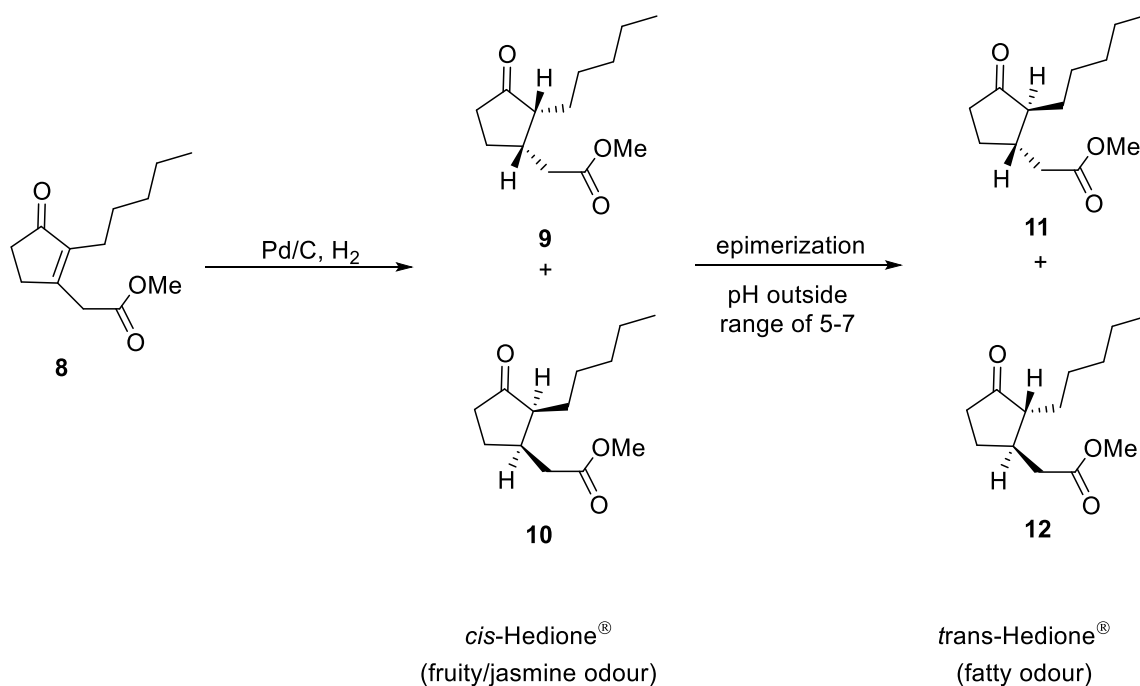
An interesting application of enantioselective hydrogenation in the fragrance industry is the synthesis of dihydromethyl jasmonate by hydrogenation of a tetra-substituted olefin with a Ru diphosphine. Initially marketed under the tradename Hedione® by Ferminich in 1970, dihydromethyl jasmonate was sold as the10% (+-)*cis* and 90% (+-)*trans* (**9**-**12**) equilibrium mixture.[31a] All four stereoisomers have different odour qualities and intensities.[31b] Perfumers established that only one isomer has the strong floral jasmine odour, while the other isomers result in a less desirable odour and the performance of the final perfume product.[31c] The initial synthesis focused on the racemic cis isomer called the *cis*-Hedione®. Acids or bases catalyse epimerization at C(2) of the *cis* isomer to produce the more stable *trans*-Hedione®.[31a] As shown in Scheme 1.2, hydrogenation over Pd under neutral conditions formed Hedione-VHC® (very high *cis*) in ~90% trans, 10% cis.[31b, e] *Cis* enriched VHC was described as "powerful and tenacious" and used in the perfume bestsellers *Pleasures* (Estee Lauder, 1995, 6.3%) and *Juicy Couture* (E. Arden, 2010, 6%).[31b]

(1.1)
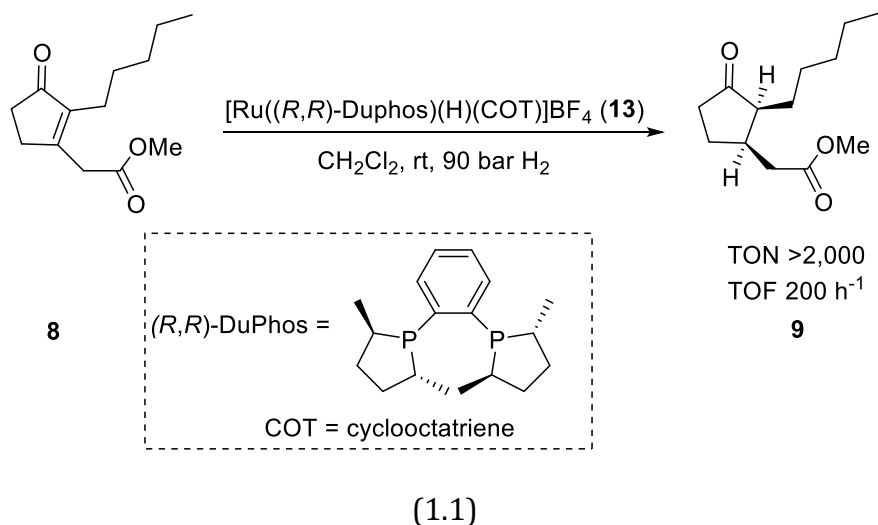
The stereoisomer (+)-*cis*-[1(*R*), 2(*S*)]-methyl dihydrojasmonate **9** has a scent that is 800 times more powerful than its enantiomer, and it is marketed under the trade name Paradisone®.[31b] It is the highest quality material sold by Ferminich, and it is used in a variety of perfumes, e.g. *Valentina* (Valentino, 2011, 7%).[31b] Paradisone® is made by enantioselective hydrogenation of the tetra-substituted alkene **8** (methyl-3-oxo-2-pentyl-1-cyclopentene-1-acetate) using [Ru ((*R*,*R*)-(Me)-DuPhos)(H)(COT)]BF₄ (**13**) (Me-DuPhos = 1,2-bis(2,5-methylphospholanyl)benzene, COT = cyclooctatriene) as the catalyst (eq 1.1).[31b, c, d, f] The reaction was carried out at 90 bar H₂, with an *er* = 82:18, TON = 2,000, TOF = 200 h⁻¹, and 90% conversion.[31c] With (*R*,*S*ₚ)-JosiPhos (JosiPhos = (*R*)-1-[(*S*ₚ)-2-(diphenylphosphino)ferrocenyl]ethyldicyclohexylphosphine) as the diphosphine, in *tert*-butyl methyl ether solvent, er = 94:6, TON = 2000, and 90% conversion was obtained with *cis*:*trans* >99:1.[31c]

Ruthenium diphosphine based catalysts have been shown to hydrogenate a wide variety of functionality, such as C=C, C=O, and C=N.[26a-f] The most notable application is the Noyori's bifunctional RuCl₂(diphosphine)(diamine) catalyst system for C=O hydrogenations.[2]
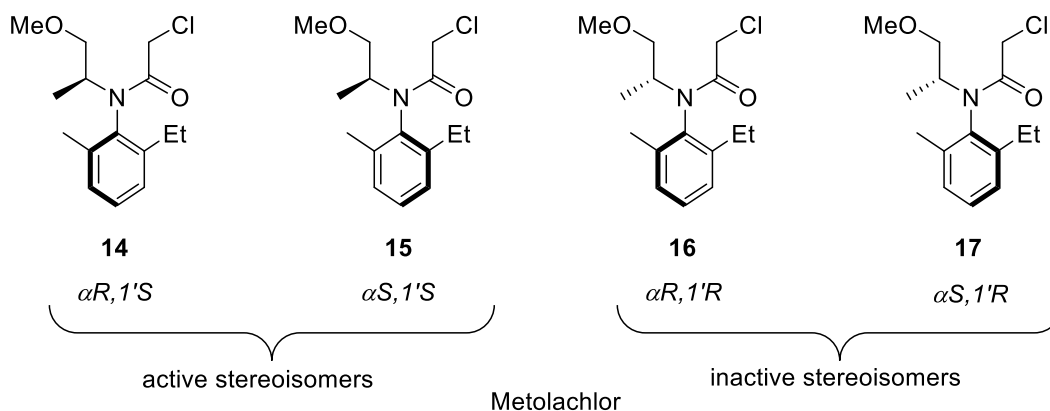
Figure 1.3 *Stereoisomers of Metolachlor.*

Iridium-based catalysts also are widely used for enantioselective hydrogenation of substrates, including imines, heteroaromatic compounds, unprotected enamine derivatives, and unfunctionalized olefins.[13, 26a, c, d, e, 27a, b] The most remarkable example is the synthesis of (*S*)-Metolachlor in agrochemical industry.[32a]

Metolachlor is a grass herbicide that is widely sold under the trade names Dual Magnum® and Dual Gold®. It should be noted that Metolachlor has two chiral elements: a chiral axis (atropisomerism, hindered C_{Ar}-N axis) and a chiral centre, giving rise to four possible stereoisomers (Figure 1.3).[32a] Interestingly, about 95% of the herbicidal activity of metolachlor results from (*1'S*)-diastereomers **14** and **15**.[32b]

10

Scheme 1.3

18

19
80% *ee*, TON 2,000,000
TOF 400,000 h^{-1}

20
(*S*)-metolachlor

Xyliphos =

R = 3,5-Me$_2$C$_6$H$_3$
21
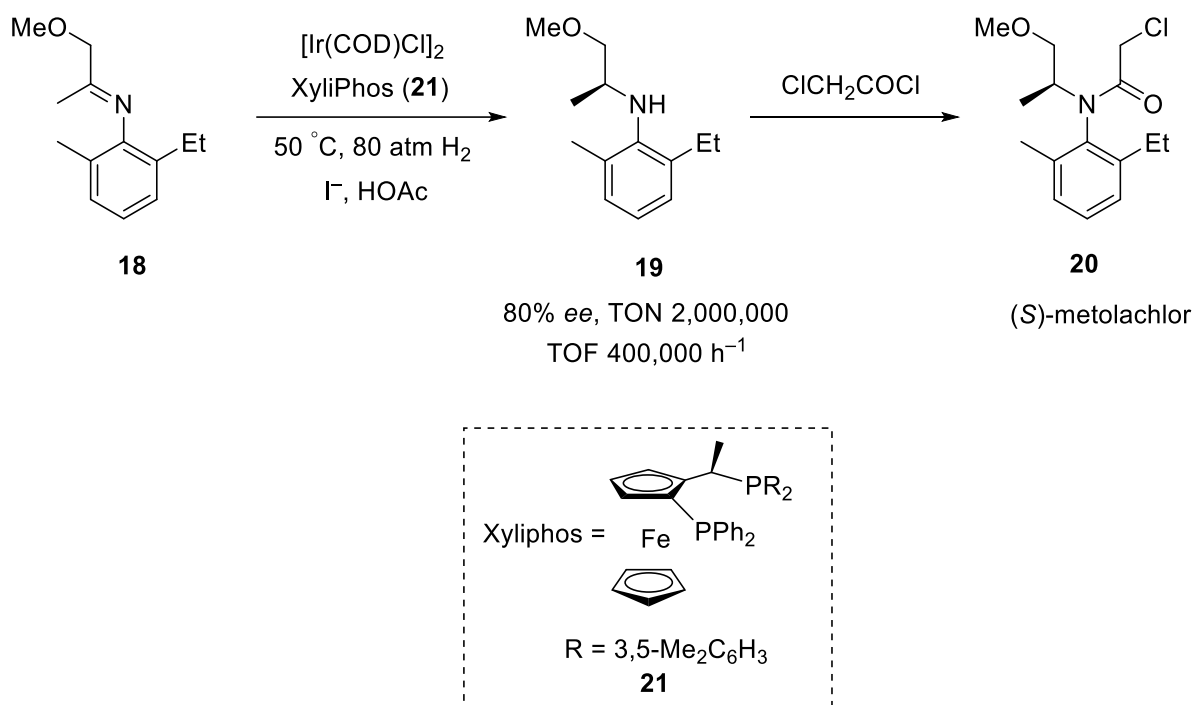
As shown in Scheme 1.3, the key step in the synthesis involves hydrogenation of the imine **18** using in-situ Ir XyliPhos (**21**, XyliPhos: (*R*)-1-[(*S$_p$*)-2-(diphenylphosphino)ferrocenyl]ethyldi(3,5-xylyl)phosphine) catalyst obtained from [Ir(COD)(Cl)]$_2$. The hydrogenation proceeds with high selectivity (80% *ee*) at 80 atm H$_2$ and 50 °C using 30% acetic acid and I$^-$ as additives. The hydrogenated product **19** was reacted further with ClCH$_2$COCl to obtain the target (*S*)-Metolachlor **20**. With a TON of 2,000,000 and a TOF of 600,000 h^{-1}, the cost and toxicity of the catalyst are insignificant. About 10,000 tons of metolachlor are produced per year, and it is the largest scale enantioselective hydrogenation on the planet.[32a,c]

Much research has been carried out with chiral complexes of non-traditional transition metals, such as cobalt-, copper-, iron etc.[13, 26d, 33a-e] However, these non-traditional

metal complexes have yet to be applied industrially, and Rh, Ir, and Ru are still among the most common metals of choice for their excellent catalytic efficiency.[13]

1.5 Enantioselectivity: a Case Study on the Rh Diphosphine System

Starting from the pioneering work of Knowles and Horner, Rh phosphine-based catalysts continue to edge out in the field of asymmetric hydrogenation. Rhodium is the principal metal used in industrial enantioselective hydrogenations.[34a,b] Rigorous mechanistic studies have enabled the understanding of the fundamentals behind the functioning of these catalysts.[35a-c] Halpern and co-workers were the pioneers behind the mechanistic study of Rh diphosphine catalysis.[35b] They studied the hydrogenation of MAC (**22**, MAC: methyl-(Z)-α-acetamidocinnamate) using Rh DIPAMP catalyst.[35b]

The first step involves elimination of diolefin NBD (NBD: norbornadiene) from the precatalysts to generate the active species as $[Rh(DIPAMP)(solvent)_2]^+$ **23**. Recently, in 2014, Heller and co-workers were able to obtain an X-ray structure of the similar species $[Rh(BINAP)(MeOH)_2]BF_4$ (BINAP = (2,2′-bis(diphenylphosphino)-1,1′-binaphthyl) in perfluorinated oil.[35c] As shown in Scheme 1.4, **23** undergoes reversible binding with the olefin by forming a 5-membered metallocycle via the double bond and the acyl group.

Scheme 1.4
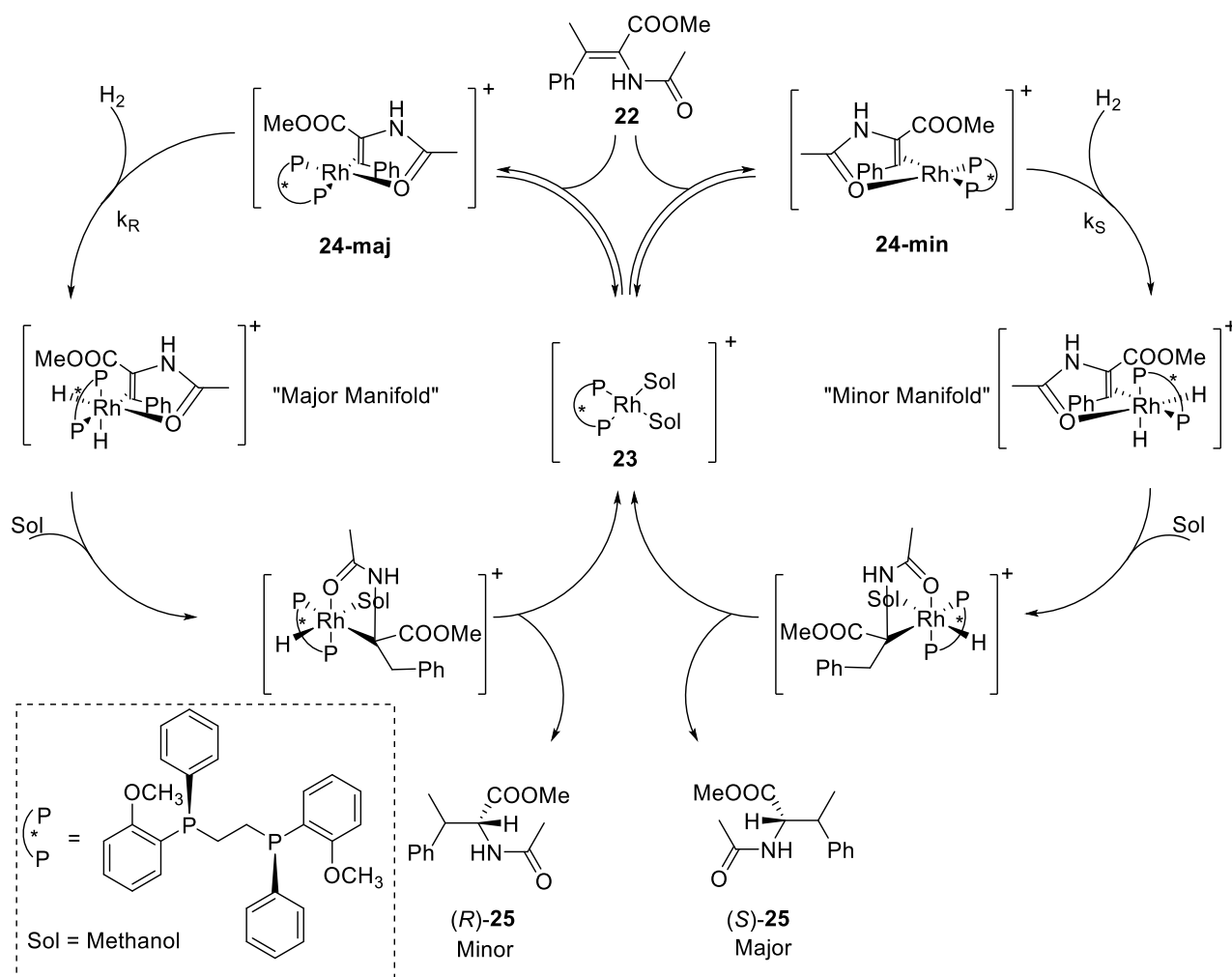
Formation of the Rh metallocycle can occur via either face of the olefin. Therefore, two different complexes are generated: **24-maj** and **24-min**. Next, the complex undergoes irreversible oxidative addition of H_2, followed by olefin insertion and further reductive elimination, leading to the reduced product and the regeneration of [Rh(DIPAMP)(solvent)$_2$]$^+$ **23** in the catalytic cycle.[35b]

$$\Delta\Delta G^{\neq}=\Delta G^{\neq}_{maj} - (\Delta G^{\neq}_{min}+\Delta G')$$

$\Delta\Delta G^{\neq}$

$\Delta G^{\neq}_{min}$

$\Delta G^{\neq}_{maj}$

$\Delta G'$

24-min

24-maj

Free Energy

Reaction Coordinate
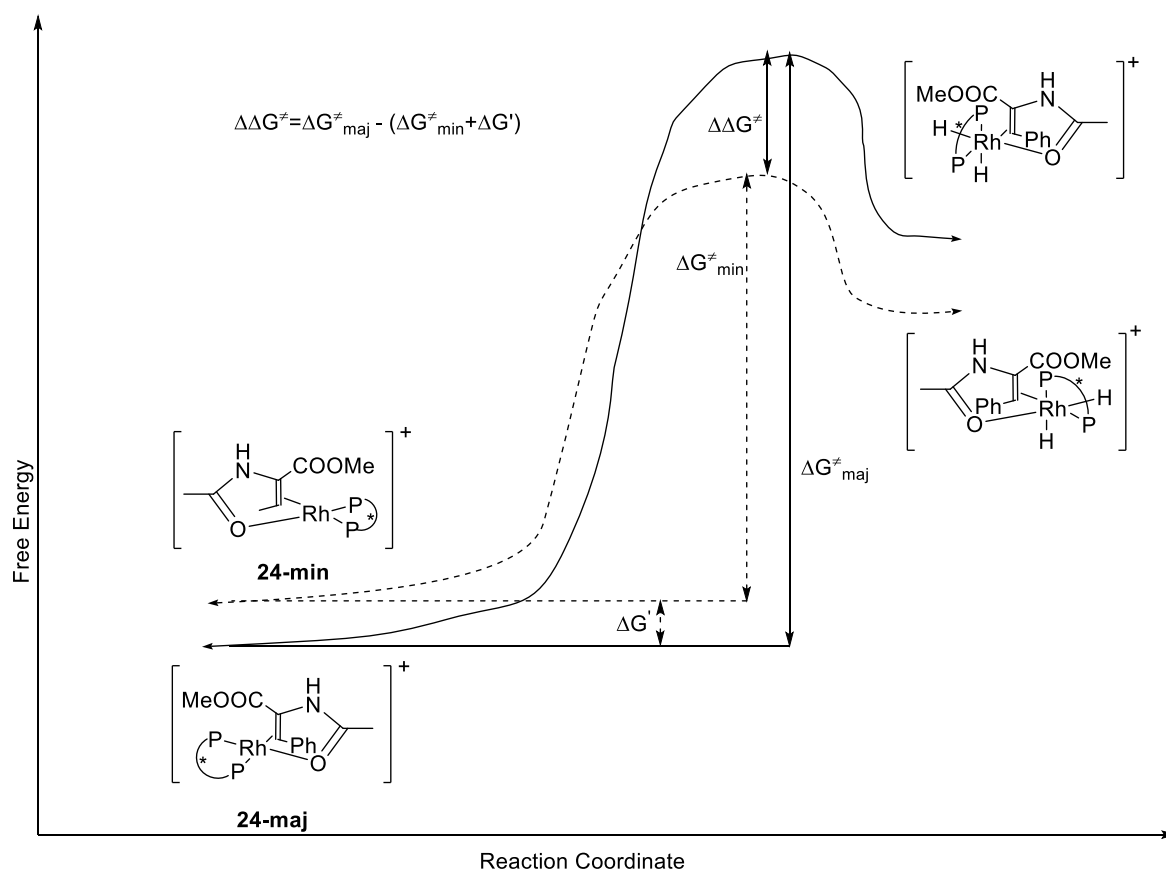
Figure 1.4 *Reaction coordinate profile for oxidative addition of H$_2$ into [Rh(DIPAMP)(MAC)]$^+$ diastereomers.*

The kinetic measurement showed that the oxidative addition of H$_2$ is the first irreversible step in the catalytic cycle, and, also the enantioselective step. It was determined that **24-maj** was a more stable complex than **24-min**. The steric interaction of olefin with the catalyst, specifically the phenyl ring on the chiral backbone of DIPAMP, differs, leading to differences in transition state energy. Surprisingly, the major complex led to the *R* enantiomer, which is the minor product, and the minor complex **24-min** led to the major *S* enantiomer product. This is because complex **24-min** is at a much higher energy, and the activation energy for the oxidative addition of H$_2$ is less than for the complex **24-maj** (Figure

1.4).[35b] Using Curtin–Hammett conditions, the *ee* of the product is determined by the difference in diastereomeric transition state energies.[35d] In this case, the enantioselectivity is determined by the difference in the Gibbs free energy of the transition state ($\Delta\Delta G^{\neq}$) for the oxidative addition of H_2 between the two complexes **24-maj** ($\Delta G^{\neq}_{maj}$) and **24-min**($\Delta G^{\neq}_{min} + \Delta G'$).[35b] The relationship between this energy difference and *ee* is calculated using eq 1.2 where K_{eq} and $\Delta G'$ are the equilibrium constant and the difference in Gibbs free energy between **24**-maj and **24**-min, respectively (Table 1.2).

$$\frac{[S]}{[R]} = \frac{k_S \times K_{eq}}{k_R} = \frac{Ae^{-\Delta G^{\neq}_{min}/RT} \times e^{-\Delta G'/RT}}{Ae^{-\Delta G^{\neq}_{maj}/RT}} = e^{\frac{\Delta G^{\neq}_{maj} - (\Delta G^{\neq}_{min} + \Delta G')}{RT}} = e^{\frac{\Delta\Delta G^{\neq}}{RT}}$$

$$\% \, ee = \frac{1 - e^{\frac{\Delta\Delta G^{\neq}}{RT}}}{1 + e^{\frac{\Delta\Delta G^{\neq}}{RT}}} \times 100$$

$$(1.2)$$

Table 1.2 *Calculation of % ee predicted via diastereomeric transition state energy difference*

$\Delta\Delta G^{\neq}$ (kcal/mol)	$\Delta\Delta G^{\neq}$ (J/mol)	$\Delta\Delta G^{\neq}$/RT	% *ee*
1	4184	1.6775	68.5
2	8368	3.3550	93.3
3	12552	5.0325	98.7
4	16736	6.7099	99.75
5	20920	8.3875	99.954

Chiral rhodium complexes have an excellent catalytic efficiency (TON and TOF), enantioselectivity, a wide range of substrate scope, catalyst recycling possibilities, etc. Further, these catalysts have a high tolerance to many functional groups and excellent chemoselectivity for a C=C bond reduction in the presence of C=O and C=N groups. Typical classes of substrates include α- and β-(acylamino)acrylates, itaconate derivatives, α-substituted enamides, α-arylenol acetates, and minimal functionalized olefins.[13, 26a-f] In fact, the choice of ligand allows one to fine tune the catalyst's selectivity and make the system more versatile. Extensive libraries of ligands have been developed based upon monodentate phosphorus derivatives or bidentate chelating phosphorus compounds to hydrogenates a wide variety of substrates with excellent selectivity.[36a-e] However, under closer inspection, one would notice that very few ligands are used on a regular basis in academia and even more so in industry; they have been classified as "privileged ligands".[37] The next section will discuss one such highly significant class of privileged chiral ferrocenyl ligands.

1.6 JosiPhos Ligand Family

Blaser identified four prerequisites to make a chiral ligand attractive for an industrial chemist.

a. Information on the scope (and limitations) and the specificity should be examined well in the literature, and the catalyst should have a high functional group tolerance.

b. The catalyst should have good performance (*ee*, TON, and TOF) not just for the model substrate but for the "real world" substrate as well.

c. Ligand synthesis should be clear and simple or should be available commercially for both screening purposes and large-scale production.

d. The patent information should be clear.

JosiPhos ligands fulfill all these criteria, therefore, they are widely used in industry, particularly for the enantioselective catalytic hydrogenation of olefins, using various Ru, Rh, and Ir complexes. This section will explore the brief history behind the development of these ligands, the versatile ligand synthesis pathway that allows easy modification of the chelating groups, and the application of its Rh complexes for asymmetric.
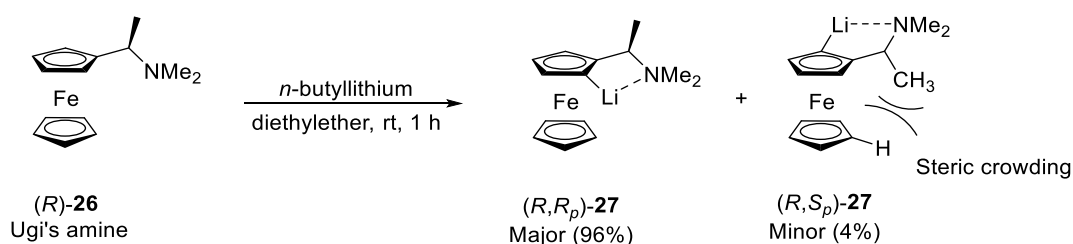
(1.3)

In 1970 Ugi and co-workers ortho-lithiated N,N-dimethyl-1-ferrocenyl-ethylamine **26** stereoselectively and functionalized it with various groups. They developed a procedure to synthesize a specific class of disubstituted ferrocenes with excellent control over planar chirality.[39a] The lithiation of optically pure (R)-**26** with butyllithium proceeds with high stereoselectivity for (R,R_p)-**27** over (R,S_p)-**27** with 96:4 ratio (eq 1.3). This selectivity arises because (R,S_p)-**27** forms an unfavorable product due to the steric repulsion between the methyl group at the chiral centre and the lower Cp ring.[39a] Next, the lithiated product was reacted with various electrophiles, such as trimethylsilane chloride, formaldehyde, and benzophenone, to form a variety of disubstituted ferrocenes. [39a] It should be noted that the major diastereomer can be isolated in high optical purity by column chromatography.[39b]

In 1974, Hayashi and Kumada utilized the diastereoselective lithiation chemistry and chlorophosphines as electrophiles to prepare the first ferrocenyl phosphine ligands **28** for application in catalytic asymmetric hydrosilation (eq 1.4).[39c]
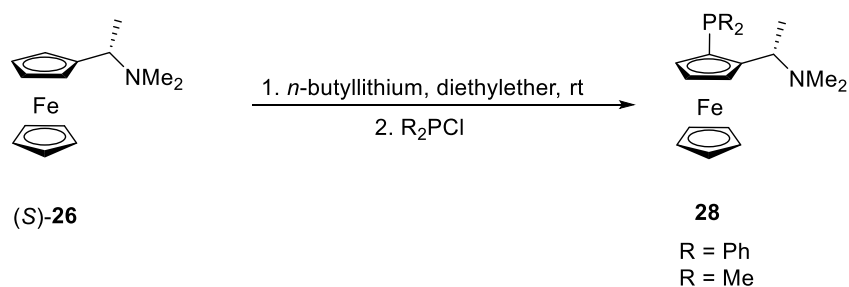
(1.4)

Ugi and colleagues had shown that the amine auxiliary of the ferrocene **26** could be substituted with acetate with complete retention of the absolute configuration at the α carbon to obtain **29**.[39d] A S_N1 type pathway was proposed, which proceeds through a configurationally stable α-ferrocenylethyl carbonium ion intermediate **30**.[39d] This stabilization is believed to be due to an interaction between the carbocationic centre and iron from the ferrocene backbone, as shown in Scheme 1.5.[39d]

Scheme 1.5
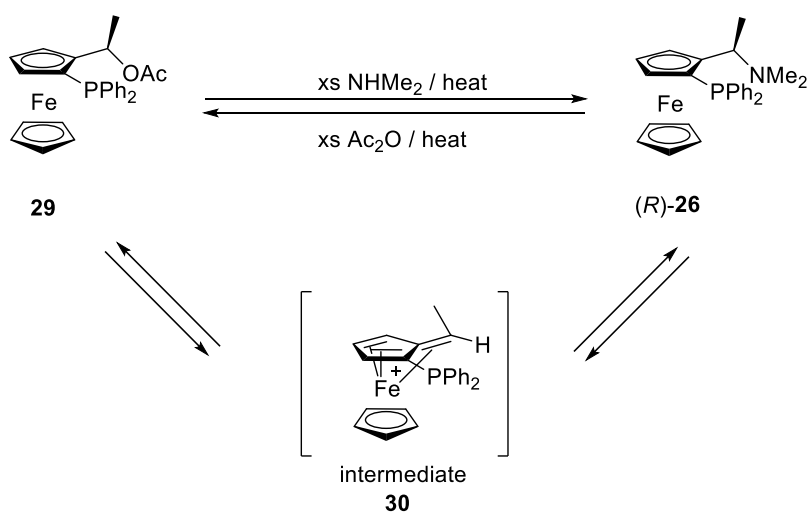
Further, Antonio Togni made an important discovery that the acetate group at the chiral centre could be substituted with nucleophilic thioacetate using KSAc in acetic acid, also with retention of the absolute configuration (eq 1.5). [39e]

(1.5)
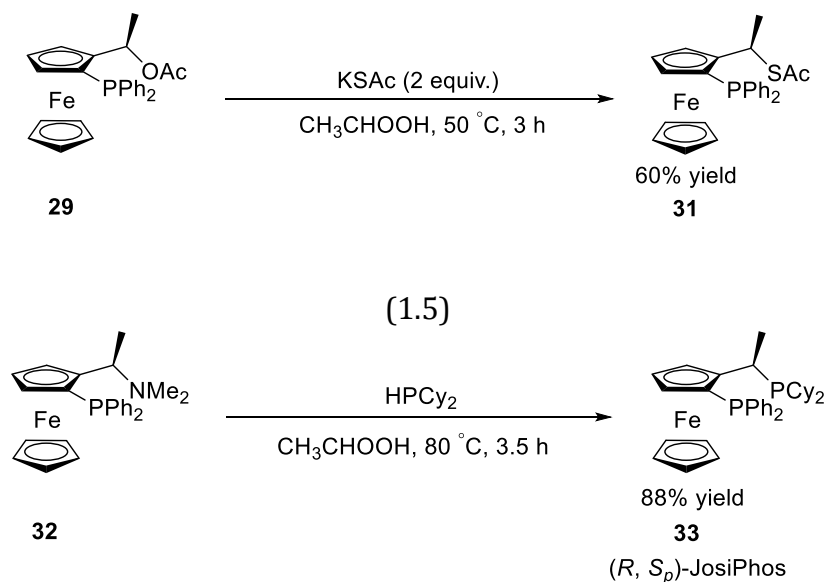
(1.6)

This finding led to the idea, developed together with Felix Splindler, to use secondary phosphines as the nucleophile to replace the acetate group; this would result in novel diphosphine ligands bearing two different phosphine groups.[38a] The first ligand synthesized using dicyclohexyphosphine was name JosiPhos after Josi Puleo, a technician who prepared it (eq 1.6).[38a] The ligand showed tremendous potential right from the very beginning. Rhodium JosiPhos complex had excellent selectivity toward the asymmetric hydrogenation of a wide variety of "privileged substrates".[38a, f] As shown in Scheme 1.6, hydrogenation of MAC proceeded with excellent selectivity with 96% *ee* and 100 TON. The reaction was carried out at 35 °C and 1 bar H_2 in methanol for 25 min using 1.0 mol% catalyst prepared in situ by reacting [Rh(NBD)$_2$] BF$_4$ and (R,S_p)-JosiPhos. However, the hydrogenation of α-

acetamidocinnamic acid gave only 84% *ee* in ethanol at 5 °C. Another derivative, MAA (MAA: methyl acetamidoacrylate), was hydrogenated with 88% *ee* in methanol at 40 °C.

Scheme 1.6

MAC	100% yield, 96% *ee*
	100 TON, 240 h^{-1} TOF

100% yield, 84% *ee*
ethanol, 5 °C

100% yield, 88% *ee*
methanol, 40 °C, 0.5 mol% cat
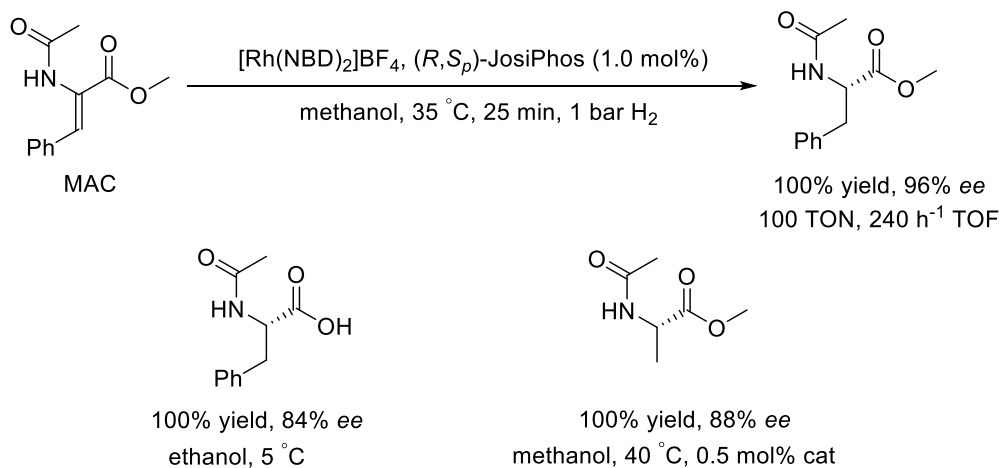
Hydrogenation of DMI (DMI: dimethyl itaconate) proceeds with exceptional selectivity (eq 1.7). The reaction was carried out at room temperature and 1 bar H_2 in methanol for 30 min using 1.0 mol% catalyst. The reaction went to completion in 0.5 h and gave 100 TON and 98–99% *ee*.

DMI

100% yield, 98–99% *ee*
100 TON, 200 h^{-1} TOF
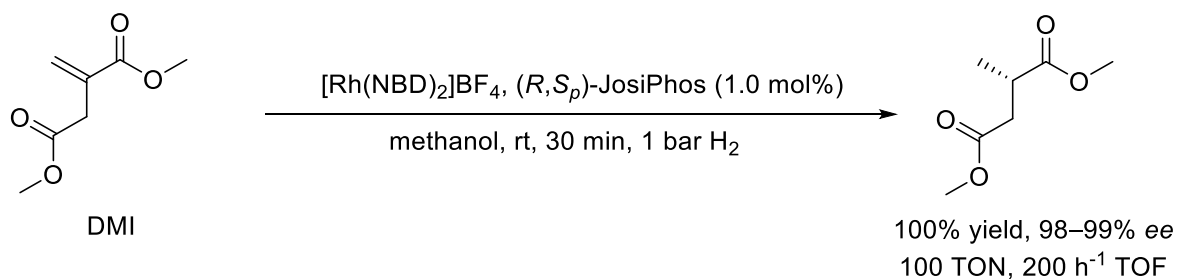
(1.7)

Rh (*R,Sp*)-JosiPhos complex also was used to hydrogenate a β-keto ester. Hydrogenation of ethyl 3-oxobutyrate was carried out at 20 bar H_2 and room temperature

(eq 1.8). The reaction went to completion in 15 h with 97% *ee* and 100 TON. Surprisingly, methyl 3-oxobutyrate hydrogenation gave a much lower selectivity of 84% *ee*.

100% yield, 97% *ee* (R = Et)
100% yield, 84% *ee* (R = Me)
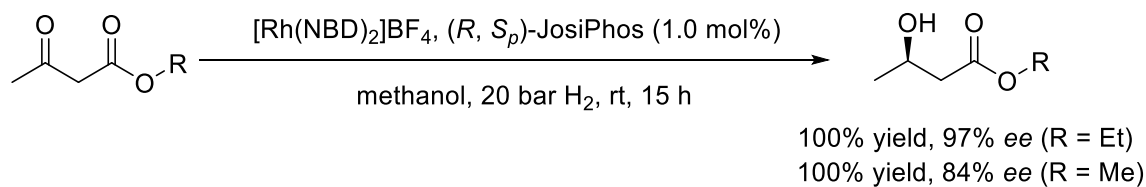
(1.8)

However, the story of the ligand didn't end here. The two-step ligand synthesis starting from Ugi's-amine, consisting of diastereoselective ortho-lithiation and absolute configuration, while retaining nucleophilic substitution of the amine group, was a versatile pathway. One could use any derivative of alkyl- or aryl- secondary phosphines in the synthesis and easily modify the electronic and the steric environment of the final catalyst. A whole family of ligands was developed using this methodology, and now all are referred to as JosiPhos ligands.[28a] Excellent control of the stereoselectivity and the high yielding synthesis makes this ligand highly attractive for industrial use. A version of the JosiPhos with xylyl phosphine, also called XyliPhos, proved to be a major success for the synthesis of (*S*)-metolachlor (Section 1.4). To run the largest enantioselective catalytic reaction on the planet, XyliPhos is synthesized on a kilogram scale every year.[32c] JosiPhos ligands are used widely in many sectors of fine chemical industry, primarily in enantioselective catalytic hydrogenation. Together with the synthesis of agrochemical (*S*)-Metolachlor[32c] and redolent Hedioine®,[31c] JosiPhos ligands are used widely in pharmaceutical industry for the synthesis of many active pharmaceutical ingredients (APIs); the reader is recommended to the literature.[28a]
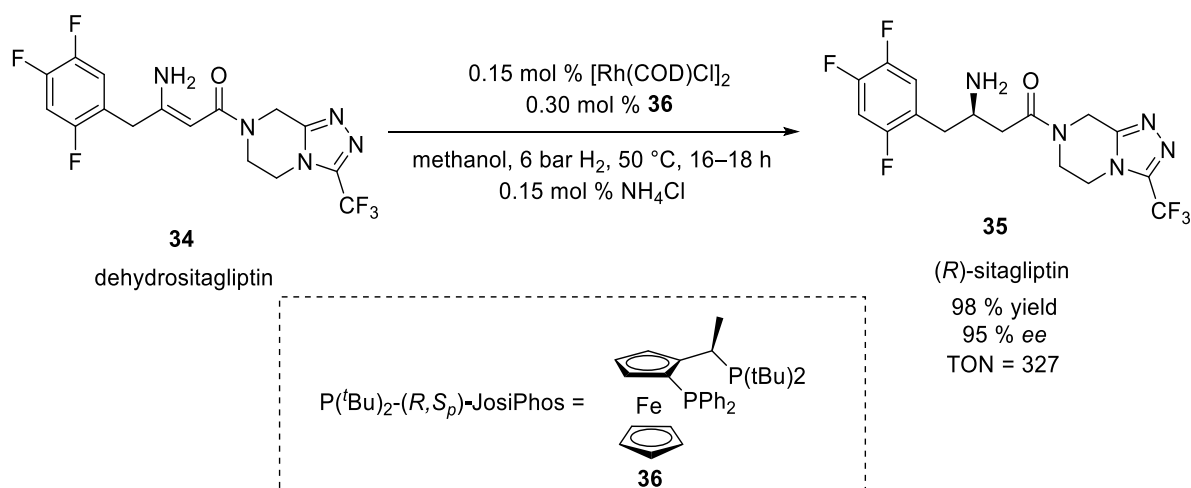
(1.9)

An important application of JosiPhos ligand involves the synthesis of Sitagliptin, which is used as a DPP-4 inhibitor for the treatment of type 2 diabetes. It is marketed in the USA by Merck & Co. under the brand name Januvia® and is sold either alone or with a combination of drug metformin.[40a] (R)-Sitagliptin is prepared by the enantioselective hydrogenation of the dihydrositagliptin **34** using Rh P(^{t}Bu)$_2$-(R,S_p)-JosiPhos (**36**, P(^{t}Bu)$_2$-(R,S_p)-JosiPhos: ((R)-1-[(S$_P$)-2-(Diphenylphosphino) ferrocenyl]ethyldi-*tert*-butylphosphine) complex made in situ by reacting dimer [Rh(COD)Cl]$_2$ and **36** (eq 1.9). In an example, the reaction was carried out using an in situ mixture of 0.15 mol% of [Rh(COD)Cl]$_2$ and (0.3 mol%) P(^{t}Bu)$_2$-JosiPhos as the catalyst.[40b] Hydrogenation was carried out under 6 bar H$_2$ at 50 °C in methanol, and the reaction gave 98% yield and 95% *ee* in 16–18 h.[40a] NH$_4$Cl was used as an additive, which seems to improve the consistency of the catalyst performance (*ee* and TOF), although the exact role is not quite obvious.[40-b-d] A previous study had shown that adding too much acid resulted in dimerized product **37** formed from of the starting enamine (eq 1.10) and the hydrogenated product, therefore, the optimized amount of 0.15% NH$_4$Cl was used for best results.[40b, c]

F

F

NH_2 O

N N N

N

CF_3

+

F

F

NH_2 O

N N N

N

CF_3

Acid →

F

F

F

O

N N N

N

F_3C

NH

O

F

F

F

N N N

N

CF_3

37

(1.10)
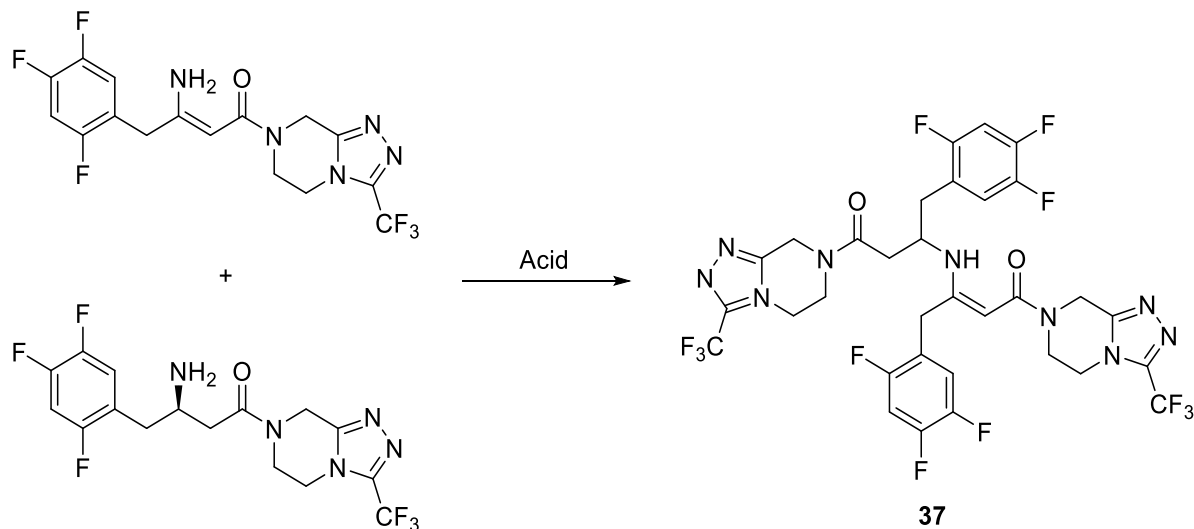
Although this is the first example of direct enantioselective hydrogenation of an unprotected enamine, the mechanistic study reveals possible tautomerization, as shown in Scheme 1.7, where the resulting imine is hydrogenated instead. When hydrogenation was carried out in D$_2$, deuterium was detected at the β-position carbon in the product **38**.[40b-d] One of the critical issues with prior enamine reduction was the use of an acyl protecting group on nitrogen.[40e] However, the authors claim that this use of a protecting group is not very attractive and a significant drawback due to difficulties in the preparation of this substrate at high *E/Z* ratio, and the protection/deprotection step would require elevated temperatures and strong acidic/basic conditions.[40b] The direct hydrogenation of enamine was more environmentally friendly as a significant amount of waste was reduced using this pathway. The authors claim a reduction in total organic waste to just one-fifth of the previous amount (250 kg to 50 kg).[40b] This reaction now is carried out on a multi-ton scale per year.[38a] This reaction uses a relatively high loading of Rh at 0.30 mol%. However, the authors showed

that Rh could be recovered using 10 wt % Ecosorb C-941, a polymer impregnated with activated carbon.[40c]

Scheme 1.7
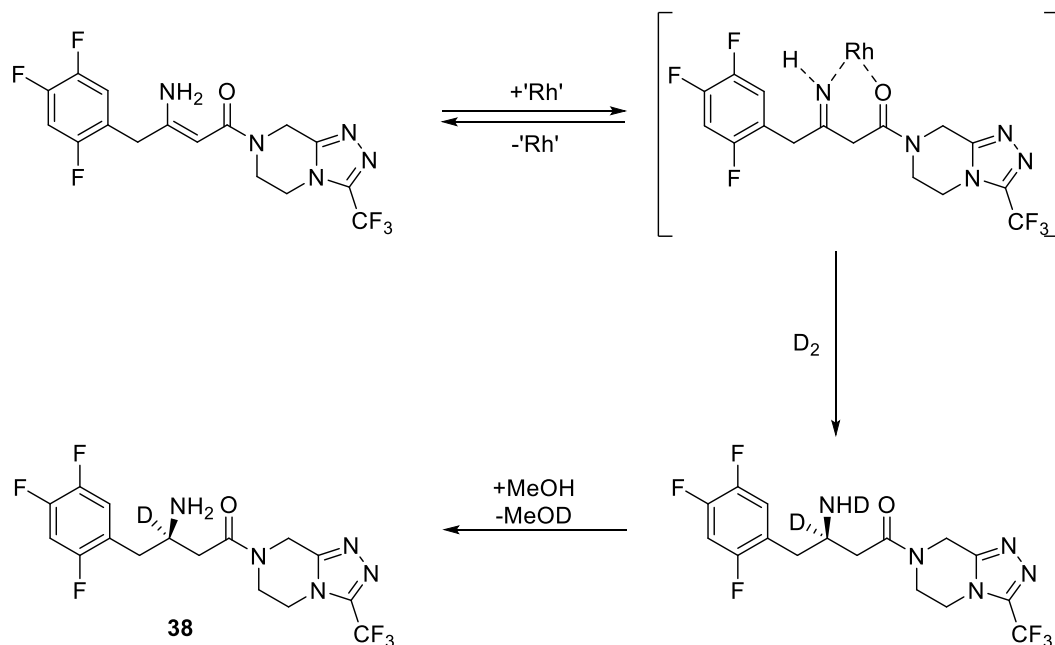
It is important to point out that this metal removal step is a principal issue with all homogeneous hydrogenation, especially in the synthesis of fine chemicals, which are heavily regulated for obvious health concerns about toxic heavy metals.[41] The next section will explore some of the challenges in homogeneous hydrogenation and the motivation behind the development of immobilized catalysts.

1.7 Challenges in the Homogeneous Hydrogenation

Enantioselective catalytic hydrogenations primarily are carried out using a homogeneous catalyst. However, due to the toxicity as well as the heavy regulation of trace metals in fine chemicals, the catalyst must be removed from the final product.[41a] For example, the

pharmaceutical industry limits the amount of allowed residual metal impurities to less than 10 ppm.[41b] However, the costly and time-consuming purification processes add a significant cost to the development and production processes, while they increase the amount of waste significantly. It is more often the case that these catalysts are air and moisture sensitive. Therefore, specialized handling techniques and precautions are taken during the operation, and recuperating the activated catalyst after a reaction is often unfeasible. However, these chiral catalysts, and especially the chiral ligands, are quite expensive. For example, 1 g of Rh metal costs 39.22 USD, whereas 1 g of P(^{t}Bu)$_2$-(R,S_p)-JosiPhos in Sigma Aldrich costs 541.91 USD.[42] The raw cost of 1g of Rh P(^{t}Bu)$_2$-(R,S_p)-JosiPhos complex would come to around 461.75 USD. In fact, the price of the ligand contributes to about 98% of the metal complex.[42] While metals usually are recovered after purification, recuperating the ligand for reuse is impractical. However, it is necessary to reduce chemical waste and improve the efficiency of the synthetic process to enact much needed green chemistry principles in chemical and pharmaceutical industries. This pressure to drive toward more sustainable scientific technologies has been a driving force toward the development of asymmetric synthesis using a heterogeneous catalyst.[43]

The use of a heterogenous catalyst addresses the above shortcomings by allowing easy recovery of the catalyst from the product. This directly reduces the rigorous purification of the product from heavy metals and allows the reuse of the expensive chiral catalysts. Further, heterogeneous catalysis in continuous-flow operations offers a safer and more efficient alternative to traditional batch reactors.[44] Immobilization of the homogeneous catalysts is a popular method that utilizes the advantages of catalyst recovery and recycling

as well as the high catalytic efficiency of the homogeneous molecular catalyst; it will be the discussion topic of next section.

1.8 Immobilized Asymmetric Hydrogenation Catalysts

A plethora of immobilization methods, which use various interactions to tether the catalysts out from reaction phases, exists in the literature. They are primarily classified into two types: covalent and non-covalent interaction.[45, 46]
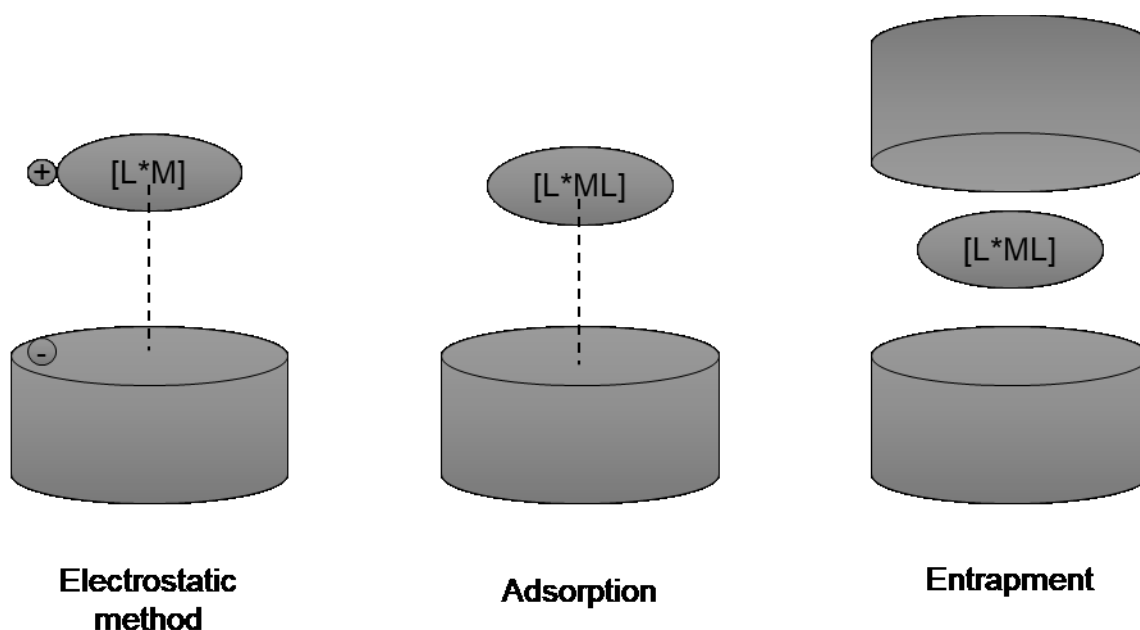
Figure 1.5 *Non-covalent methods of immobilization.*

Non-covalent immobilization strategy utilizes interactions such as electrostatic,[46] adsorption,[47] encapsulaton[48] (Figure 1.5), etc. The focus of this thesis, the electrostatic method, is quite a conventional methodology in immobilization, especially of cationic organometallic complexes[45]. This is because, cationic complexes of Rh diphosphine containing a non-coordinating counteranion, such as PF_6, BF_4, etc., can be deposited on

anionic supports with ease.[45] Furthermore, Rh remains charged all along the asymmetric hydrogenation catalytic cycle, therefore, remains bound to the support.[35b] This method circumvents the often-time-consuming ligand modification steps required in covalent tethering methods.

The electrostatic method was the first non-covalent immobilization method ever to be referred to in the literature. In 1980, Riocci and co-workers used clays as anionic supports to immobilize perchlorate salts of a Rh diphosphine complex.[46a] Clays are aluminosilicate or magnesium silicates with a two-dimensional ordered structure. Each clay sheet is composed of an Al_2O_3 or MgO layer sandwiched between SiO_2 layers. The isomorphic substitution in the crystalline structure, for example with lithium instead of magnesium or magnesium instead of aluminum, results in charge defaults. This is counterbalanced by hydrated cations (lithium, sodium, ammonium) in interlamellar space, and these cations are the key to the ionic exchange property of the overall material.[45a]

Riocci and the co-workers immobilized [Rh(PNNP)(COD)]ClO$_4$ (PNNP: *N,N'*bis(*R*(+)α-methylbenzyl)-*N,N'*bis(diphenylphosphino)ethylenediamine) in Hectorite clay by stirring the complex solution in methanol at rt for 2 h.[46a] The solid was washed with anhydrous methanol until there was complete absence of Rh in the filtrate, monitored via atomic absorption spectroscopy. This method resulted in a typical Rh loading of 1.3–1.5 % (w/w). Interestingly, the solid catalyst needed to be pre-activated by stirring in ethanol and a high pressure of H_2 (20 atm).

(1.11)
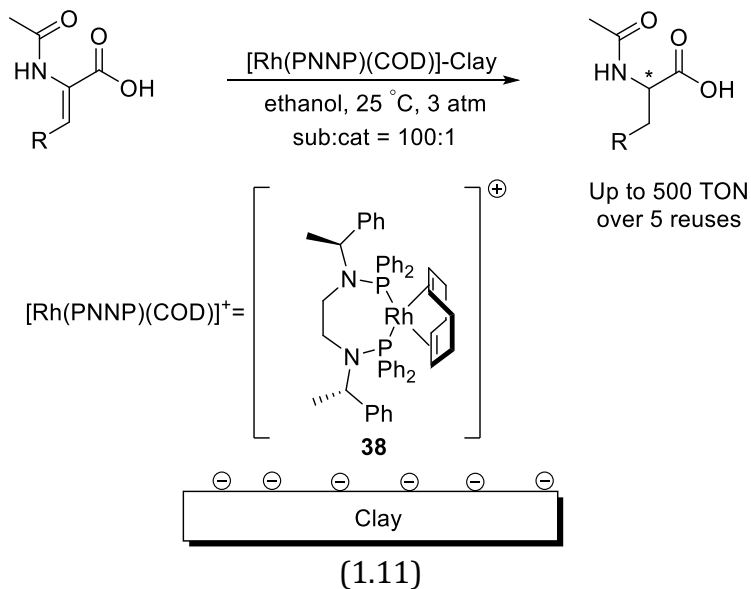
Table 1.3 *Tabulation of hydrogenation results for MAC acid and its derivatives using Hectorite deposited [Rh(PNNP)(COD)]+ 38[46a]*

Sub[a]	% ee				
	Run 1	Run 2	Run 3	Run 4	Run 5
	72.0	72.0	75.0	70.0	69.0
	49.0	38.0	24.0	-	-
	72.0	58.0	47.0	-	-

[a]Reaction was carried out in ethanol with sub:Rh at 100:1 (3 atm H_2, 25 °C). All reactions went to >95% conversion, confirmed via NMR.

A typical hydrogenation was carried out in ethanol with a Rh:Substrate ratio of 1:100 at 3 atm H_2 and stirred at 25 °C (eq 1.11). Each run went to 95–100% conversion, monitored via NMR. Hydrogenation of 2-acetamidoacrylic acid proceeds with a 72% *ee*. The catalyst was reused four times with moderate and stable *ee* in the rage of 69–72% (Table 1.3). However, the reaction had to run 7 h longer than the first run, which was carried out for only 1 h. This suggested a slow deactivation of the catalyst. Hydrogenation of cinnamic substrates showed a massive drop in *ee* during three reuses. In comparison, between the first and the third run, the *ee* had dropped from 49% to 24% for the (*Z*)-2-acetamidocinnamic acid and from 72% to 47% for the (2*Z*)-*2*-acetamido-3-(4-acetoxy-3-methoxyphenyl)-acrylic acid (Table 1.3).[46a] Although the activity and selectivity were much lower than in the homogeneous system, this was rather a pioneering work, which showed the feasibility of the electrostatic immobilization method and set up the foundation for further advances. Various anionic supports have been developed since then, consisting of inorganic or organic materials.

Derivatives of aluminosilicates are convenient inorganic supports. Silicates, when substituted with Al, result in Brönsted acidity of the overall material. Therefore, by controlling the amount of Al in silicates, one can fine tune the acidity and the ion-exchange capability of the whole material with ease.[46] To account for the mass-transport, aluminosilicate derivatives are synthesized as mesoporous materials. Promising results have been obtained by immobilizing various cationic Rh phosphine complexes on mesoporous aluminosilicate Al-MCM-41[46g] and AlTUD-1.[46h, i]

In one example, Sheldon and co-workers immobilized Rh phosphoramidite complex **39** onto mesoporous aluminosilicate ALTUD-1[46h] and used the obtained catalyst for the

hydrogenation of MAA.[46i] In one case, the hydrogenation was carried out in ethyl acetate at 5 bar H_2, 20 °C, and 10 min, which gave 99% conversion, corresponding to 217 TON and 93% *ee* (Table 1.4). When CH_2Cl_2 was used as a solvent, the activity of the catalyst was close to that of the homogeneous analog (TOF of 1600 h^{-1} vs. >1700 h^{-1}). However, the *ee* was drastically lower (83% vs. 97%). Further, the AAS (Atomic Absorption Spectroscopy) analysis of liquor showed 4.5% and 2.9% of Rh leaching in ethyl acetate and CH_2Cl_2, respectively. This catalyst also was tested for reuses, where up to four runs were carried out while maintaining the activity and the selectivity. Because of leaching issues in this system, the activity most likely would drop with further reuses.[46i]

Table 1.4 *Tabulation of hydrogenation results carried using aluminosilicates as supports*[46g, i]

Support	Cat	Sub	Activity	Comment
ALTUD-1[a] (mesoporous aluminosilicate)	 **39**	MAA	~880 TON, 1300 h^{-1} TOF[c], and ~93% *ee* during 4 reuses.	Excellent activity. Mild leaching (4.5%) and lower *ee.*
Al-MCM-41[b] (mesoporous aluminosilicate)	 **40**	DMI	4930 TON, 2000 h^{-1} TOF[c], and 94–90% *ee* during 10 reuses.	Excellent activity. Drop in selectivity during reuses.

[a]Hydrogenation carried out in ethyl acetate at 5 bar H_2, 20 °C, and 10 min, [b]Hydrogenation carried out in methanol at 5.5 bar H_2, 20 °C, and 15 min. [c]average TOF.
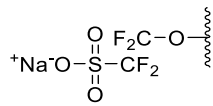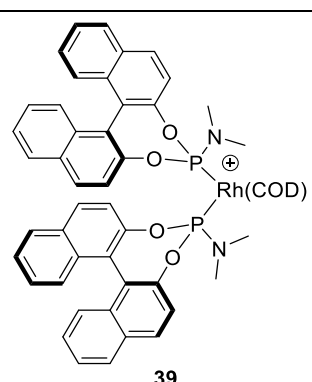
In another example, Hutching and co-workers used a different acidic mesoporous aluminosilicate, Al-MCM-41, which has a one-dimensional pore system in comparison to the three-dimensional pore system of AlTUD-1. Rh (R,S_p)-JosiPhos catalyst was immobilized on the protonated H^+Al-MCM-41 via a simple ion-exchange. The cationic [Rh((R,S_p)-(JosiPhos)(COD)]BF$_4$ solution in methanol was stirred at 55 °C for 1 h. This catalyst containing support was washed further with methanol and dried ([Rh] = 0.1g Rh/gram of support). Then, this heterogenized version of the catalyst was tested for batch hydrogenation of DMI using 0.2 mol% Rh under 6.5 bar H$_2$ and 20 °C. After 15 min, the catalyst was left to settle, and the liquor was decanted. A new batch of substrate and methanol was added, and the catalyst was reused using the same conditions. These reactions were set up by pressurizing and depressurizing with H$_2$ at 5.5 bar five times to displace N$_2$. However, this process was not taken into account for the timing of the reaction. The catalyst gave 99–98% conversion over 10 reuses, corresponding to an average TOF of 2000 h^{-1} and a combined TON of 4930 TON (Table 1.4). Unfortunately, a continuous drop in *ee* was observed over the runs. The first run gave 94% *ee*, which is slightly lower than the homogeneous version of the catalyst (96% *ee*) tested under the same conditions. The selectivity had dropped to 90% by the tenth run. No information was provided on Rh leaching nor any explanation of this issue with long-term catalyst stability, which probably is due to oxidation by exposure to traces of air.
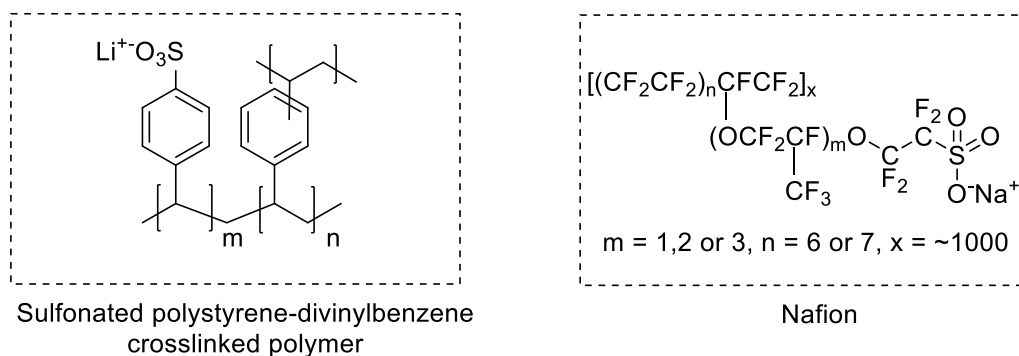
Figure 1.6 *Organic anionic supports.*

In addition to inorganic supports, various organic-based anionic supports have been developed.[46b, e] These supports primarily consist of polymer resins based on polystyrene or crosslinked polystyrene-divinylbenzene and sulfonic groups (Figure 1.6). The sulfonic group participates in the ionic exchange.[46b, e] An alternative organic support includes Nafion, which is a solid equivalent of triflic acid with an organic Teflon backbone (Figure 1.6).[46i, 49] Triflic acid is a super-acid that can participate in the ion exchange by giving off H^+ for Rh^+ and is less coordinating in comparison to the sulfonic group.[45a, 49] However, Nafion has a relatively low surface area in comparison to mesoporous inorganic supports. Therefore, Nafion has been dispersed into a mesoporous solid, such as porous silica, to improve the mass-transport during catalysis. For example, the typical surface area of Nafion resin at 0.02 m^2g^{-1} was increased to 102 m^2g^{-1} by dispersing nanosized Nafion particles (20–60 nm) onto a porous silica matrix.[46i]

Table 1.5 *Tabulation of hydrogenation result carried using Nafion based support*[46i]

Support	Cat	Sub	Activity	Reuses
Nafion[a] (Teflon polymer with triflate groups) $^+Na^-O-S-CF_2$ (O=S=O), F_2C-O	**39**	MAA	220 TON, 11 h^{-1} TOF[c], and 97% *ee* in one run. <20 TON, <11 h^{-1} TOF[c], ~97 *ee*. during 4 reuses.	Low Rh uptake. Poor catalytic performance. Mild leaching (2.3%).
SAC-13[b] (Nafion/mesoporous silica-matrix)	**39**	MAA	230 TON, 460 h^{-1} TOF[c], and 98% *ee* in one run. ~920 TON, 460 h^{-1} TOF[c], and ~98–97% *ee* during 4 reuses,	Excellent activity. Heavy leaching (>10%) and lower *ee*.

[a]Hydrogenation carried out in ethyl acetate at 5 bar H$_2$, 20 °C, and 1200 min for one run and 30 min for reuse experiments. [b]Hydrogenation carried out in methanol at 5.5 bar H$_2$, 20 °C, and 30 min. [c]Average TOF.

Sheldon and co-workers immobilized Rh bis phosphoramidite complexes onto the sodium salt of Nafion and SAC-13 (silica-Nafion composite).[46i] These heterogeneous catalysts were tested for hydrogenation of MAA. Rh uptake during the deposition for Nafion support was highly dependent on the solvent. The morphology of Nafion is affected drastically by the solvent[49], and the use of methanol significantly improved the Rh uptake by allowing easier access to the negative triflate group. Hydrogenation of MAA was carried out at 5 bar H$_2$ and 20 °C. The activity of Nafion was rather poor in ethyl acetate as it took 20 h to obtain 220 TON (95% conversion and 97% *ee*) (Table 1.5). Although changing the solvent

to methanol improved the activity, the *ee* had dropped to 75%, and up to 40% of Rh had leached. The Rh uptake during the deposition in SAC-13 was about three times higher in comparison to Nafion, most likely due to the high surface area and the morphological stability aided by the porous silica matrix. Subsequently, better catalytic performance was obtained with SAC-13 support. In an example, the hydrogenation of MAA was carried out in ethyl acetate at 5 bar H_2, 20 °C, and 30 min, and 97% conversion, corresponding to 230 TON and 98% *ee*. The TOF increased from 460 h^{-1} to 1180 h^{-1} when CH_2Cl_2 was used as a solvent (Table 1.5). However, the *ee* dropped from 98% to 86%. Both supports are plagued by massive leaching issues with >10% Rh leaching, depending on the solvent of choice. Interestingly, both Nafion and SAC-13 were reused four times with no significant drop in activity and selectivity.[46i] However, the reused runs were carried out with a relatively low substrate loading, and the leaching issue most likely would hinder the catalytic performance over the reuses.

In comparison to organic anionic supports, use of aluminosilicates resulted in better catalytic activity and lower metal leaching. However, Sheldon and co-workers made a direct comparison of Nafion, SAC-13, and ALTUD-1 with another immobilization method involving heteropoly acid, which anchors cationic Rh complexes on an alumina. The authors concluded that use of an anchoring agent was the best method among all the electrostatic immobilization methods because of its superior catalytic performance and minimum leaching.[46i]

Heteropoly Acid as the Anchoring Agents in Immobilization of Cationic Rh Complexes

Augustine and co-workers developed a straightforward immobilization method to deposit cationic complexes of Rh onto alumina using heteropoly acid as the anchoring agent.[50a-e] Phosphotungstic acid (PTA: $H_3PW_{12}O_{40}$) is the most common heteropoly acid used in the preparation.[50a-e] An alumina/PTA support can be prepared readily by adding a PTA solution into 95% ethanol slurry of neutral γ-alumina. PTA is a strong acid, therefore, binds to alumina by interacting with a basic hydroxyl group moiety of an alumina surface. However, the exact details were not provided by the authors.[50c, d] It is well known that a strong acid reacts with alumina to form the Al-conjugate base and release H_2O.[51] This method requires no synthetic modification on the ligand or the metal complex, and a homogeneous solution of cationic complexes is added directly to a slurry of alumina/HPA support. The immobilization process is simple, easy, and takes only a few hours. Immobilization has been carried out by adding a cationic Rh precursor, such as $[Rh(COD)_2]BF_4$, first, and only then adding the ligand of choice.[52] In fact, Johnson Matthey has commercialized the $Al_2O_3/PTA/[Rh(COD)_2]BF_4$ mixture under the tradename CATAXA®.[52]

$[Rh(P-P)L_2]^+$ complex

Phosphotungstic acid
as anchoring unit

γ-Al$_2$O$_3$ as the solid support
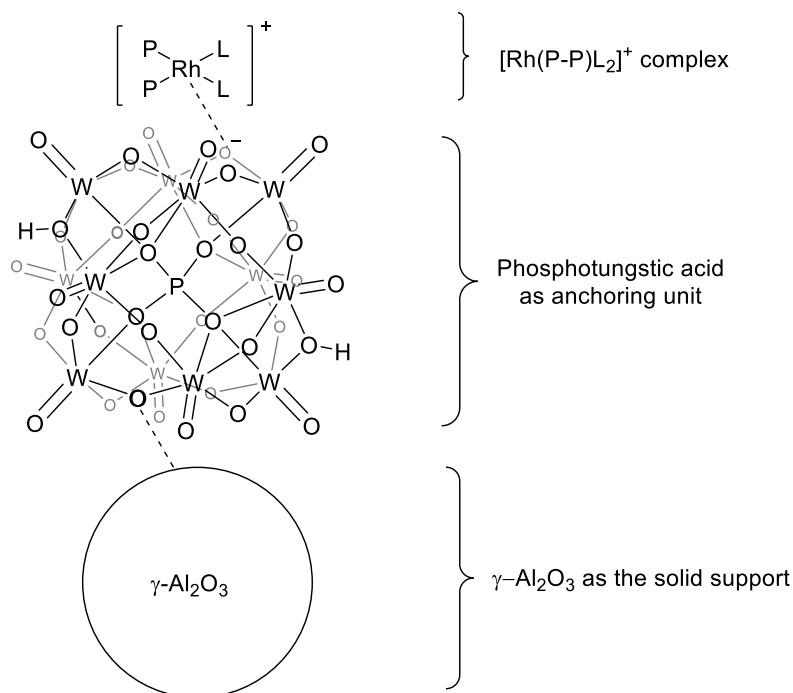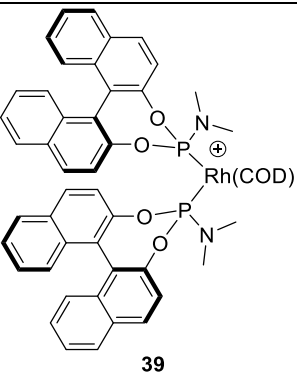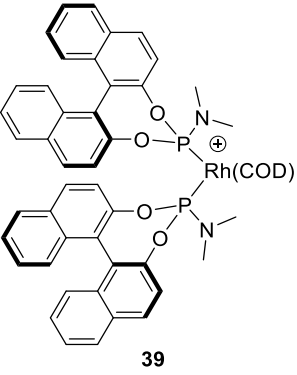
Figure 1.7 *Depiction of immobilized cationic Rh diphosphine complex onto solid alumina using PTA as an anchoring agent.*

Phosphotungstic acid forms a cage-like structure with a phosphate core, also called a Keggin unit, named after J. F. Keggin who determined it (Figure 1.7).[53a] It is believed that the PTA anchors the Rh centre via anionic oxygens by forming a direct rhodium–oxygen bond, or via electrostatic interaction between the cationic Rh and the anionic oxygen on the PTA.[50c] The authors claim that the heterogeneous catalysts can be just as selective as the homogeneous counterpart because immobilization occurs via the metal centre, and the ligand chirality is not altered.[50d] However, later research showed that there is a direct interaction between the active organometallic complex and HPA, and the nature of HPA has a significant influence on both the activity and the selectivity of the final catalyst.[50c] Further, phosphotungstic acid decomposes to PO_4^{3-} and WO_4^{2-} in basic conditions, therefore, the

integrity of the Keggin unit must be considered when determining the substrate or the hydrogenation conditions.[53b]

Table 1.6 *Tabulation of hydrogenation results of MAA carried out using Al_2O_3 and ALTUD-1 deposited* ***39***[46i]

Support	Cat	Sub	Activity	Comment
ALTUD-1[a] (mesoporous alumina)	 **39**	MAA	~880 TON, 1300 h^{-1} TOF[c], and ~93% *ee* during 4 reuses.	Excellent activity. Mild leaching (4.5%) and lower *ee.*
PWTUD[b] (PTA on mesoporous alumina)	 **39**	MAA	1000 TON, 2300 h^{-1} TOF[c], and ~97% *ee* during 4 reuses.	Excellent activity and mild leaching (<0.7%). Drop in selectivity over reuses.

[a]Hydrogenation carried out in ethyl acetate at 5 bar H_2, 20 °C, and 10 min. [b]Hydrogenation carried out in ethyl acetate at 5 bar H_2, 20 °C, and 7 min. [c]Average TOF.
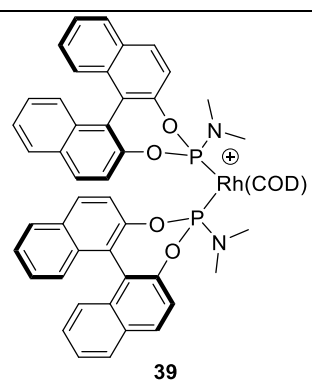
Sheldon and co-workers synthesized mesoporous alumina (TUD) and developed the anionic support called PWTUD by adding PTA.[46i] Rh phosphoramidite complex **39** was immobilized in PWTUD by merely stirring in 2-propanol for 3 h to obtain the final catalyst with 1.4mg Rh/g support loading. This catalyst was tested for the hydrogenation of MAA carried out in ethyl acetate, 5 bar H_2, and 20 °C. The reaction went to 83% conversion in just

7 min, corresponding to 2300 h^{-1} TOF and 97% *ee*. The AAS of the filtrate showed 0.7% Rh

leaching. In comparison to AlTUD-1 (1300 h^{-1} TOF, 92% *ee*, and 5.5% Rh leaching), PWTUD

was a much better support in terms of both catalytic performance and metal leaching (Table

1.6). The authors concluded that the minimum leaching with PWTUD is due to the direct Rh

and O interaction and that the use of Al$_2$O$_3$/PTA is the best support for electrostatic

immobilization.[46i]

In another example, Cole Hamilton and co-workers utilized Al$_2$O$_3$/PTA as the support

to immobilize the Rh (*R,R*)-Me-DuPhos based catalyst and used it in a flow reactor to

hydrogenate dibutyl itaconate.[54] The catalyst was synthesized by simply stirring the

Al$_2$O$_3$/PTA slurry in ethanol and adding [Rh (*R,R*)-Me-DuPhos(COD)]BF$_4$ (Rh:Al$_2$O$_3$:PTA =

1:106:8.4).
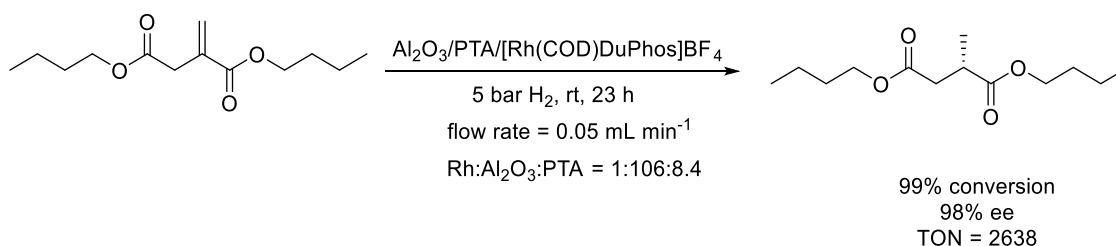
(1.12)

After optimization, the hydrogenation was carried out at 5 bar H$_2$ and rt with a flow

rate of the substrate at 0.05 mL/min (eq 1.12). For the first 23 h, the hydrogenation went to

99% conversion and 98% *ee*, corresponding to a TON of 2638. However, a massive drop in

ee was observed afterward, although the conversion was steady at 99% till 47 h. Next, the

conversion also declined rapidly, reaching 68% by 83 h. The authors correlated this to the

catalyst degradation, and no further explanation was given about the stability issues. Rh

leaching was determined by ICP-MS to be 45 ppb for the first 23 h, which increased to 625

ppb during four days of operation.[54] This is quite promising; however, a massive amount of support was used in comparison to the normal support to Rh ratio. This system is limited to one substrate and requires excess hydrogen. Also, the catalyst stability is a primary concern after a day of use.

Only a brief example was found in the literature where a JosiPhos type ligand was immobilized in Al_2O_3/PTA. Poliakoff and co-workers used CATAXA® (Al_2O_3/PTA/[Rh(COD)$_2$]BF$_4$) to immobilize Rh (R,S_p)-JosiPhos ligand and tested the obtained heterogeneous catalyst for hydrogenation of DMI in a flow reactor using supercritical CO_2 as the carrier solvent.[52] An *ee* of 58–83% was achieved with 24–35% conversion, determined by analyzing several reaction mixtures over a 20 min interval. Hydrogenation was carried out at 160 bar using supercritical CO_2 at a flow rate of 0.5 mL/min and a substrate flowrate of 0.15 ml/min (2.5 M dimethyl itaconate solution in 2-propanol). The authors concluded that it was possible to obtain good *ee* in a supercritical CO_2 hydrogenation reactor and that further optimization could improve the results.[52] However, no significant advances have been made in immobilization of a Rh JosiPhos type complex using Al_2O_3/PTA as the support. Nonetheless, use of heteropoly acids as anchoring agents is a quick, easy, and reliable immobilization method for cationic Rh diphosphine complexes.

Electrostatic immobilization has an important niche in non-covalent methods, especially of cationic Rh complexes. The diverse range of anionic supports has allowed the straightforward approach to heterogenize Rh complexes with simple ionic exchange, circumventing any catalyst modification. Nonetheless, many of these methods, including other non-covalent immobilized catalysts, suffer from metal leaching and subsequent loss in activity.[45-48, 50, 52, 54] An alternative would be to tether the catalyst onto supports via a much

stronger interaction, such as a direct covalent bond that could minimize the leaching issues of the non-covalent immobilization method. Covalent immobilization method is a popular tool in heterogeneous catalysis and is carried out using a direct ligand-support or a metal-support (Figure 1.8).[55-59] However, use of a direct bond can change the electronic environment of the catalytic sites significantly, resulting in unpredictable catalytic performance. Therefore, many polymer supported catalysts have been developed because polymer units can be modified easily with a plethora of synthetic tools, and subsequent, polymerization techniques allow a significant degree of control over the electronic environment of catalytic sites.[55g]
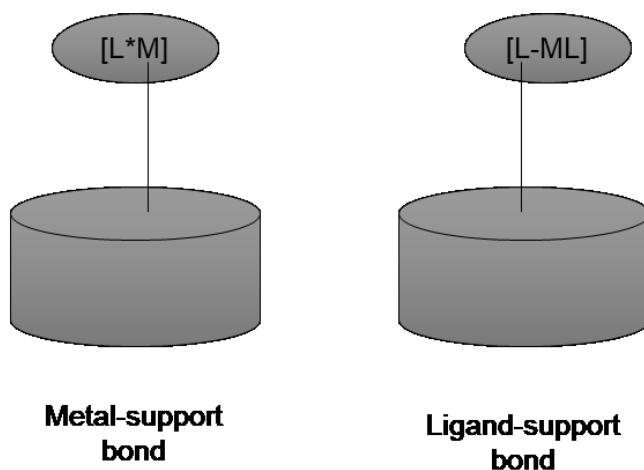
Figure 1.8 *Covalent methods of immobilization.*

Scheme 1.8
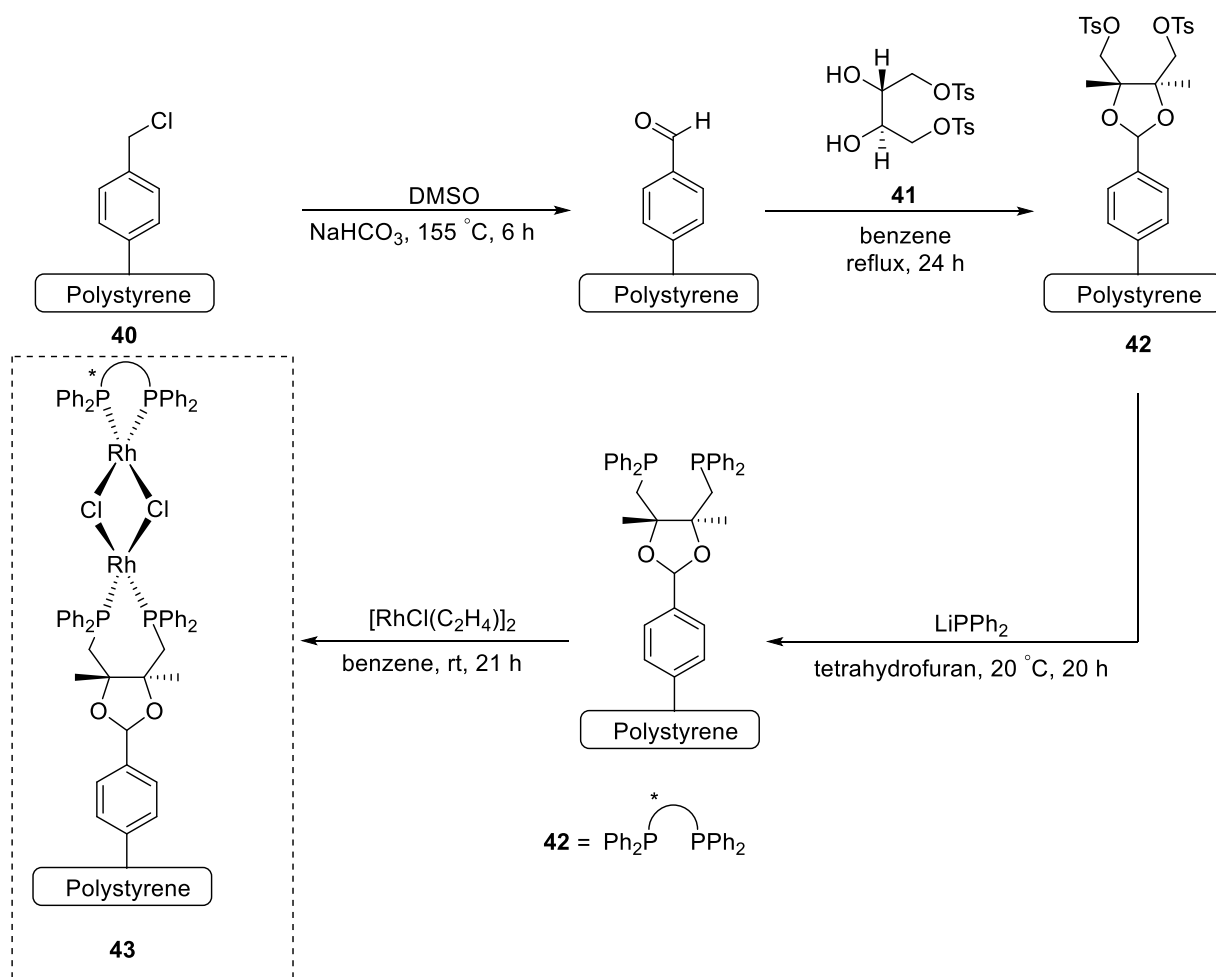
As shown in Scheme 1.8, one of the earliest works in covalent immobilization of an asymmetric hydrogenation catalyst was carried out by Kagan and co-workers in 1973, where they immobilized the DIOP ligand onto polystyrene and used it for the hydrogenation of various alkenes.[56a] Merryfield resin (0.7 mequiv of Cl/g, 200–400 mesh, 2% divinylbenzene) **40** was oxidized using the Frechet and Schuerch method.[56b] Elemental analysis was carried out to confirm that the resin was free of chlorine. Next, the aldehyde group was condensed with chiral diol **41**, and phosphine groups were introduced using diphenylphosphide to obtain a polymer-supported DIOP ligand **42**. The polymer was metallated using Cramer's

compound, $[RhCl(C_2H_4)_2]_2$, by stirring in benzene at rt for 21 h. The loss of color in the liquor was used to confirm the complexation, and the final polymer-supported chiral rhodium-DIOP catalyst was obtained.[56a]

Next, this immobilized catalyst was tested for asymmetric hydrogenation of simple prochiral olefins. In one example, α-ethylstyrene was hydrogenated at 1 bar H_2 and rt for 12 h and an optical yield of only 1.5%. However, the homogeneous Rh-DIOP catalyst hydrogenates the same substrate in 5 h and 15% optical yield. Therefore, the activity and selectivity of the immobilized catalyst were poor in comparison. This catalyst was filtered off and reused under the same the conditions as above. However, the alkene was reduced quantitatively in a much longer time of 30 h and a mere 0.6% optical yield. An attempt to hydrogenate α-acetamidocinnamic acid was unsuccessful. The poor solubility of the acid in benzene leads to the addition of ethanol as a co-solvent. The authors reasoned that this inactivity was due to poor mass transport resulting from the contraction of the hydrophobic polymer in the polar solvent.[56a] Interestingly, catalyst **43** was unable to hydrogenate even simple olefins when a polar solvent was used. This work set up a foundation for the idea of using an immobilized chiral catalyst. Many more advances have been made since then, however, many challenges, such as mass transport, accessibility of catalytic active sites, and catalyst long-term stability, continue to shadow the research field.

In an interesting example, Ding and co-workers utilized multitopic ligands to synthesize self-supported highly branched polymer frameworks called dendrimers.[57a] A multitopic ligand contains multiple metal–coordinating ligand moieties in one structure, therefore, it can be co-polymerized via complexation with metal precursors. As shown in Scheme 1.9, multitopic BINOL derivative **45** was synthesized using the Pd-catalyzed

Songashira cross-coupling reaction of methoxymethyl (MOM)- protected 6-ethylnyl-substituted BINOL derivatives **44** and 1,3,5-tribromobenzene, followed by removal of the MOM group.[56b] This resulting multitopic BINOL derivative **45** was reacted with tris(dimethylaminophosphine) to obtain the final multitopic phosphoramidite ligand. Addition of a metal precursor resulted in copolymerization to obtain the polymeric self-supported framework **46** with a monoPhos ligand to Rh ratio close to 2 to 1. This was confirmed later via elemental analysis of the polymer. The obtained polymers were 2–10 micrometer particles with an amorphous nature, confirmed via SEM (SEM: Scanning electron Microscope) and XRD (X-Ray diffraction).[57a]

Scheme 1.9

$$1 \text{ mol \% cat } (\mathbf{46})$$
$$3 \text{ atm } H_2{}^*, \text{ rt, toluene}$$
$$\text{Sub:Cat} = 100{:}1$$

95–97% *ee*, 67–85% conversion
754 TON and 170–31 h^{-1} TOF
over 10 reuses
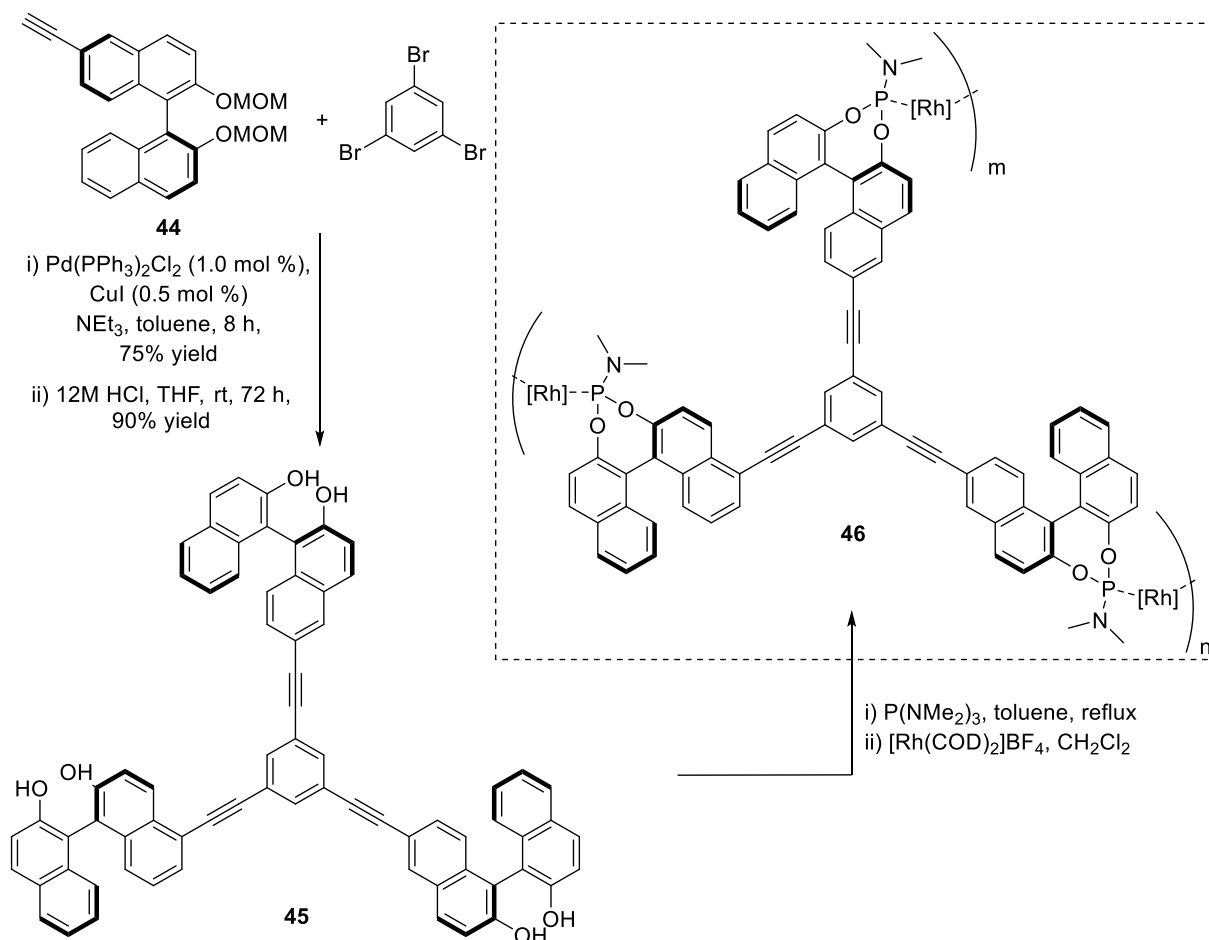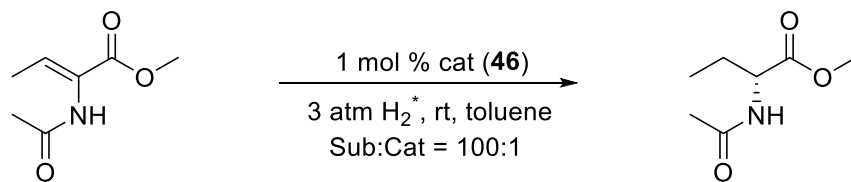
*Note: First two run carried
out at 2 atm H_2
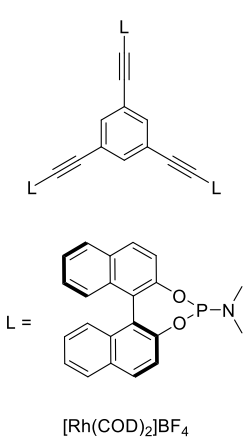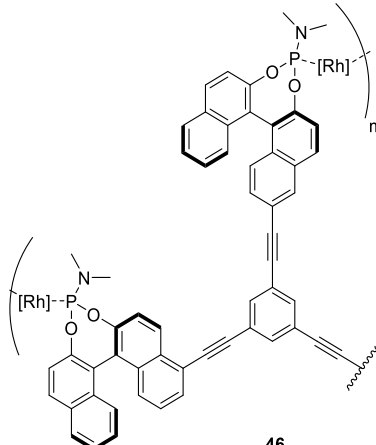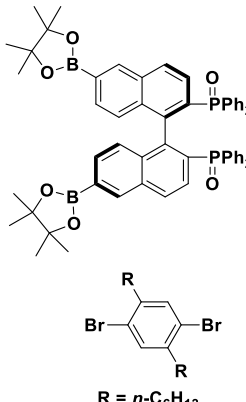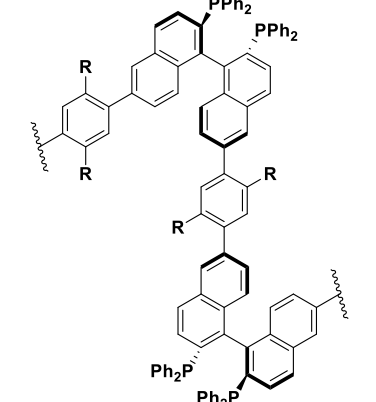
(1.13)
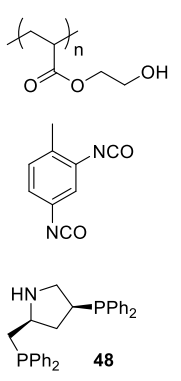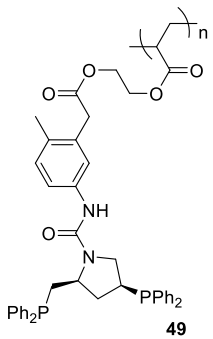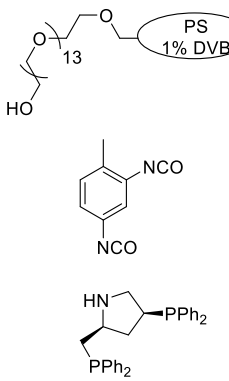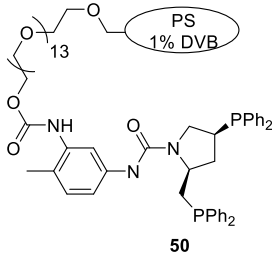
The obtained solid catalyst was tested for asymmetric hydrogenation of (*Z*)-methyl-2-acetamidobut-2-enoate. A typical run was carried out in toluene, 3 atm H_2, and 25 °C in a glass reactor (eq 1.13). Each run was stopped at around 70% conversion. At the end of each run, the catalyst was canula filtered, and a fresh batch of substrate and solvent was added. During 10 reuses, remarkable stability in *ee* was observed with fluctuation within the 95–97% range. However, the activity of the catalyst dropped significantly from a TOF of 170 h^{-1} in the first run to 31 h^{-1} in 10th run; there was no clear explanation for this deactivation. ICP-AAS (Inductively Coupled Plasma Atomic Absorption Spectroscopy) of the filtrate showed a Rh leaching of less than 1 ppm. The authors noted an improved activity with use of a different version of the catalyst (disubstituted linker) when filtration was carried out in H_2 instead of N_2, however, the selectivity dropped from 95% to 89% over seven reuses. [57a] No clear explanation exists for this common stability issue of all the immobilized catalysts, especially during reuses.

Including Ding's multitopic ligand copolymerization, many other techniques that allow synthesis of a self-supported polymeric framework via a ground-up approach are listed in the literature. Some of these polymerization methods include Friedel-Crafts alkylation between aromatic ligands and crosslinkers,[58a] radical copolymerization of vinyl

derivatives of arenes and phosphines,[58b, c] condensation reactions between amines or alcohols with acid derivatives,[58d] condensation polymerizations between amines and isocyanates,[58e] Suzuki-type couplings,[58f, g] etc.[58h] Different approaches involving grafting the ligand onto a polymer resin directly or via linker have been explored as well.[58i-l] Some of the examples are highlighted in the Table 1.7.

Table 1.7 *Tabulation of polymer-based organic/organometallic frameworks and their application in asymmetric hydrogenation*[57a, 58g, k]

#	Methods	Starting units	Organic frameworks	Performance comments
1	Multitopic ligand[a] and metal complexation polymerization	[Rh(COD)$_2$]BF$_4$	**46**	Rh polymer complex was used to hydrogenate(*Z*)-methyl-2-acetamidobut-2-enoate. 754 TON, 170–31 h^{-1}, ~70% conv., and 95–97% *ee* during 10 reuses. Excellent selectivity, drastic catalyst deactivation. Minimal leaching (<1 ppm).
2	Suzuki-cross coupling[b]	R = *n*-C$_6$H$_{13}$	**47**	Rh polymer complex was used to hydrogenate (Z)-methyl α-(benzamido) cinnamate. ~50 TON, 99% conv., and 75% *ee*. Reused once with same conv. and *ee*.

3	Isocyanate linked diphosphine on 2-hydroxyethyl methacrylate[c]	**48**	**49**	Rh polymer complex was used to hydrogenate MAC. ~100 TON, 1320 h^{-1} TOF, 50% conv., and 95% *ee*. Activity similar to homogeneous system. Reuse not attempted.
4	Isocyanate linked diphosphine on PS-1%-DVB-PEG[c]		**50**	Rh polymer complex was used to hydrogenate MAC. ~100 TON, 420 h^{-1} TOF, 50% conv., and 90% *ee*. Activity just one-third of the homogeneous system. Reuse not attempted.

[a]Hydrogenation carried out in toluene at 3 atm H$_2$ and 25 °C. Reaction stopped around ~70% conversion. [b]Hydrogenation carried out in tetrahydrofuran at 30 psi H$_2$ and rt. [c]Hydrogenation carried out in methanol/tetrahydrofuran (3.5:1 v/v) at 1 bar and 25 °C.

The common issues with polymeric catalysts are depicted in all the examples above. Use of a soluble polymer (Table 1.7, entry 2 and 3) tends to give good activity due to better mass transport in comparison to the insoluble catalyst.[55c] Pu and co-worker's Suzuki-cross coupling based soluble organic BINAP framework **47** was used to synthesize an in situ Rh BINAP derivative and tested it for the hydrogenation of (*Z*)-methyl-α-(benzamido) cinnamate.[58g] The hydrogenation gave 99% conversion (~50 TON) and 75% *ee*, which the authors concluded was close to the homogenous Rh BINAP system (~50 TON, 76% *ee*). Although comparing the TOF values would be a better way to evaluate the two systems, no information was provided on the reaction time, and the catalyst was reused just once using

the precipitation and filtration method from Chan.[58d, g] Similarly, Pugin and co-workers synthesized a soluble non-crosslinked polymer based on 2-hydroxyethyl methacrylate, where diphosphine **48** (**48**, 4-(diphenylphosphino)-2-(diphenylphosphinomethyl)-pyrrolidine) was linked into the polymer via a condensation reaction between the isocyanate group with the amine and the alcohol group.[58e] Hydrogenation of MAC was carried out using the Rh complex of the polymer **49** obtained in situ. Again, the activity of the soluble polymer (95% *ee* and 1320 h^{-1} TOF) was confirmed to be very close to the homogeneous Rh diphosphine (96% *ee* and 1320 h^{-1} TOF) system. Therefore, the soluble polymer can match the catalytic performance of the homogeneous system.

The challenges for the reuse of soluble polymer are well known. Precipitation could be used to recuperate the soluble polymer; however, it requires various solvents that could interfere with following hydrogenations.[58e] Another way would be to use ultrafiltration, but this needs specialized equipment.[58e] The resting state of the catalyst after the end of a run is hard to predict, especially in the heterogeneous system. This activated catalyst is often highly air-sensitive, and an increase in the amount of handling during the resting state increases the chances of catalyst decomposition. Therefore, crosslinkers are used to obtain solid polymer resins instead. In one example, Pugin and co-workers also immobilized diphosphine **46** onto an insoluble support based on polyethylene glycol bound to polystyrene cross-linked with 1% divinylbenzene.[58e] When the Rh complex of the ligand-grafted polymer **50** was tested for the hydrogenation of MAC, the catalytic activity (90% *ee* and 420 h^{-1} TOF) was only one-third that of the homogeneous system; the *ee* had dropped to 90% as well. Overall, the soluble polymer gave a much better catalytic performance in comparison to the crosslinked insoluble polymers, which are often plagued with mass-transport issues.[55c]

Another key factor to consider with the use of an insoluble polymer resin is the hydrogenation solvent, which has a significant effect on the selectivity of the catalyst as well as the morphology of the polymer. Often, it is tedious to find a solvent that allows both good polymer swelling to allow access to active sites and good selectivity during catalysis. Pugin and co-workers used a methanol and tetrahydrofuran solvent mixture (3.5:1 v/v, Table1.7, entry 3 and 4) to allow good polymer swelling; fortunately, this did not affect the selectivity during hydrogenation.[58e]

Pugin, Blaser, and co-workers also carried out one of the most extensive studies in the development of the covalent immobilization method for JosiPhos type ligands.[55c, 58k] A primary motivation behind the project was to develop a heterogeneous catalytic system for the synthesis of (S)-metolachlor. Pugin *et al.* used the methodology developed by Togni to derive the amine functionalized XyliPhos ligand (**51**) and attached it to silica gel and polystyrene solid supports using different linkers.[58k]

Scheme 1.10
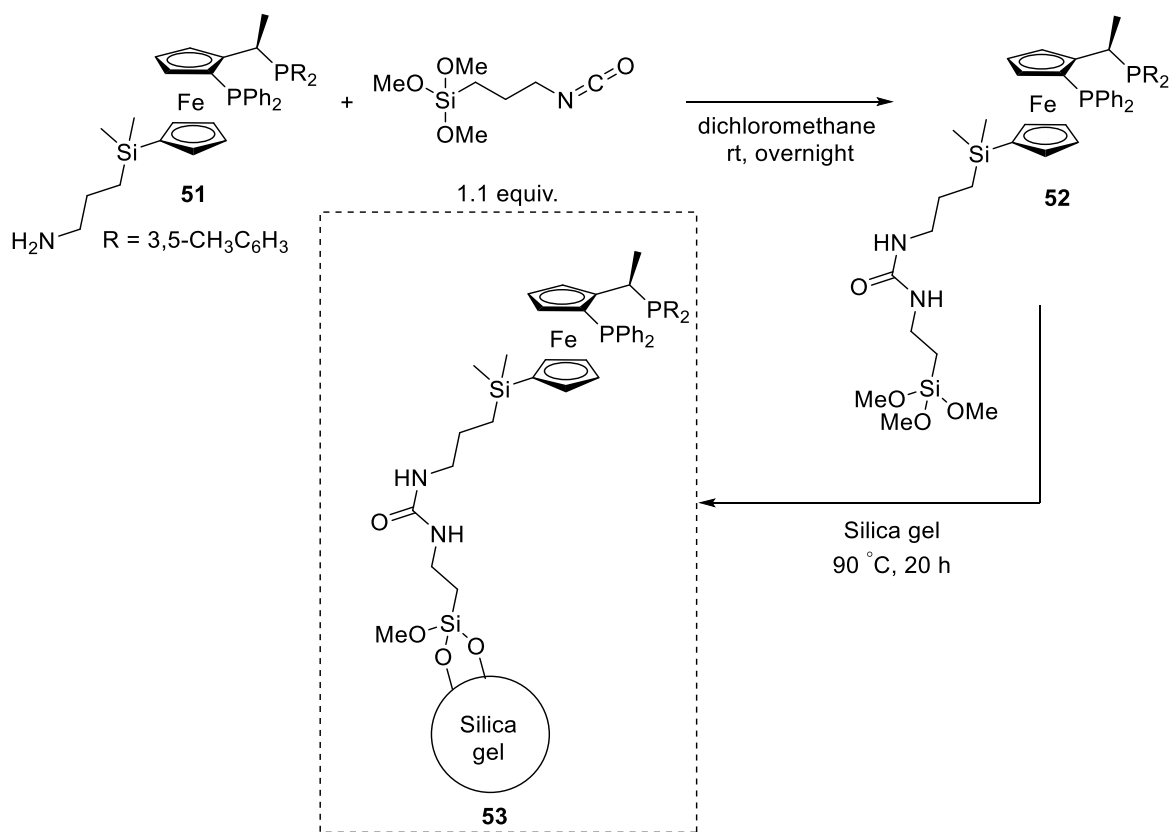
As shown in Scheme 1.10, a silica gel bound ligand was synthesized in two steps. First, the amine functionalized Xyliphos ligand **51** was reacted with 1.1 equivalent of 3-isocyanato-propyltrimethoxysilane by stirring overnight in dichloromethane to obtain **52**. The trimethoxysilane group was condensed with silica GRACE 332 by stirring in toluene at 90 °C for 20 h and vacuum dried to obtain the final silica gel bound Xyliphos derivative **53**.[58k]

Scheme 1.11
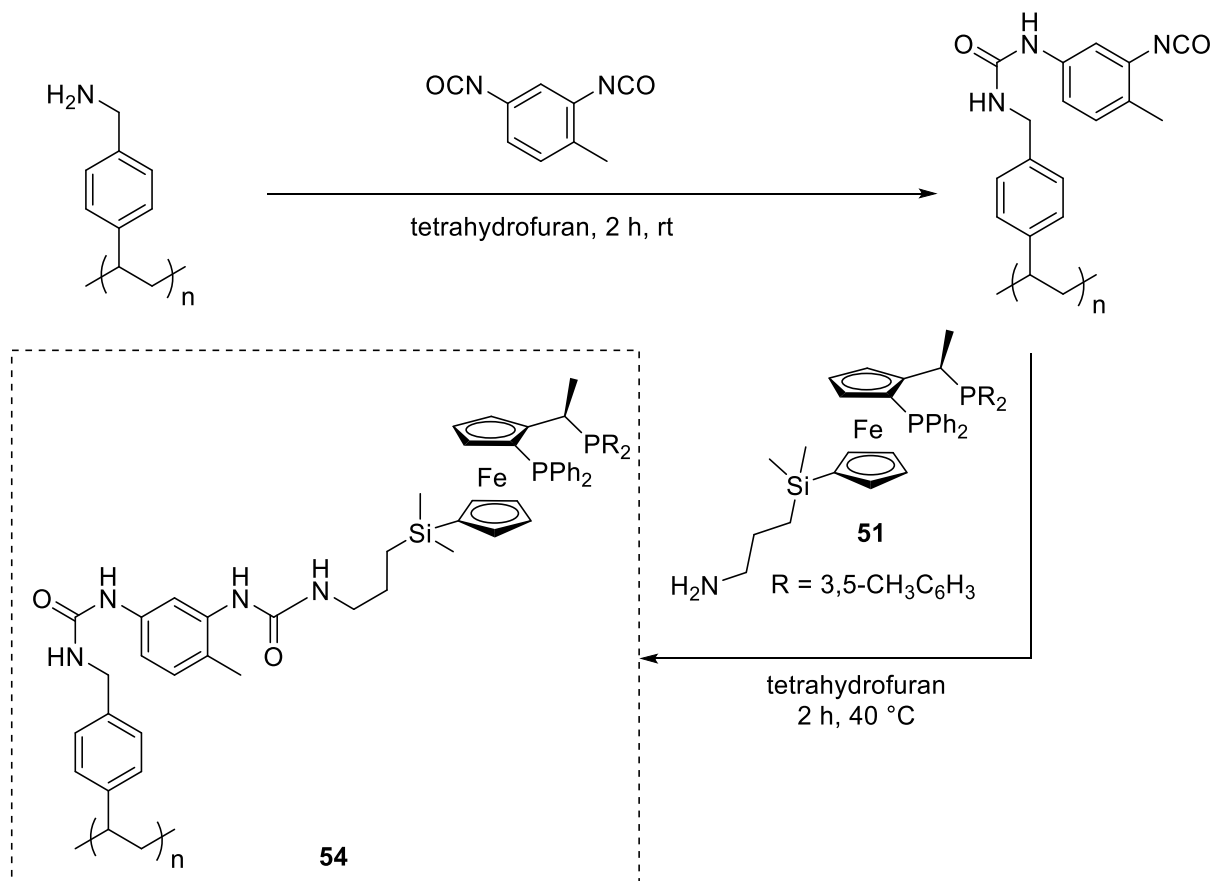
Polystyrene bound XyliPhos was synthesized in two steps, according to Scheme 1.11. First, the aminomethylated polystyrene was reacted with the linker tolylene-2,4-diisocyanate as a slurry. The least hindered isocyanate group was proposed to react with the amine. After 2 h, the excess unreacted linker was removed by washing with tetrahydrofuran. Then, this intermediate was reacted with the yellow solution of **51** in tetrahydrofuran. The liquor decolorized after 2 h. Next, the remaining isocyanate group on polymer was quenched by reacting it with ethanol overnight in the presence of catalytic amount of DABCO (DABCO: 1,4-diazobicyclo[2.2.2] octane). The phosphorous content was analyzed by microanalysis to obtain the catalyst loading. The silica gel bound ligand (0.042 mmol/g) and the polystyrene bound ligand (0.116 mmol/g) were tested for hydrogenation of imine **18**.[58k]

Both versions of immobilized ligands were metallated by adding a [Ir(COD)Cl]$_2$ solution in tetrahydrofuran at a ratio of Ir:ligand at 1:1.2. The dimer Ir precursor can bind to two ligands, therefore, crosslink the ligands. However, no further study was done on the extent of the metalation step. The solution was removed under high-vacuum, and the resulting solid was used directly for hydrogenation of the imine **18** (eq 1.14).

*Sub (19.5 g), HOAc (2.0 mL), ^{t}BuNH$_2$Cl (10 mg)
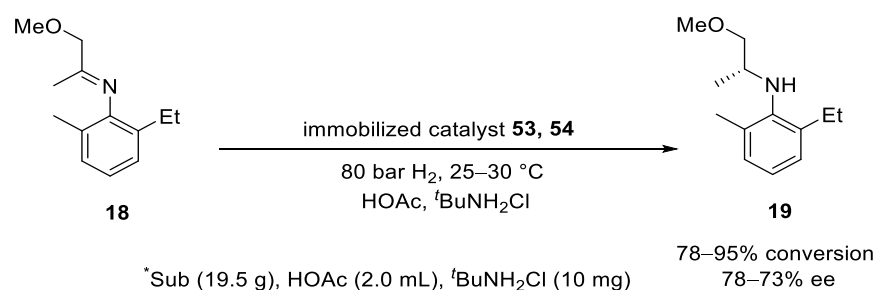
(1.14)

Table 1.8 *Tabulation of imine **18** hydrogenation results for homogeneous and immobilized Ir-Xyliphos catalysts*[58k]

Entry[a]	Catalyst	Catalyst support	Sub:Cat ratio	TOF (h^{-1}) [b]	Conversion (%)	ee (%)
1	[Ir(XyliPhos)(COD)Cl]$_2$	Homogeneous	50,000	60,000	100	79
2	[Ir(**53**)(COD)Cl]$_2$	Silica gel	20,000	20,000	100[c]	76
3	[Ir(**53**)(COD)Cl]$_2$	Silica gel	50,000	6,000	100[d]	78
4	[Ir(**53**)(COD)Cl]$_2$	Silica gel	250,000	9,750	78[c]	75
5	[Ir(**54**)(COD)Cl]$_2$	Polystyrene	50,000	1,140	95	73

[a]Reaction was carried out at 80 bar H$_2$ and 25–30 °C. [b]Overall TOF reported. [c]Ligand:Ir = 2:1. [d]Attempt to reuse, however no reaction observed after 2 h.

In comparison to the polymer bound catalyst [Ir(**54**)(COD)Cl]$_2$, the silica gel bound catalyst [Ir(**53**)(COD)Cl] gave a much better performance in terms of both the activity and the selectivity. In one example, using the silica bound catalyst, 20,000 h^{-1} overall TOF and 20,000 TON was obtained with 76% *ee* (Table 1.8, entry 2). In a high turnover reaction with a substrate:catalyst loading of 250,000:1, the reaction went to only 78% conversion and corresponds to 9,750 h^{-1} TOF and 195,000 TON (Table 1.8, entry 4). Interestingly, both of these runs were carried out using the catalyst prepared with the ligand to Ir ratio of 2:1.[58k] In another example, with the normal ligand to Ir ratio, a much smaller TOF of 6,000 h^{-1} was observed, corresponding to 50,000 TON and 78% *ee* (Table 1.8, entry 3). The rate as well as the selectivity are much lower than the control run carried out using homogeneous catalysts (Table 1.8, entry 1). The polystyrene bound catalyst gave an even worse result, which the authors reasoned was due to poor mass transport (Table 1.8, entry 5). This immobilized catalyst was unsuitable for reuse as complete deactivation was observed after the first run (Table 1.8, entry 3). Although the authors gave no explanation for using higher amounts of ligands per Ir (Table 1.8, entry 2, 3, and 4), most likely it is to compensate for the poor metalation resulting from the restriction of phosphine sites in the solid matrix.

Incomplete metallation leads to waste of ligand sites, therefore, the performance of the heterogenized systems is often poor in comparison to the homogeneous counterpart.[59c] Although polymerization of the metal-containing monomers (MCM)[55g] can address this issue, distribution of a metal-ligand complex within the polymer matrix must also be taken into consideration because it directly effects the mass transport during the catalysis. Therefore, control over the distribution and the accessibility of active sites are both essential to the final heterogenized catalyst's performance and reproductivity between different

batches. To address these issues, Bergens and co-workers developed a unique method, called alternating-ring opening olefin metathesis polymerization (alt-ROMP), and implemented it to develop Ru-BINAP and Rh-BINAP based polymer frameworks.[59a-d]

Alternating-Ring Opening Metathesis Polymerization

Alt-ROMP involves polymerization of metal-containing monomers, which eliminates the difficulties of the metalation step. Further, the modified ligand–metal complex and spacer alkene are copolymerized with excellent control over the distribution. Hence, this method addresses some of the fundamental challenges involving the distribution and accessibility of catalytic sites in polymer-based catalysts.[59a-d]

Scheme 1.12

55   56   57
89% yield
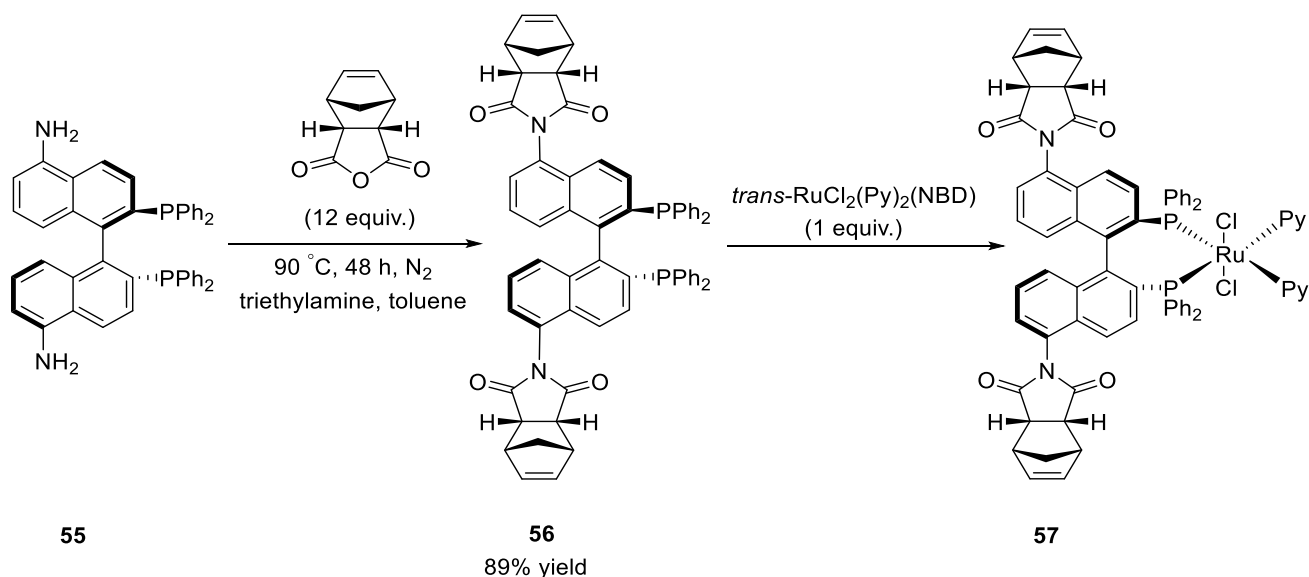
     In an example, Bergens and co-workers developed a high yielding synthetic route to functionalize the BINAP ligand with the alt-ROMP active norimido group.[59b] The privileged chiral diphosphine BINAP was the ligand of choice due to its diverse range of application in asymmetric catalysis.[60] As shown in Scheme 1.12, this high yielding synthesis led to three

atropisomers resulting from the orientation of norimido groups along the arene–nitrogen bond. This modified BINAP **56** (N-BINAP) was complexed with trans-RuCl$_2$(Py)$_2$(NBD) (Py: pyridine) in dichloromethane by stirring at 40 °C for 48 h. The final MCM **57** was obtained as a mixture of three diastereomers resulting from the orientation of the norimido group along the arene-N bond.[59b]

Scheme 1.13

Ru-BINAP:Grubbs:COE =1:0.05:4

57   **58**
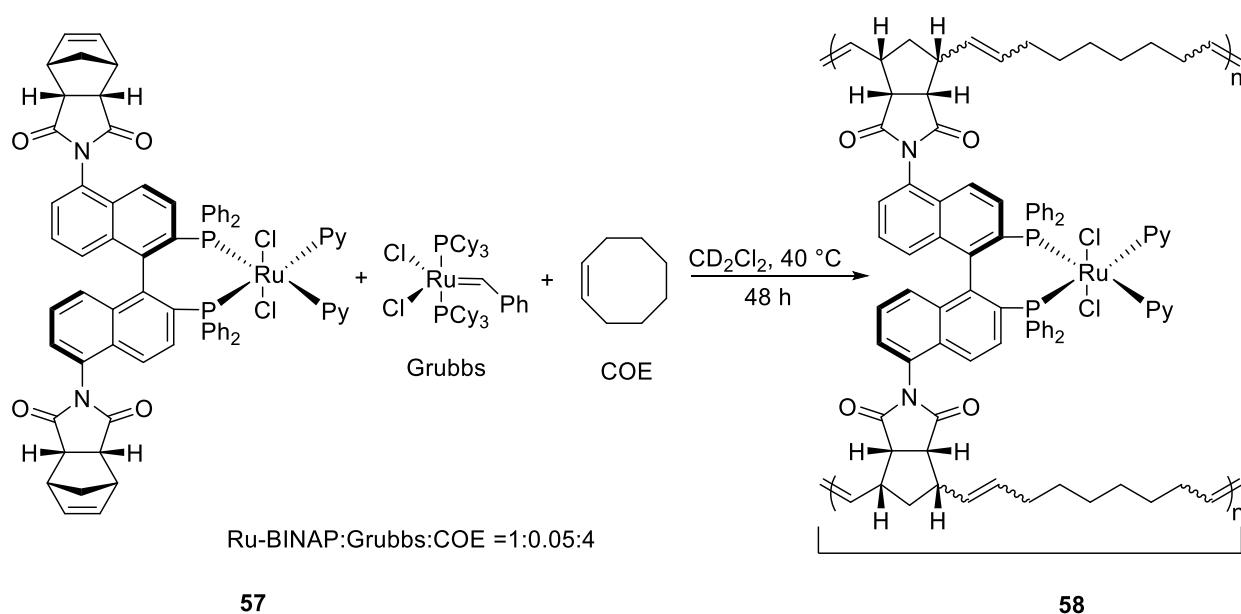
The norimido olefin groups are strained, making them intrinsically reactive towards ROMP. These norimido groups are also crowded, therefore, prevent copolymerization. The norimido group reacts with the metathesis catalyst to form an intermediate, which then prefers to react with the less crowded cyclooctene (COE). Insertion of the C8-spacer reduces crowding and allows another norimido group to react. As shown in Scheme 1.13, the result is an alternating catalyst-organic framework **58**. As the polymer grows, it can cross-link to form a three-dimensional organometallic framework because of two norimido groups in one monomer.[59b] A typical polymerization was carried out using 5% Grubbs I catalyst and 4

equivalents of COE in CD_2Cl_2 at 40 °C, which went to completion in 48 h. NMR analysis showed that the degree of alternation between the norimido and the COE was around 1.8 to 1. The Py (Py: Pyridine) ligands at the Ru centres were replaced in 100% yield by reaction with (*R,R*)-dpen (dpen: *R,R*-1,2-diphenylethylenediamine). This obtained polymer was deposited on a solid-support ($BaSO_4$) as a thin-film to aid in mechanical support during filtration and to improve mass transport.

polymer catalyst
supported on $BaSO_4$

10 bar H_2, 2-propanol
KO^{t}Bu, ~21 h, 35–40 $^\circ$C
Substrate:Base:Ru = 1:20:1000

95–96% ee
100% conversion
25 runs without loss
in converstion or *ee*
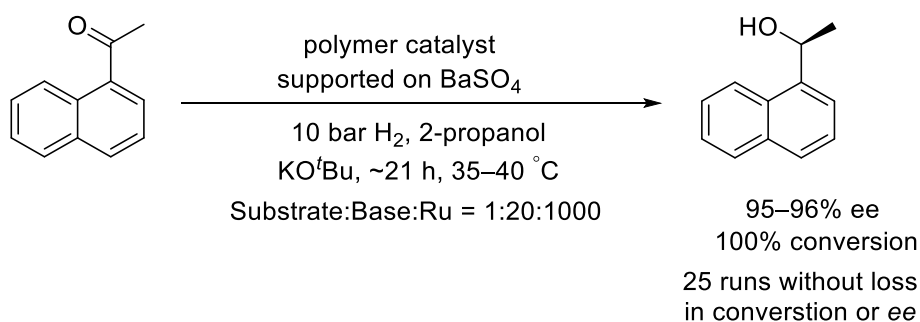
(1.15)

Next, the heterogeneous catalyst was tested for the enantioselective ketone hydrogenation of 1-acetonaphthone, with a typical run carried out using substrate:KO^{t}Bu:Ru at a ratio of 1:20:1000, 10 bar H_2, and 35–40 °C for ~21 h (eq 1.15). The catalyst was left to settle, while the liquor was cannula filtered. Later, a fresh batch of reactants was added to set the new run. The reaction gave high TON per run (≥1000) for 25 reuses before any significant loss in activity. These 25 reuses were carried out without loss in *ee* or detectable Ru leaching over 25 days of operation. At the end of 29 runs, a change in the stirring pitch was noted, and the drop in the activity on the consequent runs was due to a mechanical fault with stirring. It led to splashing of the catalyst along the hydrogenation vessel walls. Opening the bomb confirmed this; the stir bar was worn out completely due to the month of continuous stirring.

The use of the alt-ROMP polymer based immobilized catalyst led to an unprecedented number of reuses together with excellent catalytic stability and selectivity. It, therefore, occupies a niche as an attractive tool in polymer-based immobilization methods.[59b] Bergens and co-workers applied this versatile polymerization method to immobilize a Rh-BINAP based catalyst as well and used it for the intramolecular cycloisomerization of 1,6 enynes[59c] and the isomerization of secondary allylic alcohols into ketones[59d] with excellent reusability and catalytic performance.

Miscellaneous Immobilization Methods

Ionic liquids are organic salts with low melting points (<100 °C), yet have low volatility due to remarkably low vapor pressures.[61a] Using the ionic liquid [OMIM]BF$_4$ (**40**, [OMIM]BF$_4$: 1-methyl-3-octylimidazolium tetrafluoroborate) and water, Feng and coworkers developed a biphasic system to carry out the reusable asymmetric hydrogenation of olefins using Rh JosiPhos based catalyst.[61b]
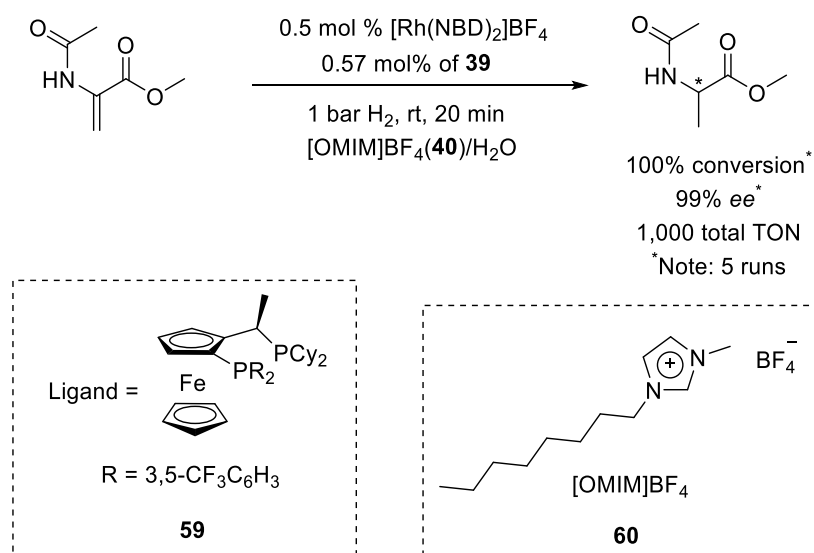
$$(1.16)$$

In one example, MAA was hydrogenated using the cationic Rh complex prepared by reacting [Rh(NBD)$_2$]BF$_4$ with **39.** The ionic nature of the Rh complex allows it to remain in the ionic liquid phase, while the hydrogenated product stays in the water. Hydrogenation was carried out at 1 bar H$_2$ for 20 min (eq 1.16). After the reaction, the aqueous phase was simply decanted, and a new run was set. Each run went to completion with 200 TON and 99% *ee*, however, catalyst deactivation was observed in the sixth run, which the authors proposed was due to the result of oxidation from traces of air exposure during work up. Rhodium leaching for the first run was determined using ICP-MS as 0.9 ppm, which corresponds to 0.5% of the total catalyst.[61b]

Other biphasic systems include ionic liquids and supercritical CO$_2$.[61c, d] The supercritical CO$_2$ itself is considered a green alternative to organic solvents as it is non-toxic, inflammable, abundant, and has excellent potential for recycling.[461a] Interestingly, CO$_2$ is soluble in ionic liquids, whereas the ionic liquid is virtually insoluble in CO$_2$. By using supercritical CO$_2$ as a solvent, reactant and products can be transported efficiently into and out of ionic liquids. Therefore, biphasic systems, consisting of supercritical CO$_2$ and ionic liquids, are common in multi-phase catalysis.[61a, c-d] Nonetheless, the massive drop in selectivity and activity over an extended period are common issues. Further drawbacks include high moisture sensitivity and the requirement of significant energy and highly specialized equipment for the pressurizing/depressurizing process of supercritical CO$_2$.[61c, d]

Immobilization methods highlighted in this section outline some of the common challenges in heterogeneous catalysis, such as low catalytic activity, issues with long-term catalyst stability, leaching of metal, mass transport, etc. Therefore, some of the goals of our

research objective regarding the development of immobilized catalysts were to address these issues. Further, immobilized molecular catalyst performance and its applicability is dependent directly on the choice of molecular catalysts and, specifically, on the ligand itself. Therefore, it has been logical for our industrial partners and us to pursue relevant privileged ligands for the development of immobilized chiral catalysts. Specifically, immobilization methods involving JosiPhos-type ligands suffer from limited reusability and poor catalytic performance. Apart from Hutching's Al-MCM-41 based support, no reliable system exists in the literature, and even this method is plagued with catalytic stability issues as evident from a drop-in selectivity during reuses.[46g, 52, 58k 61b] Therefore, we intended to use our pioneered alt-ROMP method combined with the Al_2O_3/PTA support to develop an immobilized Rh chiral ferrocenyl diphosphine complex; this will be the topic for the remainder of this thesis.

Chapter 2 Highly Reusable Cationic Rhodium Diphosphine Polymers for Heterogeneous Asymmetric Hydrogenation

2.1 Introduction

Asymmetric hydrogenation of prochiral unsaturated substrates is used extensively in the synthesis of pharmaceuticals, agrochemicals, fragrances, flavourants, etc. and is among the most efficient and reliable methodologies to synthesize one hand of chiral molecules selectively.[2, 13, 26d] The success of this technology relies on the highly effective catalysts based on chiral phosphines with transition metal complexes, commonly Rh, Ru, and Ir, which hydrogenate a broad range of unsaturated prochiral substrates with excellent selectivity and conversion.[26] In particular, JosiPhos type ligands are among the rare class of "privileged ligands" in chemical industry due to the excellent selectivity and activity that have been obtained using these ligands for the synthesis of a wide variety of highly industrially relevant chiral commodities, such as agrochemical (*S*)-Metolachlor[32c], API Sitagliptin®,[40b] redolent Paradisone®,[31c] etc.[38a] The success of this class of ligands also lies on the high-yielding and versatile ligand synthesis routes developed by Togni and co-workers.[39f] Asymmetric hydrogenation is carried out with dissolved catalysts that possess challenges, specifically, the inability to recuperate the expensive chiral catalyst after a reaction and the rigorous purification that the products must go through to remove heavy metal traces.[41a] However, the costly and time-consuming purification processes adds considerable expense to the development and production process while increasing the amount of waste significantly.

The necessity to reduce chemical waste and strive toward a more sustainable chemical production process in compliance with green chemistry principles has been the leading theme in modern chemistry and the motivation behind heterogeneous catalysis. Specifically, use of a heterogeneous catalyst in the synthesis of chiral molecules can address the issues identified with homogeneous catalysis by allowing easy recovery and reuse of the catalyst.[43] A large number of techniques have been developed in the past fifty years, aimed to immobilize the homogeneous molecular catalysts in an effort to incorporate the advantages of catalyst recovery and recycling with the high catalytic efficiency of the molecular catalyst.[45-48, 50-52, 54-59, 61] However, the majority of these immobilization methods result in a catalyst with much lower activity due to reduced mass transport, lower selectivity than the homogeneous counterpart, metal leaching, poor lifetime, etc. For a JosiPhos type catalyst, very few examples exist in the literature, and some of these immobilization methods involve a biphasic solvent,[61b] electrostatic interplay with aluminosilicates,[46h] dendrimers,[62] grafting onto silica,[58k] polystyrene,[58k] etc.[52] The majority of these methods are in accordance with the issues outlined earlier, including a dwindling number of reuses and of unexplained catalyst decompositions. Therefore, it was of interest to us and our industrial partner to explore alternatives to immobilize a JosiPhos type ligand.

As mentioned in Chapter 1, the Bergens group developed alt-ROMP method to synthesize a highly-reusable Ru and Rh BINAP based organometallic-polymer framework for asymmetric hydrogenation of ketones, intramolecular cycloisomerization, and isomerization of secondary allylic alcohols to ketones.[59] Specifically, the immobilized polymeric Ru BINAP derivative was reused 25 times for asymmetric hydrogenation of 1-acetonaphthone, with no significant drop in activity or selectivity and with no detectable

metal leaching.[59b] Such an unprecedented number of reuses made this methodology attractive from an industrial perspective and was licensed by GreenCentre Canada (GCC).[63] In collaboration with our industrial partners, Merck Research Laboratories (Merck & Co.), Chiral Technologies Inc., and Dr. Reddy's Laboratories Ltd., we developed a methodology to immobilize a JosiPhos type ligand by incorporating alt-ROMP. Our procedure consists of three major steps.

Scheme 2.1
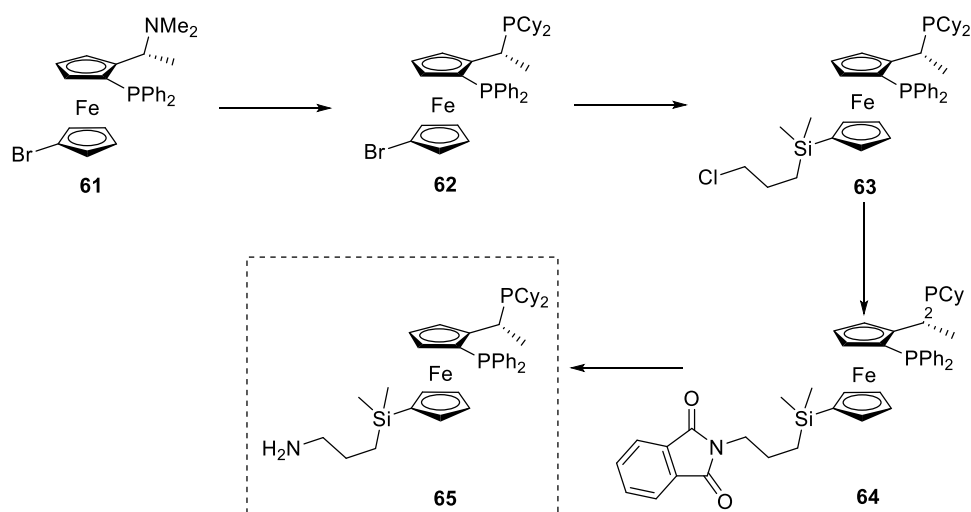
The first step involved functionalization of a JosiPhos type ligand with an amine derivative following a synthesis pathway developed by Togni, Pugin, and co-workers, as shown in Scheme 2.1.[62] We chose this pathway due to the straightforward, high yielding synthetic route and the reliable purification of the intermediate via column chromatography.[62]

Scheme 2.2
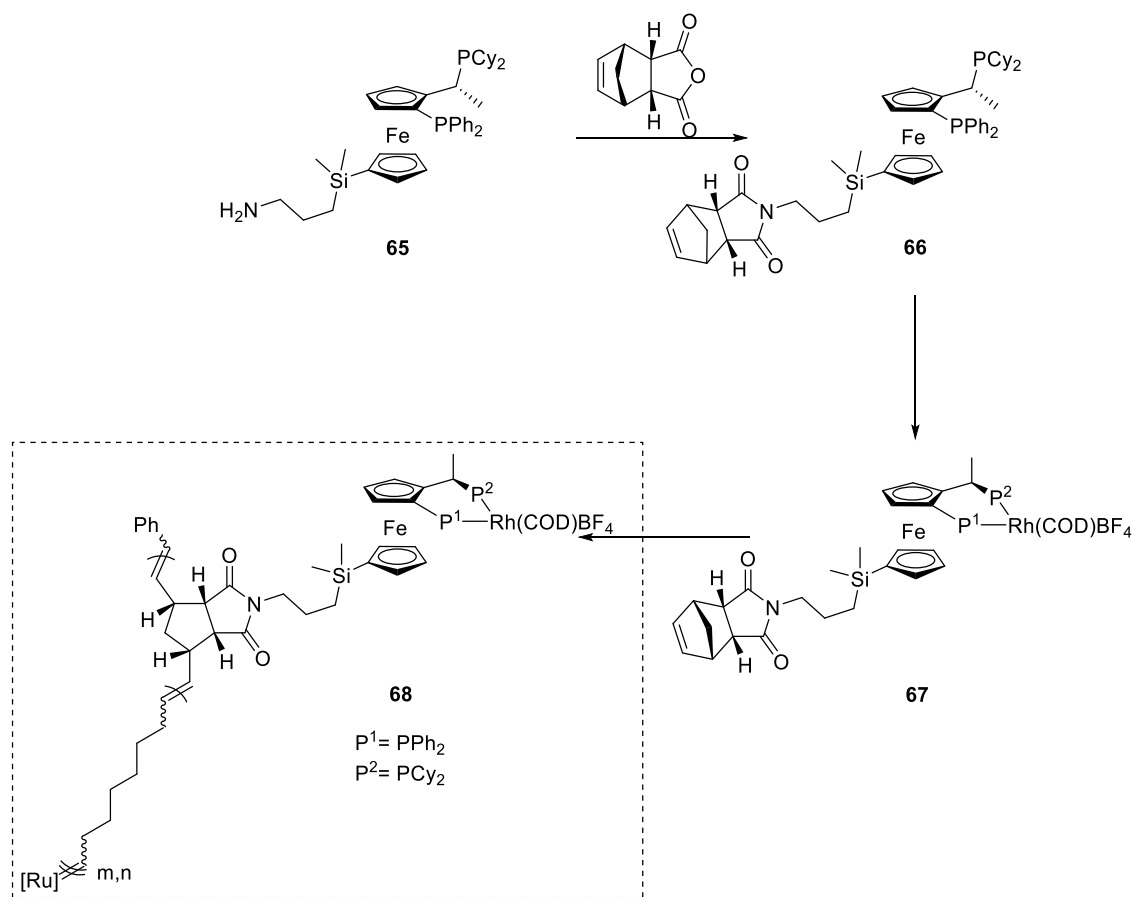
The second step, shown in Scheme 2.2 involved the synthesis of a Rh JosiPhos derivative with an alt-ROMP active group carried out via condensation of the amine **65** with *cis*-5-norbornene-*endo*-2,3-dicarboxylic anhydride, followed by complexation of the diphosphine with the Rh precursor. This cationic Rh JosiPhos derivative was used to synthesize the alt-ROMP polymer.

Finally, in the third step, the obtained alt-ROMP polymer was deposited on the solid support Al_2O_3/PTA. As identified in Chapter 1, use of an anchoring agent (PTA) with alumina was regarded as the best immobilization method compared to other electrostatic based methods because of its superior catalytic performance and minimum leaching; therefore, it

was our solid-support of choice.[46j] Immobilization of a cationic Rh diphosphine using

Al$_2$O$_3$/PTA is also quick, easy and reliable, yet has no significant limitation on the nature of

the ligand.[50] However, it has been determined that the metal leaching can increase

exponentially with solvent polarity.[46j] Further, many systems based on Al$_2$O$_3$/PTA suffer

from long-term stability and loss in selectivity over time.[50, 52, 54] However, the alt-ROMP

polymer contains multiple Rh centres after depositing on Al$_2$O$_3$/PTA, resulting in

immobilization of the whole polymer via numerous Rh-PTA interactions.

Scheme 2.3
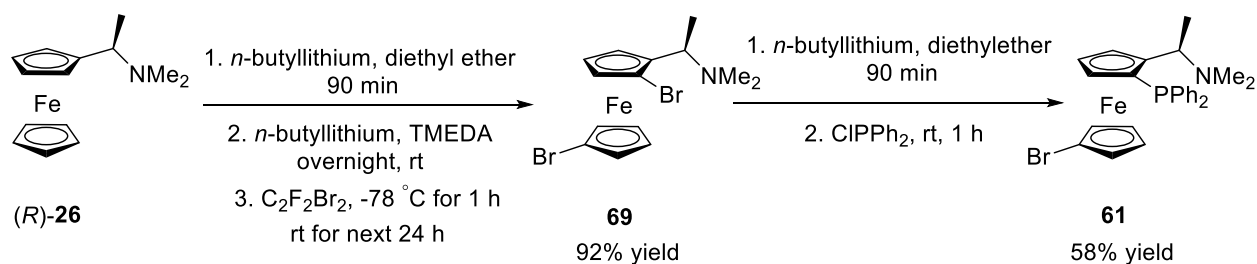
Even though the starting material **61** was supplied by Merck & Co., it is important to

have a precise and efficient way to obtain all the starting reagent for any practical use in

industry. As shown in Scheme 2.3, it can be synthesized readily from the Ugi-amine (*R*)-**26**

in just two steps. The first step involves di-bromination of the Ugi amine (*R*)-**26** via di-

lithiation. Initially, Ugi amine is reacted with *n*-butyllithium to form the diastereoselective

ortho-lithiated intermediate. The next lithiation step is carried out using a stronger

metalating reagent to metalate the other cyclopentadienyl group; *n*-butyllithium in TMEDA

was used due to the absence of directing groups. Next, addition of the brominating reagent

C$_2$F$_2$Br$_2$ led to the final dibrominated species **69** with a yield of 92% after purification via

column chromatography.[62]

The next step in the synthesis incorporates the first phosphine group at the cyclopentadienyl ring via diastereoselective ortho-lithiation at the brominated carbon, followed by reaction with chlorodiphenylphosphine to result in **61**.[62] Any phosphine derivative could be incorporated into the ligand by modifying this step.

2.2 Universal Synthesis of alt-ROMP Active Rh JosiPhos Complex

As identified in the previous Section, an alternative to our starting material **61** bearing any phosphine derivative can be synthesized readily. The first step in our ligand synthesis involved the introduction of the other phosphine group (eq 2.1).

(2.1)
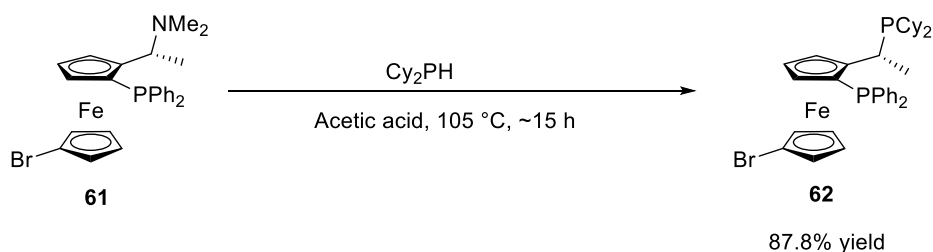
This reaction was carried out by stirring **61** in acetic acid, followed by addition of dicyclohexylphosphine. The substitution of the amine group with dicyclohexylphosphine proceeds with retention of absolute configuration, as described in Chapter 1.[39d] Pure compound bromo-JosiPhos derivative **62** ((R)-1-[(S_p)-2-(diphenylphosphino)-1'-bromoferrocenyl]ethyl-di-cyclohexylphosphine) was obtained with a yield of 88% after purification carried out via column chromatography under nitrogen. This step could be carried out with any derivative of secondary phosphine.
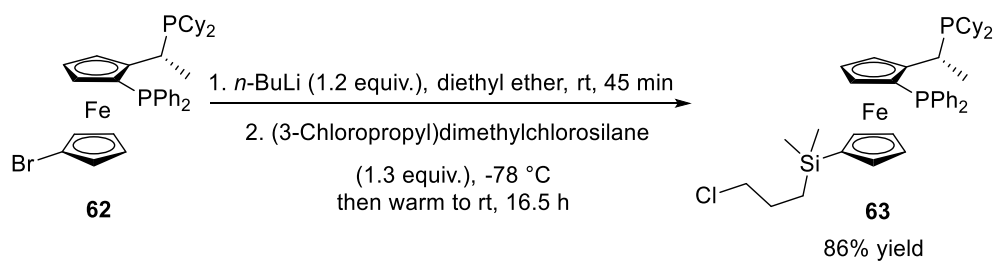
(2.2)

Next, the obtained bromo-JosiPhos derivative **62** was lithiated in situ using *n*-butyllithium via exchange of a bromine group (eq 2.2). This lithiated intermediate was cooled to −78 °C, and 3-chloropropyl dimethylchlorosilane was added slowly over a period of 20 min. The mixture was left to warm slowly to room temperature and stirred overnight. After the workup and purification steps, product **63** was obtained at a yield of 86% (NMR) with by-products proposed to be silyl ether **71** and (R, S_p)-JosiPhos **70**, based on ^{1}H NMR and ^{31}P{^{1}H} NMR analysis (Figure 2.1). The side products most likely were formed via reaction of both the excess chlorosilane and the lithium–ferrocene with water during the workup. This product was used with no further purification as the side-product doesn't interfere with the next reaction step and can be purified further by the followup column chromatography.
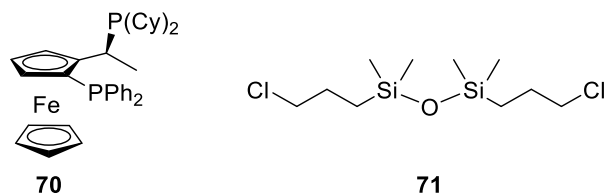
Figure 2.1 *Proposed by-products formed during preparation of (R)-1-[(S$_p$)-2-(Diphenylphosphino)-1'-(dimethyl-3'-phthalimidopropylsilyl)]ethyl-di-cyclohexylphosphine.*

(2.3)

(2.4)
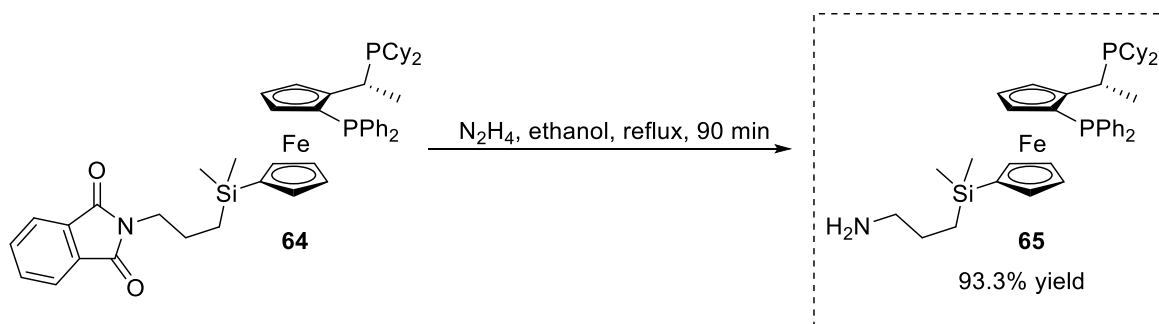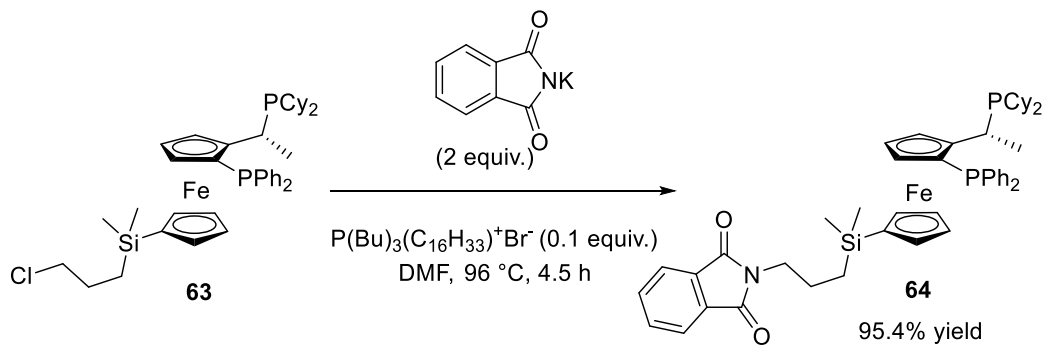
Then, compound **63** was modified with an amine group via a straightforward Gabriel

synthesis (eq 2.3, 2.4). The first step involves the formation of a phthalimido group via a S_N2

reaction using potassium phthalimide as the nucleophile in the presence of a 10% phase

transfer catalyst, hexadecyltributylphosphonium bromide (eq 2.3). This reaction proceeds

via formation of the KCl salt. The phthalimido species **64** was obtained with a yield of 95.4%

after purification via column chromatography. The second step involves liberation of free

amine via reaction of **64** with hydrazine hydrate (eq 2.4). The reaction mixture was refluxed

in ethanol for 90 min and purified via silica-gel column chromatography to yield the final

amine modified JosiPhos derivative **65** with a yield of 93.3%.
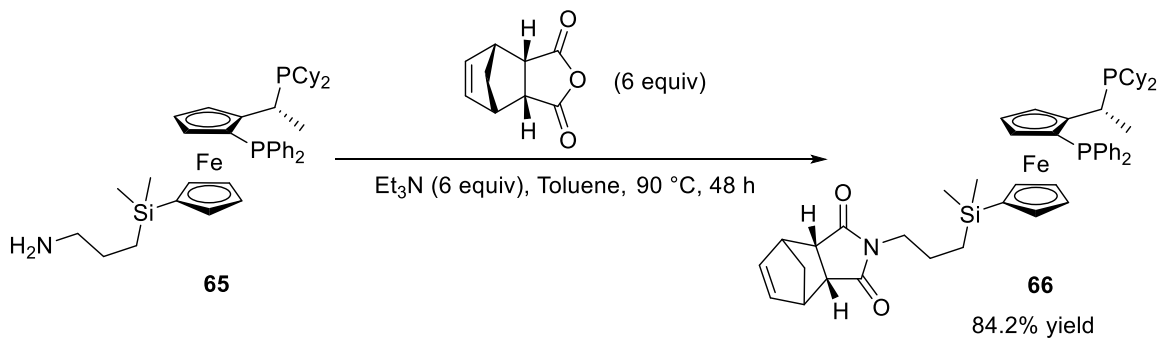
(2.5)

Next, the functionalized JosiPhos derivative **65** was condensed with norbornene *cis*-5-norbornene-*endo*-2,3-dicarboxylic anhydride (eq 2.5). The *exo*-isomers of norbornene imides are known to undergo ROMP without a need for a spacer.[64a] Therefore, we chose the *endo*-isomer to be the alt-ROMP active functional group because it has a relatively much slower propagation during ROMP and, consequently, allows a better control during the polymerization steps.[64b] The reaction was carried out with an excess anhydride to ensure complete reaction of the starting amine to product **66**. The reaction was worked up by washing the mixture with saturated $NaHCO_3$. The aqueous base reacts with the unreacted anhydride to form the maleic acid salt, which was removed via liquid–liquid extraction using water and toluene. The resulting orange solid was purified further using column chromatography to obtain the product **66** as an orange powder with a yield of 84.2%. Incorporation of the norimido group was obvious in the ^{1}H NMR. The strained olefin of the norimido backbone appeared at 6.00 ppm as a singlet (Figure 2.2) since the two olefinic protons are equivalent due to free rotation of the norimido group along the N–C bond. The remaining protons are assigned as well.
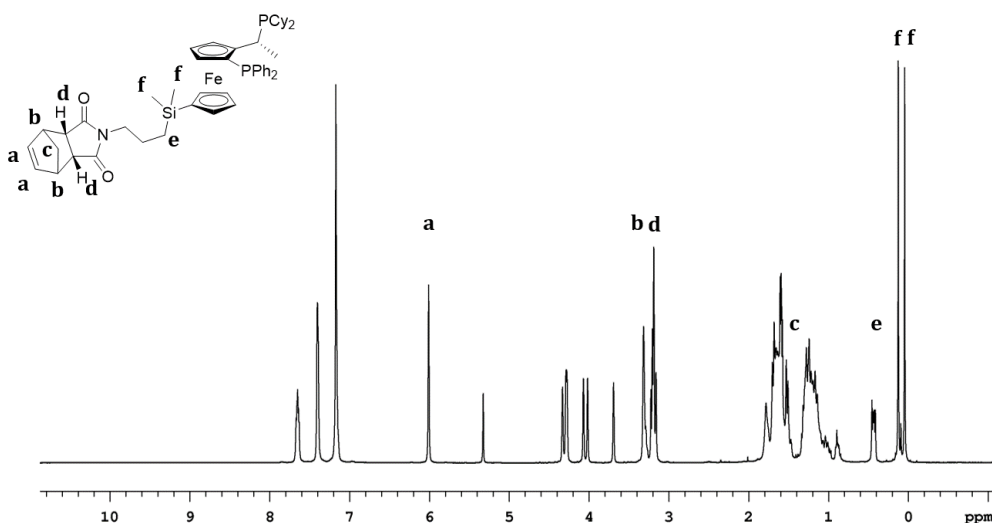
Figure 2.2 ^1H NMR spectrum of alt-ROMP active JosiPhos derivative **66** (399.975 MHz, CD$_2$Cl$_2$, 27.0 °C).

The $^{31}P\{^1H\}$ NMR consist of two doublets, one at 15.6 ppm, corresponding to the PCy$_2$ group, and the other peak at −26.3 ppm, corresponding to PPh$_2$ (Figure 2.3). This chemical shift is very similar to the starting amine **65,** suggesting that functionalization of the bottom cyclopentadienyl ring has no significant effect on the electronic environment of the phosphines. The product was characterized further via ^{13}C NMR, HRMS, and elemental analysis.

The complexation of the alt-ROMP active JosiPhos derivative was carried out using [Rh(COD)$_2$]BF$_4$ precursor (eq 2.6). The complexation took place with ease by simply stirring the precursors at rt in CH$_2$Cl$_2$ for 1 h. The crude was purified by dissolving in minimum CH$_2$Cl$_2$, followed by slow precipitation using ether. The resulting complex was obtained with a yield of 92% as a reddish-orange powder.
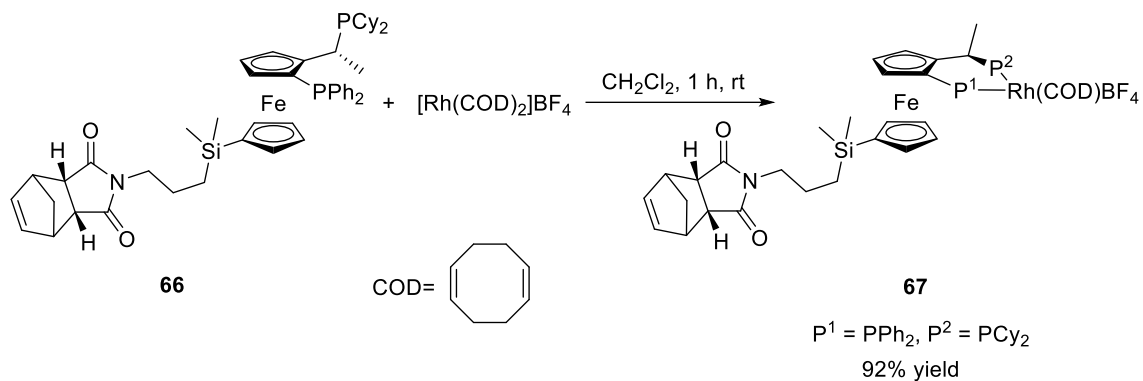
(2.6)

The $^{31}P\{^1H\}$ NMR consisted of two sets of doublets of doublets (Figure 2.3). This is because of coupling of the phosphines with each other and with Rh, which has a nuclear spin value of $I = \frac{1}{2}$. The complexation leads to a downfield shift in the phosphine signals. Peaks appeared at 52.8 ppm and 20.7 ppm, assigned to the PCy$_2$ and PPh$_2$ groups, respectively.
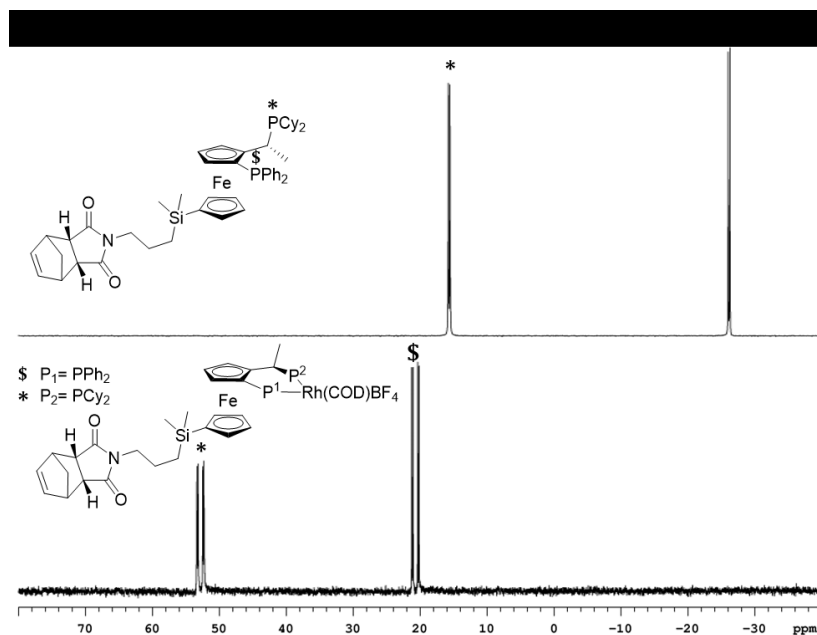
Figure 2.3 ^{31}P NMR before and after complexation of alt-ROMP active JosiPhos derivative **66** (Top: 161.839 MHz, CD$_2$Cl$_2$, 27.0 °C; Bottom: 161.914 MHz, CD$_2$Cl$_2$, 27.0 °C).
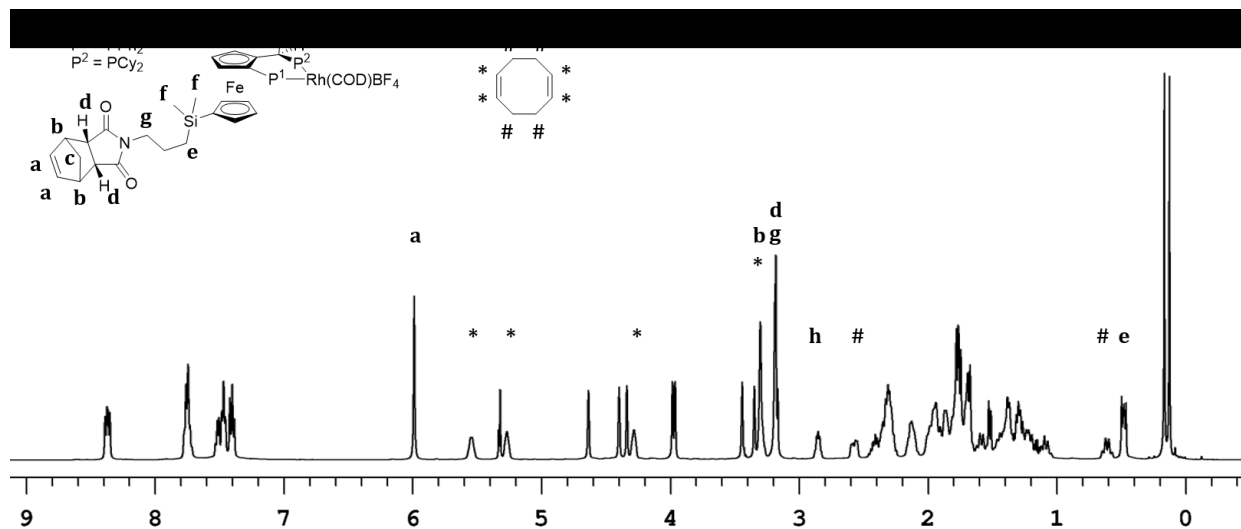
Figure 2.4 *¹H NMR of alt-ROMP Rh JosiPhos derivative **67** (499.807 MHz, CD₂Cl₂, 27.0 °C).*

In comparison to the free ligand, there was no notable change in the complex's norimido group proton signals, and this change in phosphines seems to have no effect on the chemical environment of the polymerization site (Figure 2.4). Upon complexation, the aromatic groups bonded to phosphine shifted downfield. The signals for COD were identified as well. The product was characterized further via ^{13}C NMR, HRMS, and elemental analysis.

This high yielding and versatile synthesis allows for the modification of the two phosphine groups, therefore, it is a universal route to any alt-ROMP active JosiPhos derivatives. One of us had demonstrated previously the versatility of this synthesis by changing the PCy₂ phosphine group to *tert*-butyl phosphine on the gram scale as well. The next section will discuss the polymerization of this obtained monomer **67**.

2.3 Alt-ROMP of Rh JosiPhos Derivative

Scheme 2.4
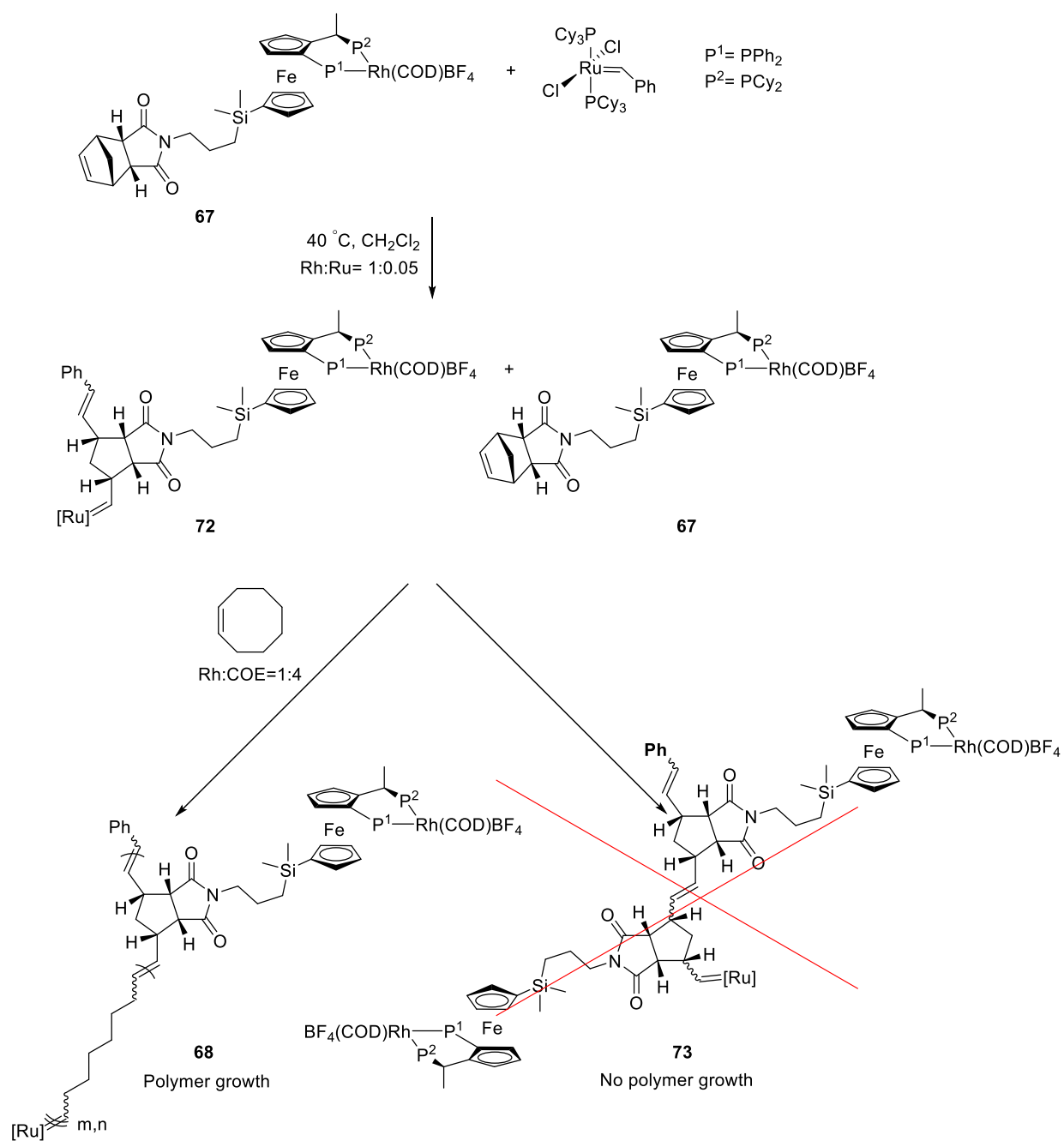
As shown in Scheme 2.4, the cationic alt-ROMP active Rh JosiPhos derivative **67** underwent

alt-ROMP easily with COE and RuCl$_2$(=CHPh)(PCy$_3$)$_2$ (COE:Rh:Ru = 4:1:0.05, 40 °C, 17 h,

CH₂Cl₂) to form the organic catalyst framework **68**. To confirm that the polymerization proceeds via an alternation ROMP of COE and monomer **67**, we carried out a test polymerization with just **68**. Even though this reaction was heated at 40 °C for 40.4 h, we observed no consumption of the norimido group via NMR. We believe that the alkylidyne intermediate **72** that formed after the reaction of the metathesis catalyst and monomer is sterically crowded. Therefore, the intermediate would prefer to react with a less crowded COE, leading to insertion of the C8 spacer. This relieves the steric hindrance of the alkylidyne intermediate and allows it to attack another norimido group. After 40.4 h, we added 4 equivalents of COE to the unreacted polymerization mixture containing just the monomer and Grubbs; as expected, polymerization did proceed further.
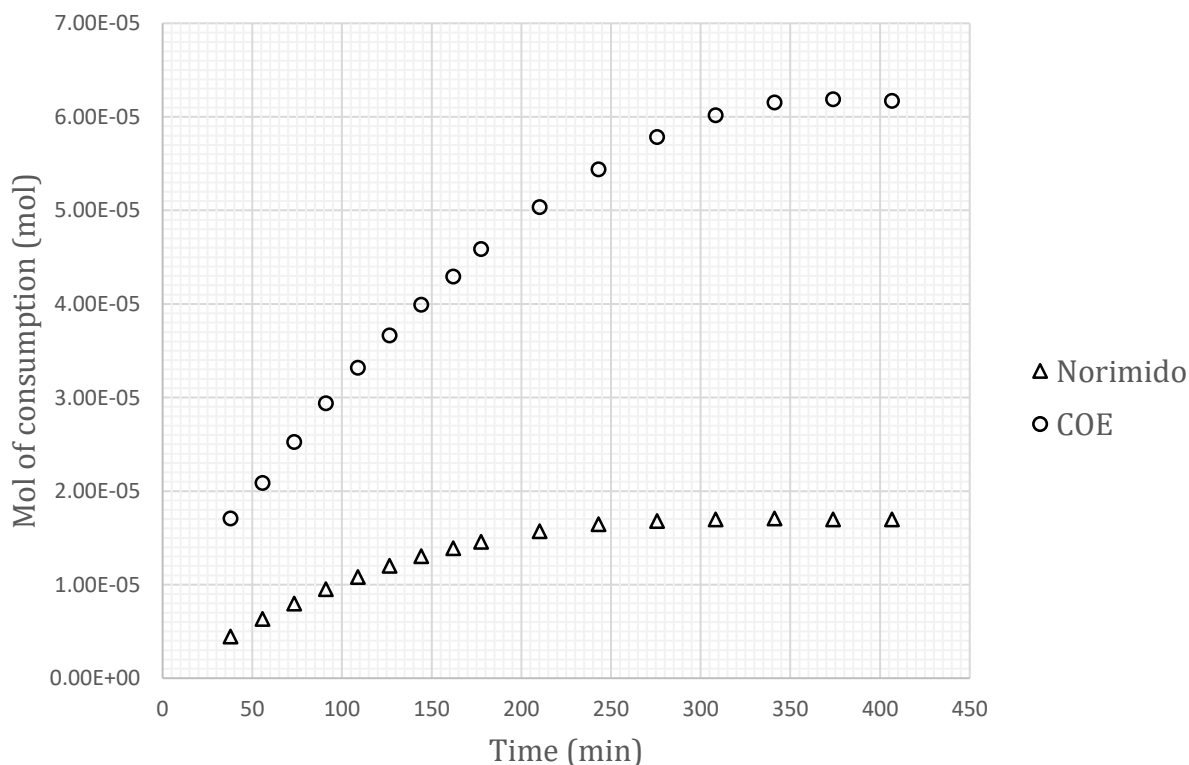
Figure 2.5 *Plot of consumption of COE and norimido backbone vs time for alternating ROMP.*

Next, we carried out a NMR study to determine the distribution of Rh diphosphine in the polymer chain. The monomer **67** and metathesis catalyst were mixed at room temperature and chilled in an ice-bath. Four equivalents of COE were added to the NMR tube and warmed to 40 °C in the NMR probe, and consumption of COE and the norimido backbone was monitored. During the first 177 min of reaction, ~85% of the monomer was consumed. The consumption of COE and the norimido group (Figure 2.5) shows a linear relationship with time, and r^2 was determined to be 0.998 and 0.981, respectively. This suggests an even distribution of COE spacer and Rh diphosphine in the polymer framework, which is crucial for mass transport during hydrogenation. The rate of consumption was calculated from the slope of the linear regression line using the first 177 min data points. The ratio of the rate of consumption of COE and monomer was used to determine the alternation ratio, 1:2.9. We previously reported that the alternation of Ru−BINAP and COE happens in a 1:1 ratio[59b] and, with a bulkier Rh−BINAP dimer, at a slightly higher ratio of 1.7:1.[59c] The alternation of **67** is much higher than that of the other reported polymers. More C8 spacer reacted to relieve the steric crowding for alternation, suggesting a much more crowded alkylidene, possibly due to the bulky ferrocene backbone in the monomer.
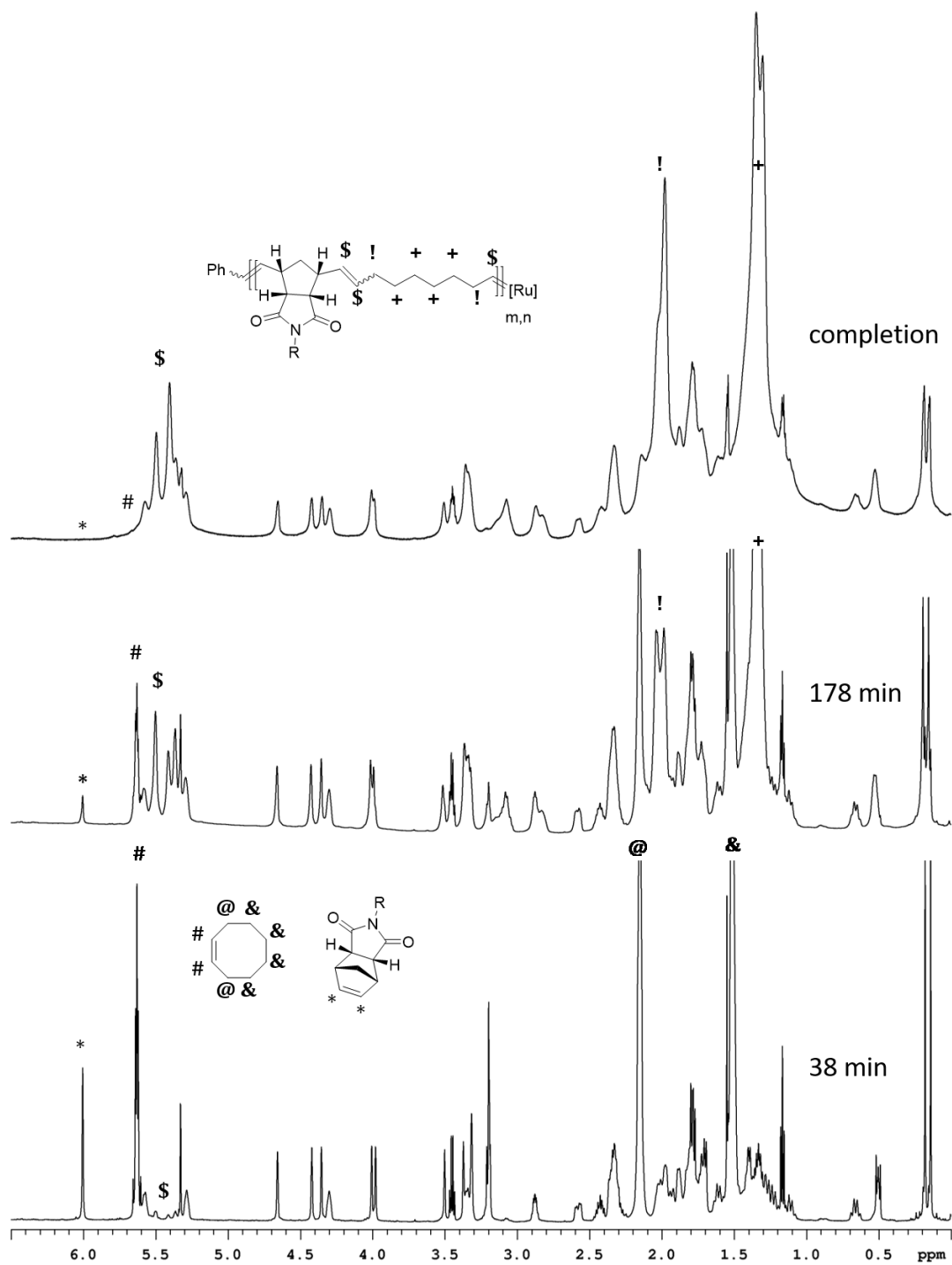
Figure 2.6 *^{1}H NMR spectra of alt-ROMP between the cationic Rh JosiPhos derivative **67** and 1,4-cis-cyclooctene at different time intervals. (599.927 MHz, CD$_2$Cl$_2$, 27.0 °C).*
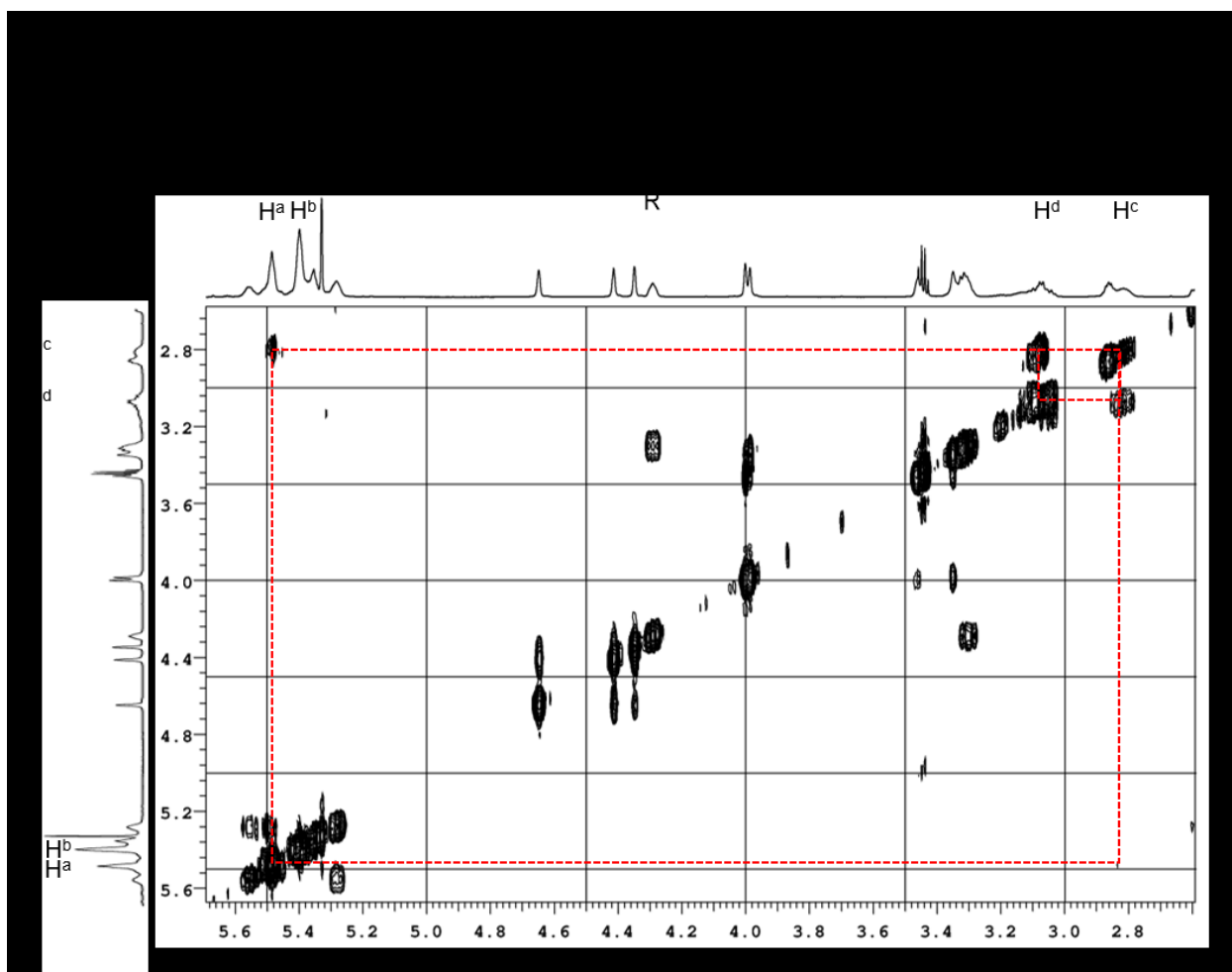
Figure 2.7 *2D-COSY NMR of the alt-ROMP polymer of Rh JosiPhos derivative.*

Upon alt-ROMP, the norimido proton signal disappeared (Figure 2.6). The peak at 2.8 ppm was assigned to H^c, which correlated to the alkene signals in the 2D-COSY experiment (Figure 2.7). The peak at 3.1 ppm was assigned to H^d, the neighboring proton to H^a. The remaining two protons corresponding to the CH_2 group in the cyclopentane were identified in the alkyl region. Protons H^c and H^d both are expected to be *cis* because the chiral centres corresponding to these protons are unaffected by alt-ROMP.

In the alkene region, three sets of signals were observed. However, only the first signal within the 5.53–5.44 ppm region correlated to the cyclopentane backbone protons. Furthermore, the integration of this region is close to the expected value of 3.9, therefore, it was assigned to H^a. Interestingly, both alkene protons resulting from alt-ROMP of the norimido group overlap. The end of the polymer consisted primarily of a poly-cyclooctene chain, as evident from the kinetic study. The formation of the poly-cyclooctene resulted in the growth of the peak in the 5.44–5.37 ppm region. By comparison to the NMR of poly-cyclooctene[64c] and further analysis, the peaks in the 5.44–5.34 ppm region were assigned to poly-cyclooctene related alkenes H^b. The stereochemistry of the alkenes is tedious to predict due to the overlap of peaks as well as the inability to distinguish the coupling constant due to broadening of the peaks. The alkene protons were also correlated to the protons of the alkyl chains. The set of protons adjacent to the alkene were assigned to the downfield alkyl region signal at ∼ 2.0 ppm, and the remaining CH_2 protons of the alkyl region were assigned to the peak at 1.2–1.5 ppm. All signals corresponding to COD remained unchanged and were unaffected by the polymerization (Figure 2.6). It was concluded that the hydrogenation catalyst active sites were undisturbed during polymerization as the ^{31}P NMR showed no shift in the signal before and after polymerization (Figure 2.8).
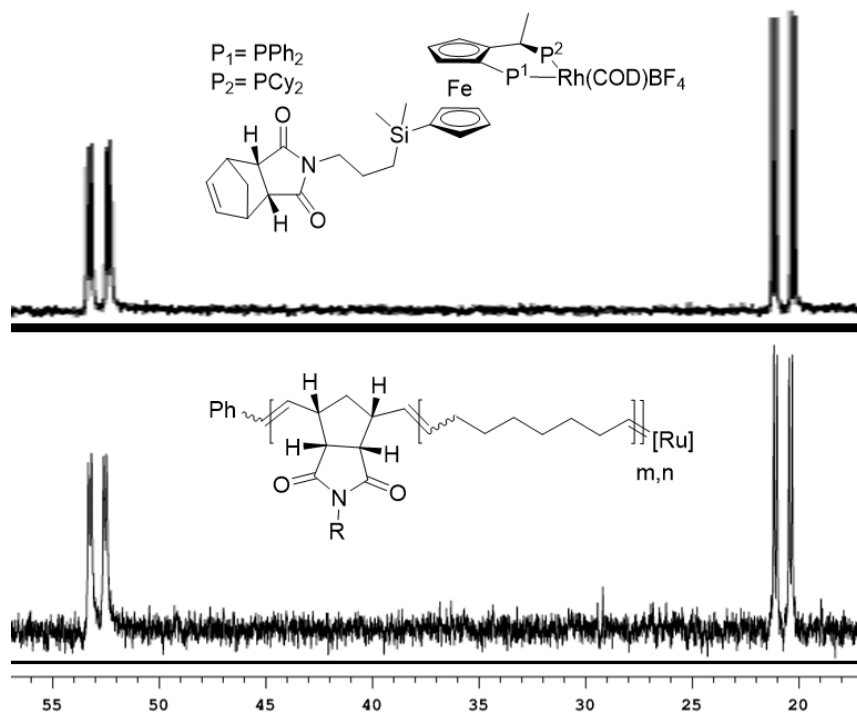
Figure 2.8 *³¹P{¹H} NMR spectra before and after alt-ROMP of the Rh JosiPhos derivative (Top: 161.914 MHz, CD₂Cl₂, 27.0 °C; Bottom: 201.641 MHz, CD₂Cl₂, 27.0 °C).*

Next, the resulting polymer needed to be deposited on a high surface area solid support to aid in mechanical stability and mass transport during catalysis. We used Augustine's well-known procedure to deposit the polymer on Al₂O₃/PTA for reasons previously discussed.[50] To our knowledge, this is the first example where an asymmetric hydrogenation catalyst incorporated into a polymer via alt-ROMP is held on the solid support via multiple electrostatic interactions. We believe that these numerous electrostatic interactions result in a stronger immobilization than the one with a single Rh centre and PTA. The resulting alt-ROMP polymer solution was diluted in CH₂Cl₂ and transferred into a rapidly stirring slurry of Al₂O₃/PTA in CH₂Cl₂. The deposition was rapid, as indicated by the loss of color in the liquor. The filtered liquor was analyzed by ³¹P and ¹H NMR and showed no

indication of any Rh diphosphine signal. The XPS spectra of Al_2O_3/PTA were recorded before and after the deposition of the Rh polymer. Figure 29A shows the Rh $3d_{5/2}$ and $3d_{3/2}$ peaks in the XPS spectrum. Figure 2.10 shows the shows the deconvoluted peaks that occur at 308.2 eV and 312.7 eV binding energies. Polzonetti and co-workers studied the oxidation of Wilkinson's catalyst, $RhCl(PPh_3)_3$, using XPS. They reported that the $3d_{5/2}$ and $3d_{3/2}$ signals for this Rh(I) compound occur at 308.0 eV and 312.7 eV.[65a] Upon oxidation to Rh(III), the binding energy for Rh $3d_{5/2}$ shifts upwards to 309.7 eV.[65a] In another example, Serp and co-workers studied carbon nanotube supported $[Rh(diphosphine)COD]BF_4$ with XPS. Rh $3d_{5/2}$ signal for these Rh(I) compounds ranged from 308.5 eV to 309.1 eV.[65b] Based upon these peak positions, we are confident that the Rh(I) centres in the polymer were not oxidized during the deposition.
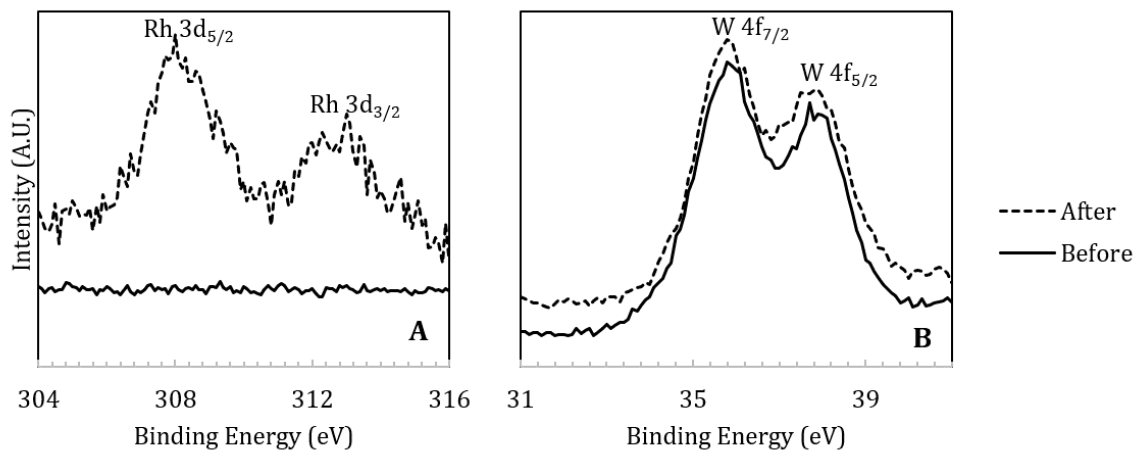
Figure 2.9 *The XPS spectra of the Al_2O_3/PTA before and after the deposition with Rh JosiPhos*

alt-ROMP polymer.
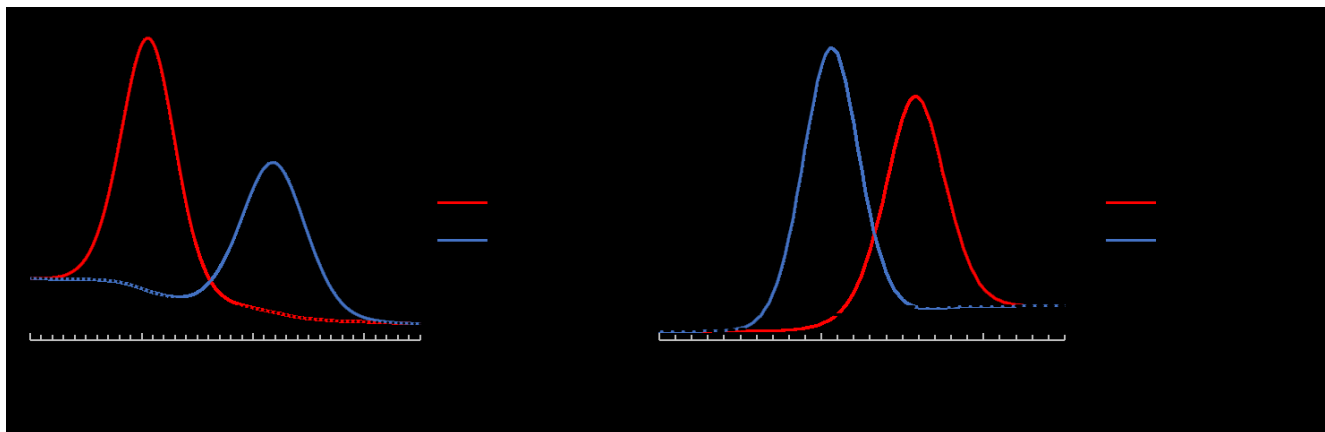
Figure 2.10 *Deconvolution of Rh and W signals for Rh JosiPhos alt-ROMP polymer deposited on Al$_2$O$_3$/PTA.*

Figure 29B shows the W 4f$_{7/2}$ and 4f$_{5/2}$ peaks in the XPS spectra measured before and after the polymer deposition. Figure 2.10 shows the deconvoluted peaks. The W 4f$_{7/2}$ and 4f$_{5/2}$ signals occurred at 35.8 eV and 37.9 eV binding energies, corresponding to W(VI) species.[65c]

2.4 Catalytic Performance Evaluation

Methyl-(Z)-α-acetamidocinnamate (MAC)

We decided to evaluate the catalytic performance of the obtained Al_2O_3/PTA deposited polymeric Rh JosiPhos derivative for the asymmetric hydrogenation using the standard substrate MAC. The reaction was carried out in methanol using 1 mol % heterogeneous catalyst at 2 bar H_2, rt, and 4 h (eq 2.7). The heterogeneous catalyst gave 100% conversion (100 TON, 25 h^{-1} average TOF) with 48% *ee*.

(2.7)
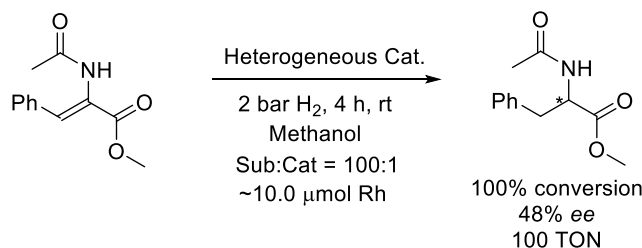
The reaction was run much longer to ensure complete conversion and does not reflect the absolute TOF of the catalyst. Nonetheless, the excellent conversion encouraged us to pursue improving the selectivity of the catalyst, which was surprisingly lower than the value reported by Togni (96% *ee*). The synthetic modification on the JosiPhos ligand seemed to have no effect on the chemical environment of the phosphine group and was unlikely to affect the selectivity. To test this, we decided to carry out a homogeneous hydrogenation using Rh complex **67** containing the alt-ROMP active JosiPhos derivative. The reaction was carried out at 35 °C and 2 bar H_2 using a much higher ratio of MAC:Rh at 500:1. The reaction went to completion in 3 h with 93% *ee*, which corresponds to 500 TON and an average of ~167 h^{-1}

TOF (eq 2.8). The catalytic performance is comparable to the literature, therefore, we concluded that the lower selectivity of the heterogenized catalyst must be due to the support itself.

(2.8)
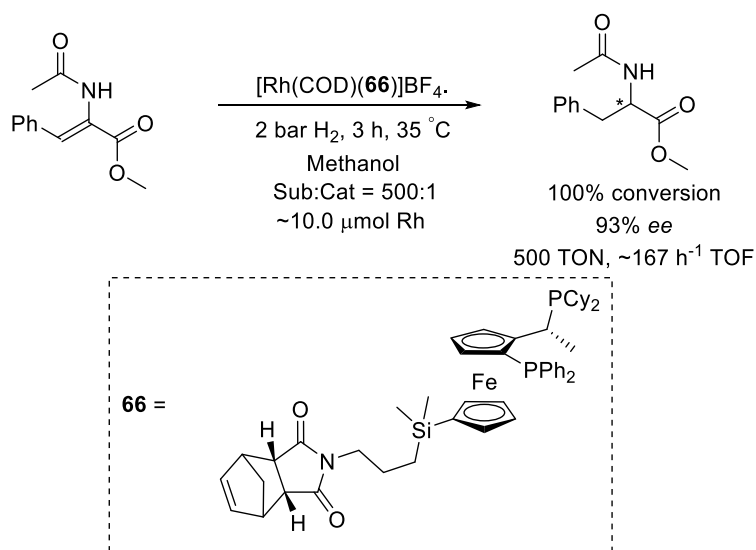
The effect of the reaction parameter on the selectivity of the catalyst is a tedious process to predict or model. As discussed in Chapter 1, the selectivity of the catalyst under Curtin-Hammett conditions is determined by the difference in the Gibbs free energy of the different diastereomeric transition states. However, the transition state free energy itself is intricate to model. In order to predict it accurately, the interaction of the catalyst with solvent needs to be considered. This is because the transition state under solvation conditions is significantly different from that of just isolated models. Solvent properties, such as polarity, hydrogen-bond donating ability (acidity), hydrogen-bond accepting ability (basicity), solubility, or direct bonding ability with the metal, add a further complexity to the system.[66] Therefore, we decided to carry out solvent screening in an effort to improve the selectivity

of MAC hydrogenation. The reaction was carried out in various solvents using 1 mol %

heterogeneous catalyst at 2 bar H_2, rt, and 4 h (eq 2.9).
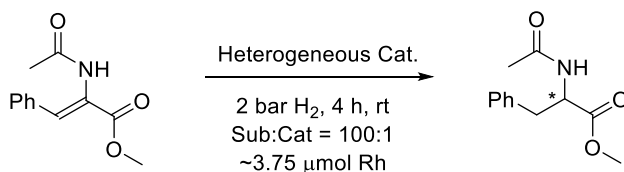
(2.9)

Table 2.1 *Results for solvent screening for asymmetric hydrogenation of MAC using Al_2O_3/PTA*

deposited polymeric Rh JosiPhos derivative

Label[a]	Solvent	Conversion[b]	% ee[c]
A	Toluene	74	21
B	Tetrahydrofuran	100	85
C	Ethyl Acetate	100	61
D	Acetone	100	87
E	Ethanol	100	56
F	Methylene Chloride	100	82
G	Tertbutyl methyl ether	85	32
H	Methanol	100	48

[a]Hydrogenation carried out at 2 bar H_2, rt, and 4 h. [b]Conversion determined via ^{1}H NMR. [c]*Ee* determined using shift reagent europium tris[3-(trifluoromethylhydroxymethylene)-(+)-camphorate].

The low solubility of MAC in toluene and tertbutyl methyl ether could be the reason

behind the poor catalytic performance (Table 2.1). Otherwise, the reaction went to

completion with the remaining solvents. The catalyst gave 56% *ee* with ethanol as solvent,

which was slightly higher in comparison to methanol (48% *ee*). Ethyl acetate gave a lower selectivity as well as 61% *ee.* However, moderate *ee* was obtained in CH_2Cl_2 and tetrahydrofuran at 81% and 85%, respectively. Acetone turned out to be the best solvent in our screenings with 87% *ee*, however, still lower than the homogeneous analog. Remarkably, we were able to improve the selectivity from 48% to 87% with just the solvent change from methanol to acetone. However, much better selectivity and activity were obtained in the initial testing of another model substrate, DMI (dimethyl itaconate). Therefore, we decided to pursue the further development of the catalyst for reusability using DMI instead.

Dimethyl itaconate (DMI)

The most significant evaluation of a heterogeneous catalyst is its reusability. To test this, we proceeded with DMI as the substrate following Togni's conditions. The reaction was carried out in methanol and room temperature with a slightly elevated pressure of 75 psig. The reaction was set up in a glass bomb loaded with the heterogeneous catalyst (Figure 2.11). The transparent reaction vessel allowed us to maneuver the filtration process and the reaction volume. DMI dissolved in methanol (Rh:DMI = 1:500) was added to the glass bomb, and the reaction was stirred at 1200 rpm for 4 h (eq 2.10).
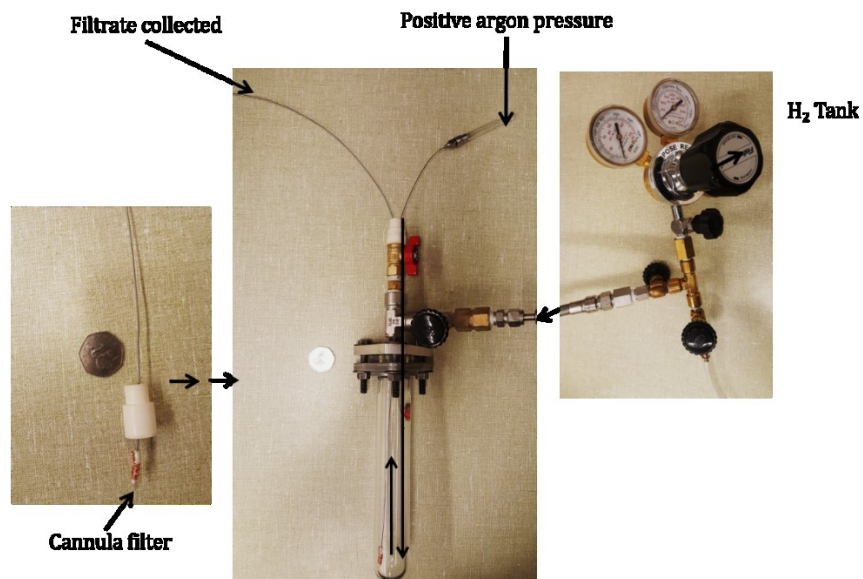
Figure 2.11 _Hydrogenation apparatus and filtration setup using the Al$_2$O$_3$/PTA deposited polymeric Rh JosiPhos derivative._

At the end of the run, the catalyst was left to settle, and the liquor was filtered to the 1.0 mL mark under Ar. This was carried out using a cannula filter and a positive argon pressure, ensuring that the catalyst always remained submerged in either DMI solution or the hydrogenation product during the filtration process. This could protect the active catalyst and allows one to control the volume of the reaction better. Next, another 500 equivalents of DMI methanol solution were added, and the reaction were continued.

Heterogeneous Cat.

6 bar, H$_2$, methanol, rt, 4 h

Sub:Cat = 500:1

100% conversion

95–87% ee, 5000 TON
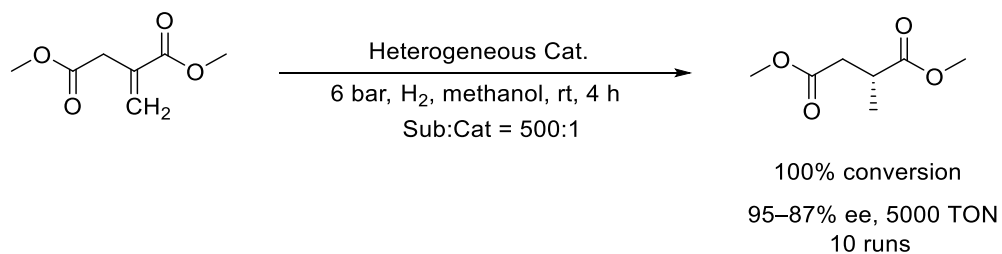
10 runs

(2.10)
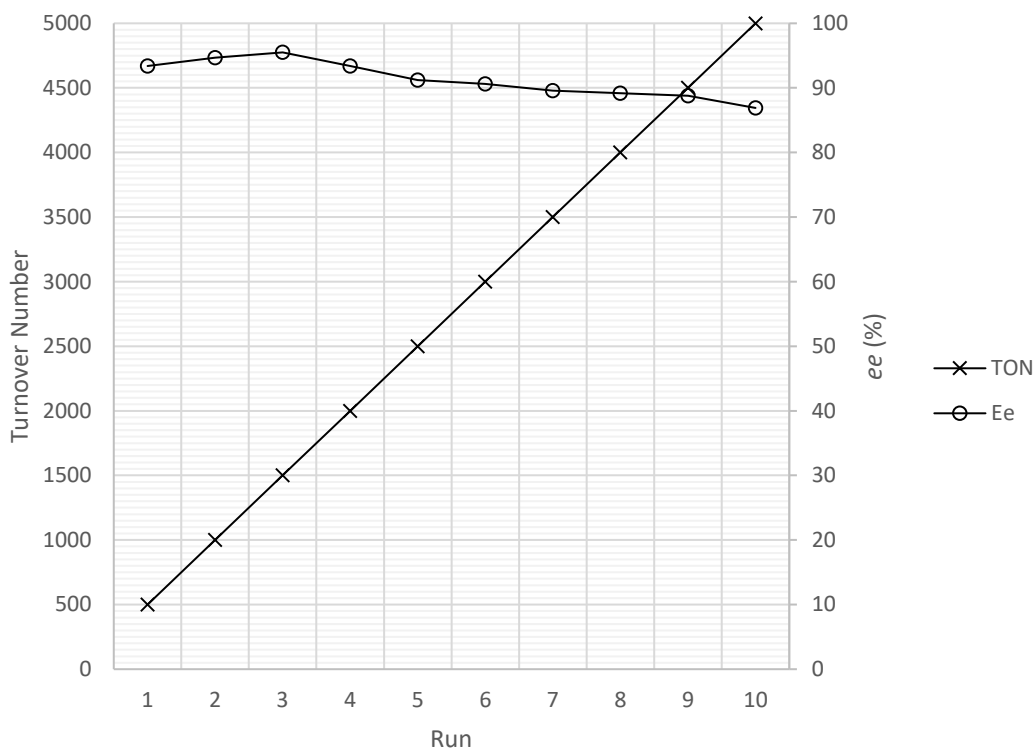
Figure 2.12 *TON and ee during hydrogenation of DMI using the deposited Rh JosiPhos catalyst in methanol, Rh:DMI = 1:500.*

The catalyst showed excellent activity and *ee* for 10 runs with a total of 5000 TON, 100% conversion, and 95−87% *ee* (Figure 2.12). The reaction mixtures froms run 1, 5, and 10 were analyzed further for Rh and W leaching using ICP-MS. Augustine and co-workers had reported a breakdown of Rh−PTA as a complex from Al_2O_3 before.[50c] Because W also was observed in the filtrate, we believe that the Rh leaching occurred as a result of the breakdown of PTA from Al_2O_3, and the Rh−PTA interaction was still intact. Nevertheless, the Rh leaching values obtained were trivial (Table 2.2), in the 0.04−0.16 ppm range. We have, therefore, succeeded in developing a method to immobilize any derivative of a Rh JosiPhos based

catalyst. We have used it for asymmetric hydrogenation with excellent reusability while maintaining excellent catalytic performance.

Table 2.2: *Rhodium and Tungsten content in the filtered liquor from batch hydrogenation of DMI*

Run[a]	Rh content (ppm)	W content (ppm)	Mol ratio of W:Rh
1	0.11	1.0	9.3
5	0.04	1.5	33
10	0.16	2.3	14

[a]Leaching was determined using ICP-MS.

Next, we carried out several test hydrogenations to gain insight into the catalyst stability and the slight drop in enantioselectivity. In the first test, hydrogenation of DMI was set up at room temperature using the same conditions as before (eq 2.10). However, an aliquot obtained after 1.5 h showed that the reaction had gone to completion with 93% *ee.* Next, the catalyst was stirred at 40 °C under 75 psig H_2 for 2 extra hours. A new run set after filtration went to 84% completion in 2 h with only 87% *ee.* The storage conditions between the runs played a crucial role in the stability and the selectivity of the catalyst.

During the 1980s, Halpern and co-workers carried out an extensive study on the hydrogenation of alkene using a Rh diphosphine catalyst. It is accepted widely that the active catalyst generated is a highly reactive [Rh(diphosphine)(solvent)$_2$]anion.[29-31] During the resting period, the catalyst is still in the product solution, which contains dimethyl methyl

succinate that coordinates to the Rh centre via two C=O groups. However, this 7-membered metallocycle is not as stable, and elimination of the product would result in the highly reactive disolvento species (Figure 2.13).
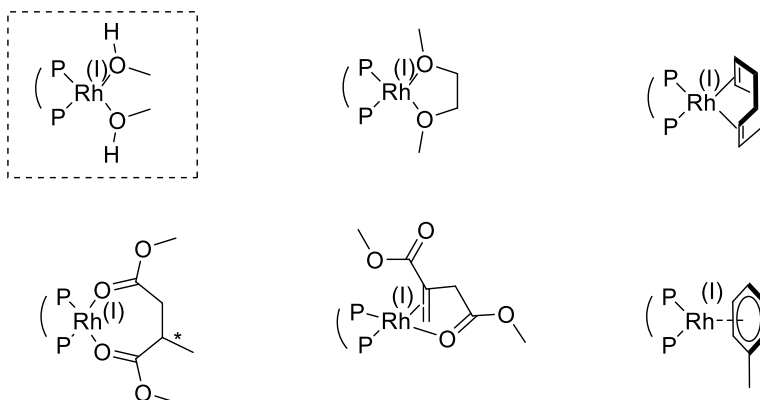
Figure 2.13 *Coordination of Rh diphosphine species with various solvents and substrates.*

Next, we decided to carry out the hydrogenation with high substrate loading and stopped it before going to completion in an effort to stabilize the active catalyst via DMI coordination better. Hydrogenation was carried out using a higher Rh:DMI ratio of 1:1000, 75 psig H_2, rt, for 1h (eq 2.11) so that most of the runs did not go to completion, and the catalyst was always under the presence of some unreacted substrate. We expected DMI to stabilize the active catalyst better than the hydrogenated product by forming a much more stable 5-membered metallocycle by coordinating via the alkene and C=O group (Figure 2.13). The selectivity of the catalyst under these conditions remained stable, with an *ee* range of 94–95% over 7 runs (Figure 2.14). Therefore, the presence of a stabilizing solvent or additives during storage could improve the stability of the catalyst; this was our next logical step.
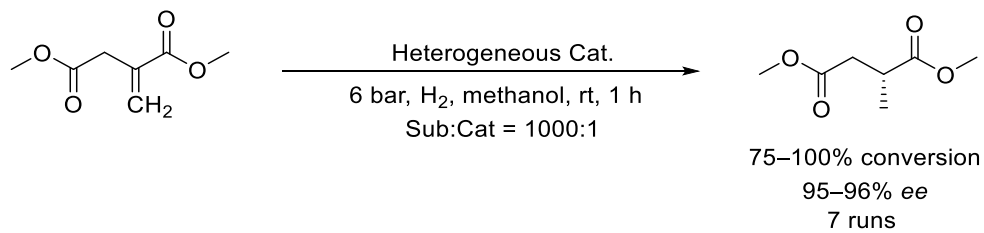
(2.11)
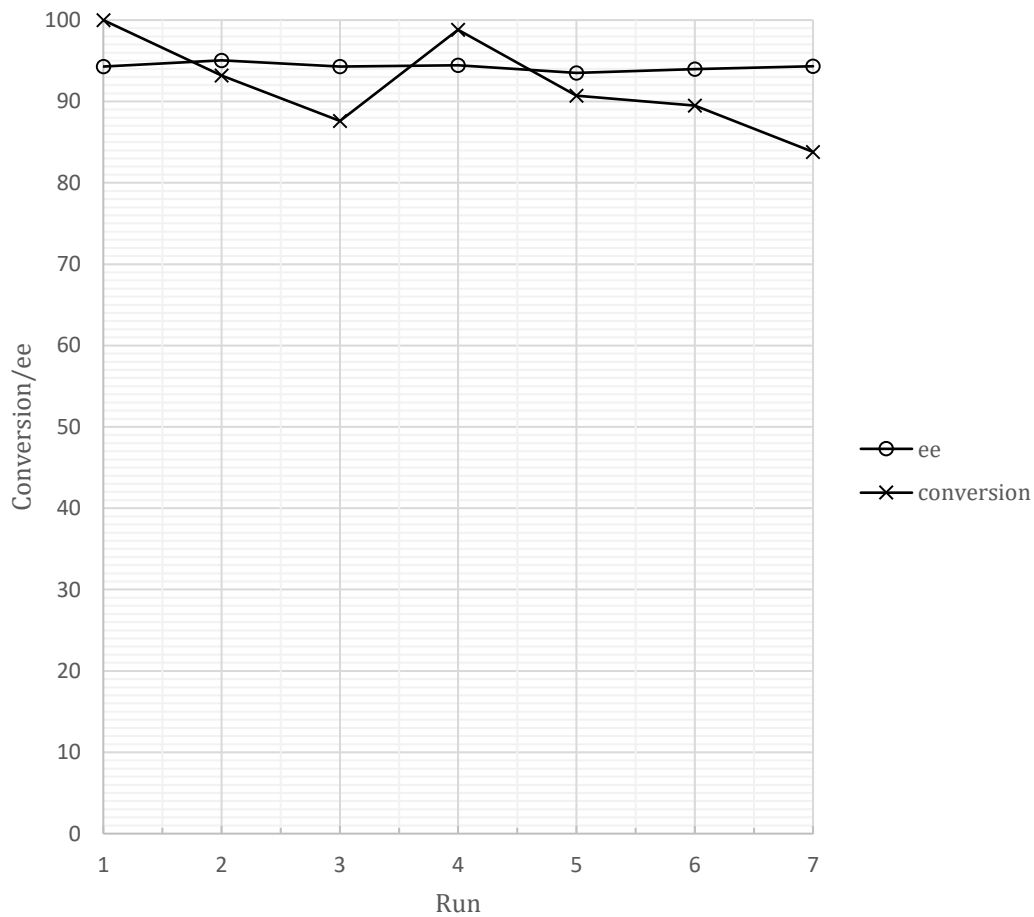
Figure 2.14 *Conversion and ee during batch hydrogenation of DMI using the deposited Rh*

JosiPhos catalyst in methanol, Rh:DMI = 1:1000.

Heterogeneous Cat.

6 bar, H₂, toluene, rt — 6 bar, H_2, toluene, rt

Sub:Cat = 500:1
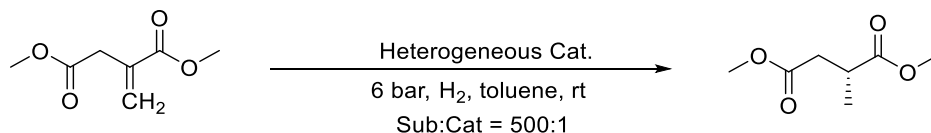
Run	Time	Conversion	*ee*
1	4 h	71%	93.0%
2	4 h	40%	91.7%
3	11h	56%	88.0%
4	24 h	19%	81.6%

(2.12)

Aryl rings can coordinate to [Rh(diphosphine)(solvent)$_2$]anion forming stable species and, in some cases, they even deactivate the catalytic cycle. For example, toluene can form the complex [Rh((S,S)-Me-DuPHOS)(η^6-toluene)]BF$_4$ (Me-DuPhos = 1,2-bis(2,5-methyl-phospholanyl)benzene).[32] Our next experiment involved a simple solvent change to toluene using the same conditions as before (eq 2.12). The first run went to 71% conversion with 93% *ee*, and the hydrogenation was much slower than in methanol. By run 4, which was carried out for 24 h, there was only 19% conversion and 82% *ee*. The rapid deactivation of the catalyst was a result of an η^6 coordination of toluene to the Rh diphosphine; however, the drop in selectivity was still unclear.

Heterogeneous Cat.

6 bar, H_2, acetone, rt, 2 h

Sub:Cat = 500:1

100% conversion

96–83% *ee*

5 runs
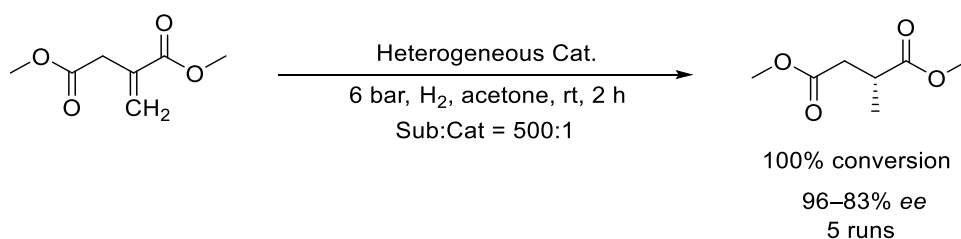
(2.13)

In another experiment, we tested acetone as the solvent. Hydrogenation was set at a Rh:DMI ratio of 1:500, 75 psig H_2, rt, for 2 h (eq 2.13). The reaction went to completion for the first five runs. However, a drastic, unexplained *ee* drop was observed between run 4 and

5 (90 % to 87% *ee*). The run was stopped after that due to a drop in both activity and *ee* (Figure 2.15).
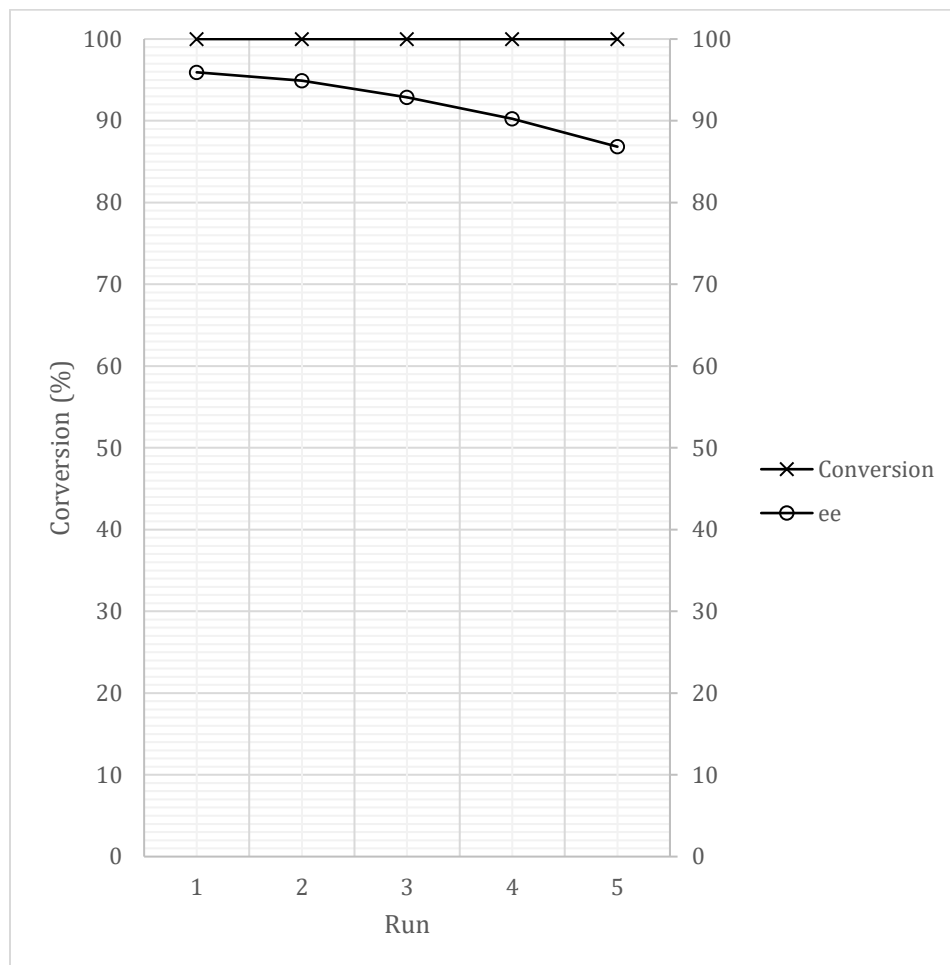
Figure 2.15 *TON and ee during hydrogenation of DMI using the deposited Rh JosiPhos catalyst in acetone, Rh:DMI = 1:500.*
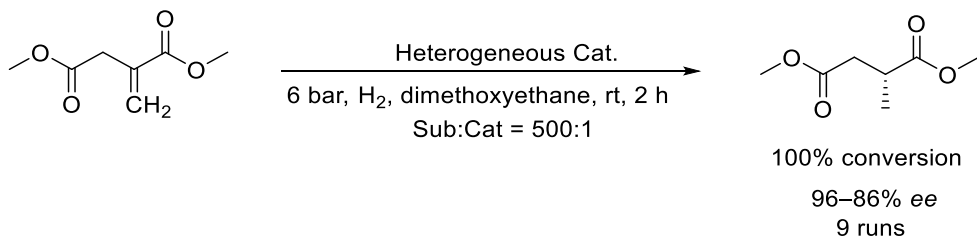
(2.14)
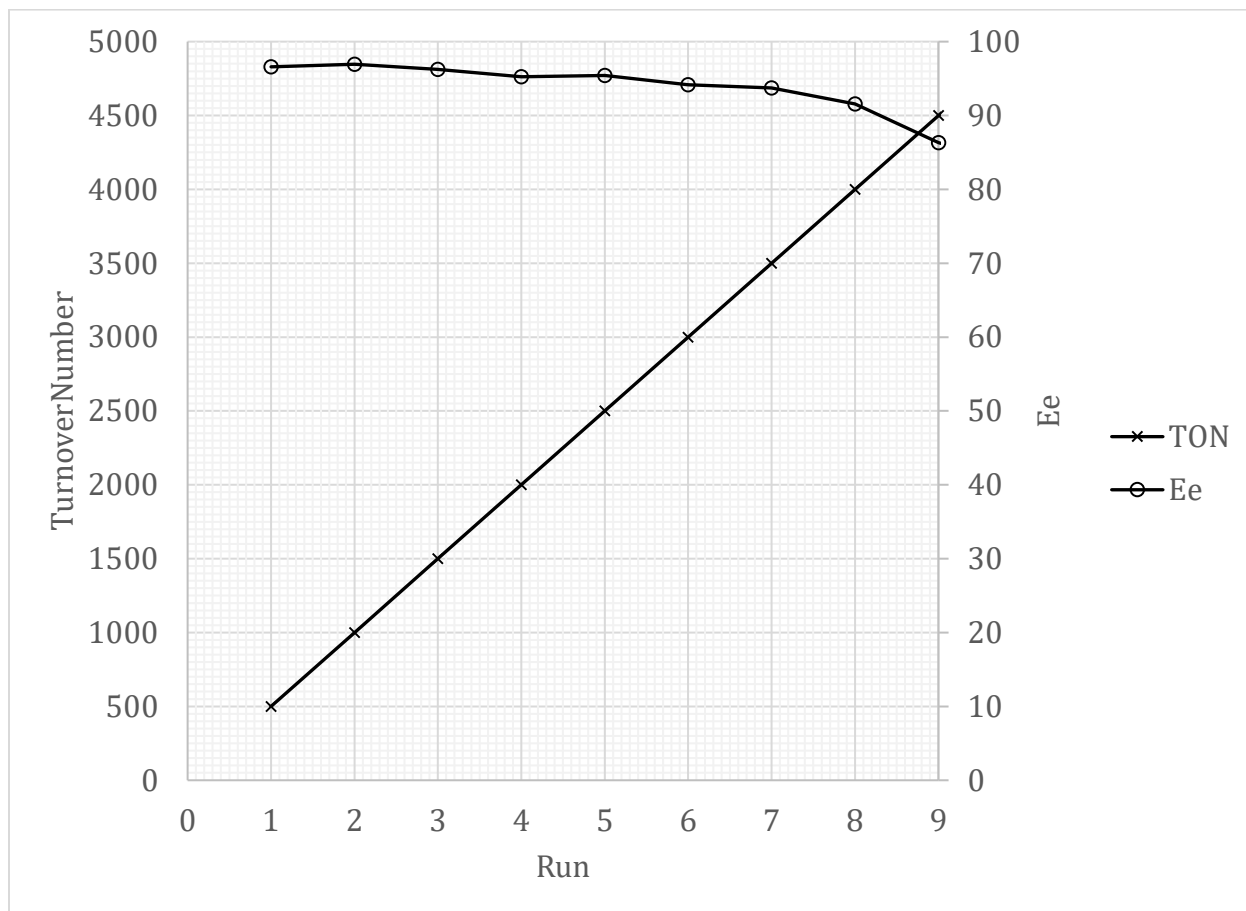
Figure 2.16 *TON and ee during batch hydrogenation of DMI using the depostied Rh JosiPhos*

catalyst in dimethoxyethane, Rh:DMI = 1:500.

Dimethoxyethane was used next as the solvent as it can coordinate to Rh via two

oxygens and form a stable 5-membered metallocycle. Hydrogenation was set at a Rh:DMI

ratio of 1:500, 75 psig H_2, rt, for 2 h (eq 2.14). The reaction showed excellent activity, giving

100% conversion over 11 runs. Until run 7, the *ee* of the reaction was above 94%. In comparison to methanol, dimethoxymethane as a solvent gave a better selectivity in the initial runs. However, there was a massive drop in *ee* from run 8 at 91% to 86% by run 9 (Figure 2.16).

Next, in collaboration with the Dr.Reddys laboratories, hydrogenation was performed by monitoring the H_2 uptake, which allowed us to take down the reaction right after completion. This was very important to our system in order to minimize the resting period during reuses. The reaction was carried out at with Rh:DMI at 1:500, 75 psig H_2, and 40 °C. The slightly higher temperature improved the activity and selectivity and allowed faster conversion, which was necessary in order to be able to carry out the most number of runs before storing the catalyst overnight.

Six runs were performed before storing the catalyst, and the *ee* ranged between 93.3% to 90.9% (Figure 2.17). This drop in the half-life of the reaction correlates with the continuous deactivation of the catalyst over the reuses. In another experiment, 20 equivalents of COD were added during the overnight storage; this didn't help. We concluded that the catalyst changes over this period to form a species that still hydrogenates DMI, but at a lower selectivity. Also, there is slow deactivation of the catalyst over this period. The literature points to this drop in *ee* with the Al_2O_3/PTA immobilized catalyst as a common issue, and no clear explanation exists.[50, 52, 54] Further mechanistic studies need to be carried out to study the effect of supports on the stability of Rh diphosphine.
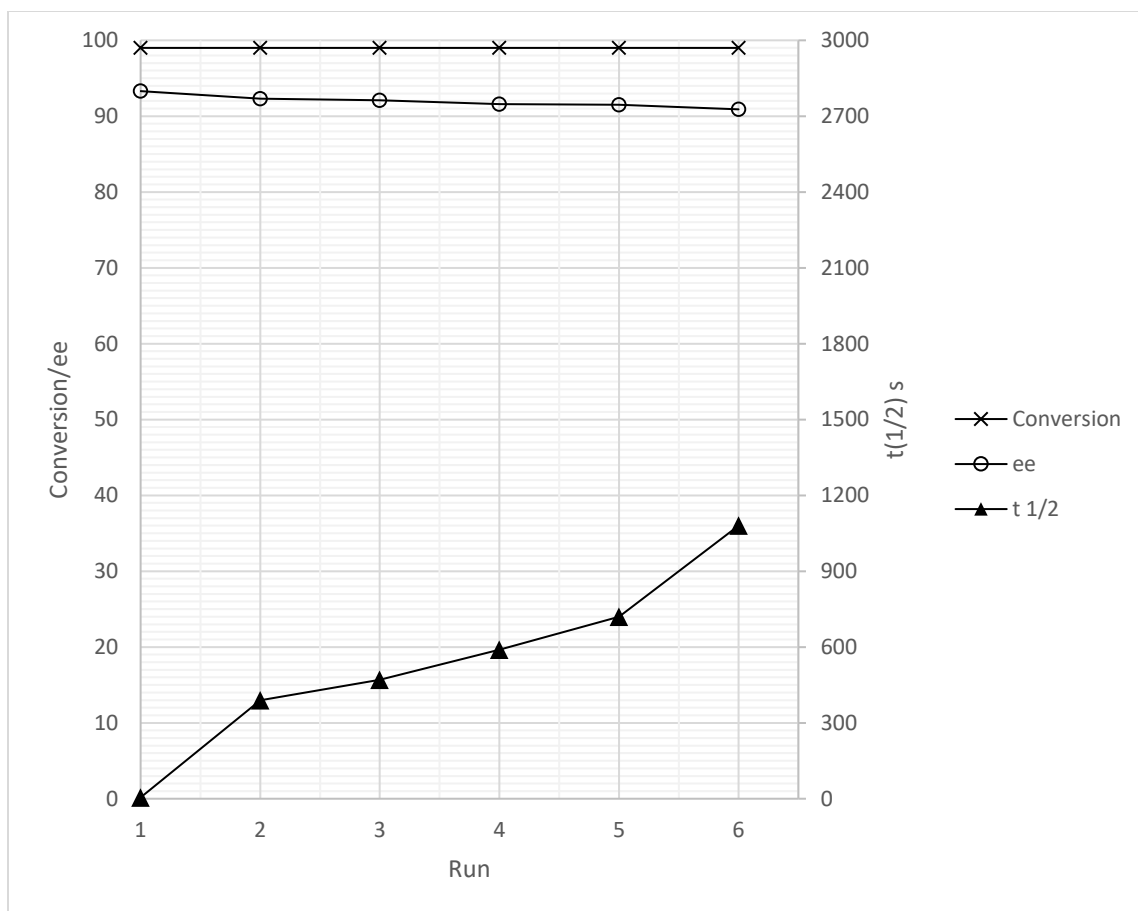
Figure 2.17 *Conversion, ee, and half-life during the batch hydrogenation of DMI using the deposited Rh JosiPhos catalyst in methanol, Rh:DMI = 1:500.*

Experimental:

The solvents tetrahydrofuran, ethyl acetate, acetone, methanol, methylene chloride and diethyl ether were purchased as ACS reagent grade, and toluene as HPLC grade from Sigma-Aldrich. Triethylamine and *N,N*-dimethylformamide were purchased from Fischer Chemicals as reagent grade. Anhydrous ethanol, hexanes (ACS reagent), glacial acetic acid, and tertbutyl methyl ether (extra pure) were purchased from Commercial Alcohols, Caledon Laboratories, Ananchemia, and Acros Organics, respectively. The solvents diethyl ether (Na/benzophenone), chloroform (CaH$_2$), methylene chloride (CaH$_2$), methanol (magnesium methoxide), toluene (CaH$_2$), triethylamine (CaH$_2$), dimethylformamide (CaH$_2$), ethanol (magnesium ethoxide), and acetone (3Å molecular sieves), ethyl acetate (CaH$_2$), tertbutyl methyl ether (CaH$_2$), tetrahydrofuran(Na/benzophenone), and hexanes (Na) were dried by distillation from the appropriate drying agent under N$_2$.. N$_2$ was bubbled through all solvents for a minimum of 40 min before use.

(*R*)- 1-[(*S*$_p$) -2-(diphenylphosphino)-1'-bromoferrocenyl]ethyl-dimethylamine **61** was provided by GCC. Other particular reagents, such as dicyclohexylphosphine (98%), *n*-butyllithium solution (2.50 M in hexanes), hexadecyltributylphosphonium bromide (97%), hydrazine hydrate (50-60%), phthalimide potassium salt (98%), *cis*-5-norbornene-*endo*-2,3-dicarboxylic anhydride (99%), and europium tris[3-(trifluoromethylhydroxymethylene)-(+)-camphorate] were all obtained from Sigma-Aldrich and used without further purification. (3-Chloropropyl)dimethylchlorosilane (>95%) and phosphotungstic acid were purchased from Fluka Chemika and Fischer Scientific, respectively, and used without further purification.

Dichloro(benzylidene)bis(tricyclohexylphosphine)ruthenium(II) (Grubbs' Catalyst) was purchased from Strem Chemicals. Bis(1,5-cyclooctadiene)rhodium(I) tetrafluoroborate was purchased from Strem Chemicals and purified further by recrystallization in dichloromethane and hexanes. *Cis*-cyclooctene (95%) was purchased from Sigma-Aldrich and purified via fractional distillation. α-Acetamidocinnamic acid (98%) was purchased from Sigma-Aldrich and used to synthesize methyl-(*Z*)-α-acetamidocinnamate ester following a literature esterification procedure using Diazald®.[67] Dimethyl itaconate (99%) was purchased from Sigma-Aldrich and purified by triple distillation under reduced pressure. Neutral, gamma, activated aluminum oxide, 60 mesh was purchased from Strem chemicals. Flash Chromatography was performed on silica gel (240−400 mesh). Florisil adsorbent, 60−100 mesh was purchased from Fischer Chemicals. Nitrogen (4.8pp), H_2 (4.4pp or 5.0pp), and Ar (4.8pp) gas tanks were purchased from PRAXAIR. Elemental Analysis data were acquired with a Carlo Erba EA1108 Elemental Analyzer. HRMS spectra were acquired using electrospray ionization in an Agilent 6220 ao TOF mass spectrometer. ICP-MS for Rh and W leaching was carried out by the Canadian Centre for Isotopic Microanalysis (CCIM). The ^{1}H NMR and ^{31}P NMR spectra were acquired using Agilent/Varian Inova 400 MHz, 500 MHz, Agilent/Varian VNMRS 600 MHz, Agilent VNMRS 700 MHz, and Varian DD2 M2 400 MHz NMR spectrometers. The ^{13}C NMR spectra were acquired using a Varian VNMRS 500 MHz and Agilent VNMRS 700 MHz NMR spectrometers. The chemical shifts are reported in ppm relative to TMS with the solvent as the internal standard. Abbreviations used in reporting of NMR data are s (singlet), d (doublet), t (triplet), q (quartet), dd (doublet of doublet), dq (doublet of quartet), m (multiplet), and J (coupling constant in Hz). The GC-MS analysis was performed by using a Hewlett Packard 5890 chromatograph equipped with a 5970B mass

selective detector and Supelco Beta DEX 225 capillary column (30 m × 0.25 mm × 0.25 μm film thickness). The sample was prepared in methanol at 0.5mg/ml, and 1.0 μL was injected in to GC-MS via 1.0 μL syringe. All the *ee*'s were confirmed by comparing the retention times and mass spectra to authentic samples.

*Synthesis of (R)-1-[(S$_P$)-2-(Diphenylphosphino)-1'-(dimethyl-3'-aminopropylsilyl)-ferrocenyl]ethyldicyclohexylphosphine using Togni's procedure **

*Note: Togni's procedure was used to prepare (*R*)-1-[(*Sp*)-2-(diphenylphosphino)-1'-(dimethyl-3'-aminopropylsilyl)-ferrocenyl]ethyldicyclohexylphosphine.[62] The NMR of the intermediates were compared to the literature and used without further purification.[62] All procedures were carried out using appropriate Schlenk techniques under an inert atmosphere. Purification steps, such as liquid–liquid extraction, filtration, recrystallization, column chromatography, etc. were all carried out under an inert atmosphere. During chromatography, the column was purged with N_2 for a minimum of 1 h. All solvents were distilled using an appropriate drying agent and degassed by bubbling nitrogen for a minimum of 40 min prior to use.

Synthesis of (R)- 1-[(S$_P$) -2-(diphenylphosphino)-1'-bromoferrocenyl]ethyl-di-cyclohexylphosphine (62).

JosiPhos precursor **61** (5.5040g, 10.580 mmol) was weighed out in a 250 mL side-arm round-bottom flask containing a 1" stir bar inside the glovebox. The solid was dissolved in 45.0 mL of acetic acid delivered via a 10.0 mL gas-tight syringe to obtain a homogeneous orange solution. $HPCy_2$ (2.63 g, 13.3 mmol) was added into the reaction flask slowly using a

5.0 mL syringe. The reaction was stirred overnight at 105 °C in a reflux apparatus for ~15 h. Next, the reaction mixture was cooled to room temperature, and acetic acid was removed using high vacuum. The resulting brown oil was treated with 25 mL of saturated $NaHCO_3$, and 30 mL of ether was added and stirred thoroughly. The organic layer was cannula transferred into a separate 250 mL side-arm round-bottom flask, and the aqueous layer was washed with ether (3 X 30 mL) and combined into the previous organic layer. The organic layer was washed further with (3 X 30 mL) water and stirred in $MgSO_4$ for 20 min. Then, the organic layer was filtered into a separate 250 mL side-arm round-bottom flask and dried using high vacuum yielding a crude orange oil (7.324 g). Next, 1.91 g of the resulting crude were chromatographed (33.1 g of SiO_2, hexanes: diethyl ether = 20:1, 2% NEt_3) to yield **62** as an orange oil (1.62 g, 87.8% yield).

^{1}H NMR: (498.118 MHz, $CDCl_3$, 27.0 °C): δ 7.71−7.68 (m, 2H, Ph−H), 7.40−7.42 (m, 3H, Ph−H), 7.71−7.25 (m, 5H, Ph−H), 3.54−4.40 (m, 7H, Cp), 3.32 (dq, $^3J_{HH}$ = 7.47 Hz, $^2J_{PH}$ = 3.0 Hz, 1H, C*H*MeP), 1.79−0.90 (m, 25H, PCy and CH*Me*P).

^{13}C{^{1}H} APT NMR: (125.688 MHz, $CDCl_3$, 27.0 °C): δ 141.1 (d, J = 7.5 Hz, 1C, PPh), 139.5 (d, J = 2.5 Hz, 1C, PPh), 135.9−127.1 (s, 10C, PPh), 103.6 (dd, J = 27.0, 18.4 Hz, 1C, Cp), 77.9 (s, 1C, Cp), 76.0 (dd, J = 12.6, 2.8 Hz, 1C, Cp), 73.0 (m, 1C, Cp) 72.6−68.5 (s, 5C, Cp), 33.0 (d, J = 21.1 Hz, 1C, PCy), 32.8 (d, J = 21.5 Hz, 1C, PCy), 31.4 (d, J = 23.0 Hz, 1C, PCy), 31.1 (d, J = 16.5 Hz, 1C, PCy), 30.1 (d, J = 6.7 Hz, 1C, PCy), 29.8 (d, J = 9.6 Hz, 1C, PCy), 27.7−27.5 (s, 3C, PCy), 27.4 (d, J = 7.4 Hz, 1C, PCy), 27.1 (d, J = 11.1 Hz, 1C, PCy), 26.6 (d, J = 5.4 Hz, 1C, PCy), 26.1 (dd, J = 23.9, 8.4 Hz, 1C, *C*HMeP), 17.4 (s, 1C, CH_3).

31P{1H} NMR: (201.641 MHz, CDCl$_3$, 27.0 °C): δ 16.1 (d, $^4J_{PP}$ = 35.7 Hz, 1P, PCy), −27.1 (d, $^4J_{PP}$ = 35.7 Hz, 1P, PPh).

Synthesis of (R)-1-[(S$_P$)-2-(Diphenylphosphino)-1'-(dimethyl-3'-chlopropylsilyl)]ethyl-di-cyclohexylphosphine (63).

16.0 mL of diethyl ether were added using a 10.0 mL gas-tight syringe into a 100 mL side-arm round-bottom flask containing precursor **62** (1.62g, 2.41 mmol) and a 1" stir bar. The mixture was stirred for 5 min yielding an orange homogeneous solution. Next, *n*-butyllithium solution (2.50 M in hexanes, 1.15 mL, and 2.89 mmol) was added dropwise over a period of 5 min using a 1.0 mL gas-tight syringe. The resulting mixture was stirred for 45 min at room temperature yielding a dark-red solution, and the flask was cooled to −78 °C using a hexanes/liquid nitrogen bath. Next, (3-chloropropyl)dimethylchlorosilane (0.512 mL, 3.127 mmol) was added slowly over a period of 20 min using a 1.0 mL gas-tight syringe. The solution was warmed slowly to room temperature and stirred overnight for a total of 16.5 h. Then, the solution was treated with 13 mL of water and stirred for 15 min. The organic phase was cannula transferred into another flask, the aqueous phase was washed with diethyl ether (3 X 20 mL), and the organic phases combined. The organic phase was washed further with water (3 X 15 mL) and dried over MgSO$_4$ for 30 min while stirring. Next, the solution was filtered and dried using high vacuum. The crude was chromatographed (33.4 g of SiO$_2$, hexane: ethyl acetate = 20:1) to yield **63** as an orange oil (1.74 g, 86% yield in situ). The NMR was compared to the literature and, even though it showed ~86% purity, it was used for the next step without further purification as the side-products do not interfere with next step.

¹H NMR: (399.794 MHz, CDCl₃, 27.0 °C): δ 7.72–7.64 (m, 2H, Ph–H), 7.36–7.44 (m, 3H, Ph–H), 7.26–7.14 (m, 5H, Ph–H), 4.36 (m, 2H, Cp–H), 4.28 (m, 1H, Cp–H), 4.05 (m, 2H, Cp–H), 3.86 (s, 5H, Cp–H)*, 3.83 (m, 1H, Cp–H), 3.54 (t, $^3J_{HH}$ = 7.2 Hz, 4H, CH₂–Cl)*, 3.44 (t, $^3J_{HH}$ = 6.8 Hz, 2H, CH₂–Cl), 3.25 (m, 1H, Cp–H), 3.24 (dq, $^3J_{HH}$ = 7.2 Hz, $^2J_{PH}$ = 3.6 Hz, 1H, C*H*MeP), 1.83–0.89 (m, 27H, PCy₂, CH₃ and CH₂C*H₂*CH₂), 0.65 (m, 2H, Si–CH₂), 0.17 (s, 3H, Si–CH₃), 0.11 (s, 12H, Si–CH₃)*, 0.09 (s, 3H, Si–CH₃).

¹³C{¹H} APT NMR: (125.688 MHz, CDCl₃, 27.0 °C): δ 141.3 (dd, *J* = 7.2, 0.8 Hz, 1C, Ph), 139.5 (dd, *J* = 9.8, 2.5 Hz, 1C, Ph), 135.9–127.0 (s, 10C, Ph), 102.0 (dd, *J* = 27.0, 18.1 Hz, 1C, Cp), 74.2 (dd, *J* = 11.2, 3.1 Hz, 1C, Cp), 74.1–73.7 (s, 3C, Cp), 73.13 (d, *J* = 1.3 Hz, 1C, Cp), 71.2 (d, *J* = 4.9 Hz, 1C, Cp), 70.4 (s, 1C, Cp), 69.4–69.2 (m, 2C, Cp), 47.9 (s, 2C, Cl–CH₂), 47.9 (s, 2C, Cl–CH₂)*, 33.0 (s, 1C, Cy), 32.7 (s, 1C, Cy), 31.4 (d, *J* = 22.9 Hz, 1C, Cy), 31.0 (d, *J* = 16.2 Hz, 1C, Cy), 30.0 (d, *J* = 6.7 Hz, 1C, Cy), 29.9 (d, *J* = 9.7 Hz, 1C, Cy), 27.7–27.5 (s, 3C, 2 Cy and CH₂*C*H₂CH₂), 27.3 (d, *J* = 7.5 Hz, 1C, Cy), 27.1 (d, *J* = 8.0 Hz, 1C, Cy), 27.1 (s, 1C, Cy), 26.5 (d, *J* = 8.0 Hz, 1C, Cy), 26.3 (d, *J* = 8.8 Hz, 1C, *C*HMeP), 17.6 (s, 1C, CH*Me*P), 15.9 (s, 2C, Si–CH₂)*, 14.6 (s, 1C, Si–CH₂), 0.3 (s, 4C, Si–Me)*, –2.4 (s, 1C, Si–Me), –2.4 (s, 1C, Si–Me).

³¹P{¹H} NMR: (161.839 MHz, CDCl₃, 27.0 °C): δ 16.1 (d, *J* = 33.3 Hz, 1P, PCy), 15.7 (d, *J* = 30.4 Hz, 1P, PCy)*, –25.8 (d, *J* = 29.9 Hz, 1P, PPh)*, –26.2 (d, *J* = 33.3 Hz, 1P, PPh).

*Note: Two side products were proposed from the reaction. The ratio of side products was determined from the NMR integration of Si–Me peaks and ³¹P NMR signals (**3:4:5** = 1:0.14:0.11). The yield was determined as 86% via NMR.

Synthesis of (R)-1-[(S$_P$)-2-(Diphenylphosphino)-1'-(dimethyl-3'-phthalimidopropyl

silyl)]ethyl-di-cyclohexylphosphine (64)

Potassium phthalimide (0.6648 g, 3.517 mmol) and hexadecyltributylphosphonium bromide (0.1816 g, 0.3472 mmol) were weighed out into a 100.0 mL side-arm round-bottom flask containing a 1" stir bar. The flask was degassed using a nitrogen/high vacuum cycle. The product mixture from the previous reaction containing **63** (1.79 mmol) was transferred into the reaction flask using 4.5 mL of DMF delivered via a 5.0 mL gas-tight syringe. An orange solution containing a white suspension was obtained, which was heated to 96 °C for 4.5 h. Next, the reaction mixture was cooled to room temperature, and 36.0 mL of H_2O were added into the flask and stirred for 10 min. The aqueous phase was extracted using toluene (3 X 20 mL), and the combined organic layer was washed further with H_2O (3 X 15 mL). The organic layer was cannula transferred into a degassed flask containing $MgSO_4$ and stirred for 30 min. The organic layer was cannula filtered and the solvent was removed using high vacuum. Next, the crude was passed through a column (36.4 g of SiO_2, hexanes: diethyl ether = 10:1, 1% NEt_3) and collected as one large fraction. A second column chromatography (32.8 g of SiO_2, hexanes: diethyl ether = 5:1, 1% NEt_3) was carried out to obtain **65** as an orange powder (1.65g, 95.4% yield).

¹H NMR: (498.118 MHz, CDCl$_3$, 27.0 °C): δ 7.87−7.82 (m,2H, phthalimide Ar), 7.73−7.69 (m, 2H, phthalimide Ar), 7.69−7.63 (m, 2H, Ph−H), 7.41−7.36 (m, 3H, Ph−H), 7.25−7.15 (m, 5H), 4.33−3.77 (m, 5H, Cp), 3.62 (tr, $^3J_{HH}$ = 7.5 Hz, 2H, NCH$_2$), 3.27−3.20 (m, 2H, CHMeP and Cp),

1.82–0.85 (m, 27H, PCy$_2$, CH$_3$, CH$_2$CH_2CH$_2$), 0.57 (m, 2H, Si–CH$_2$), 0.15 (s, 3H, Si–CH$_3$), 0.07 (s, 3H, Si–CH$_3$).

^{13}C{^{1}H} APT NMR: (125.688 MHz, CDCl$_3$, 27.0 °C): δ 168.4 (s, 2C, C=O),141.4 (d, *J* = 7.5 Hz, 1C, PPh), 139.5 (dd, *J* = 9.8 Hz, 2.26, 1C, PPh), 133.8 (s, 1C, Ar C in C$_6$H$_4$(CO$_2$)), 132.2 (s, 1C, Ar C in C$_6$H$_4$(CO$_2$)), 135.9–127.0 (s, 10C, PPh$_2$), 123.1 (s, 1C, Ar C in C$_6$H$_4$(CO$_2$)), 101.9 (dd, *J* = 27.2, 18.1 Hz, 1C, Cp), 74.2 (s, 1C, Cp), 74.1 (dd, *J* = 11.1, 2.9 Hz, 1C, Cp), 73.7 (s, 1C, Cp), 73.6 (s, 1C, Cp), 73.1 (s, 1C, Cp), 71.2 (d, *J* = 4.9, 1C, Cp), 70.5 (s, 1C, Cp), 69.3–69.2 (m, 2C, Cp), 40.9 (s, 1C, NCH$_2$), 32.9 (d, *J* = 20.9 Hz, 1C, Cy), 32.7 (d, *J* = 20.9 Hz, 1C, Cy), 31.4 (d, *J* = 22.9, 1C, Cy), 31.0 (d, *J* = 16.3, 1C, Cy), 30.0 (d, *J* = 6.8, 1C, Cy), 29.8 (d, *J* = 9.8, 1C, Cy), 27.7 (s, 1C, Cy), 27.3 (d, *J* = 7.5, 1C, Cy), 27.1 (d, *J* = 11.2 Hz, 1C, Cy), 26.9 (s, 1C, *C*HMeP), 26.5 (d, *J* = 7.8 Hz, 1C, Cy), 26.4 (d, *J* = 8.7, 1C, Cy), 23.3 (s, 1C, CH$_2$CH_2CH$_2$), 17.5 (s, 1C, CH*Me*P), 14.0 (s, 1C, Si–CH$_2$), −2.4 (s, 1C, Si–Me), −2.4 (s, 1C, Si–Me).

^{31}P{^{1}H} NMR: (161.839 MHz, CDCl$_3$, 27.0 °C): δ 16.1 (d, $^4J_{PP}$ = 34.1 Hz, 1P, PCy$_2$), −26.1 (d, $^4J_{PP}$ = 34.3 Hz, 1P, PPh$_2$).

Synthesis of (R)-1-[(S$_P$)-2-(Diphenylphosphino)-1'-(dimethyl-3'-aminopropylsilyl)-ferrocenyl]ethyldicyclohexylphosphine (65).

About 20.0 mL of ethanol were cannula transferred into 100.0 mL side-arm round-bottom flask containing ligand **64** (1.65 g, 1.96 mmol) and a 1" stir bar. The flask was stirred to obtain a homogeneous orange solution. Next, 1.15 mL (55% v/v in water solution, 19.6 mmol) of hydrazine hydrate were added via a 1.0 mL gas-tight syringe. The reaction was set for 90 min at 86 °C, and a white precipitation was observed. Cannula filtration was carried

out, the solid was washed with 3 X ~20 mL of ethanol into a 250.0 mL side-arm round-bottom flask, and the solvent was removed under high vacuum yielding an orange oil. The crude was purified further using column chromatography (28.5g of SiO_2, CH_2Cl_2, 5% NEt_3) to obtain **65** as an orange powder (1.30g, 93.3% yield).

^{1}H NMR (399.794 MHz, $CDCl_3$, 27.0 °C): δ 7.64–7.68 (m, 2H, Ph–H), 7.38–7.39 (m, 3H, Ph–H), 7.18–7.24 (m, 5H, Ph–H), 4.33 (m,1H,Cp), 4.26 (m, 1H, Cp), 4.04–4.03 (m, 2H, Cp), 3.80 (m, 1H, Cp), 3.25 (m, 1H, Cp), 3.22 (dd, $^3J_{HH}$ = 7.3 Hz, $^2J_{PH}$ = 3.3 Hz, 1H, C*H*MeP), 2.59 (m, 2H, C*H$_2$*NH$_2$), 1.79–1.02 (m, 27H, P*Cy$_2$*, CH$_2$C*H$_2$*CH$_2$, CH$_3$), 0.50 m, 2H, Si–CH$_2$), 0.15 (s, 3H, Si–Me), 0.06 (s, 3H, Si–Me).

^{31}P{^{1}H} NMR (161.839 MHz, CD_2Cl_2, 26.1 °C): δ 52.2 (s, 1P, Cy$_2$P=O)*, 16.1 (d, $^4J_{PP}$ = 33.3 Hz, 1P, PCy), −26.1 (d, $^4J_{PP}$ = 32.9 Hz, 1P, PPh), −28.0 (s, 1P, PPh)*.

*Note: 2% mono-oxide observed in ^{31}P{^{1}H} NMR

^{13}C{^{1}H} APT NMR: (125.688 MHz, $CDCl_3$, 27.0 °C): δ 141.3 (d, *J* = 6.9 Hz, 1C, PPh), 139.5 (d, *J* = 9.1 Hz, 1C, PPh), 135.9–127.0 (s, 10C, PPh$_2$), 74.1 (s, 1C, Cp), 74.0 (dd, *J* = 10.9, 3.1 Hz, 1C, Cp), 73.7 (s, 1C, Cp), 73.0 (s, 1C, Cp), 71.2 (d, *J* = 5.2 Hz, 1C, Cp), 71.0 (s, 1C, Cp), 69.3 (s, 1C, Cp), 69.3 (s, 1C, Cp), 69.2 (s, 1C, Cy), 45.5 (s, 1C, NCH$_2$), 32.9 (d, *J* =20.7 Hz, 1C, Cy), 32.7 (d, *J* = 20.9 Hz, 1C, Cy), 31.4 (dd, *J* = 22.9, 1.5 Hz, 1C, Cy), 31.0 (dd, *J* = 16.3, 1.6 Hz, 1C, Cy), 30.0 (d, *J* = 6.8 Hz, 1C, Cy), 29.8 (d, *J* = 9.8 Hz, 1C, Cy), 28.3 (s, 1C, CH$_2$*C*H$_2$CH$_2$), 27.7 (s, 1C, Cy), 27.6 (d, *J* = 12.6 Hz, 1C, Cy), 27.5 (s, 1C, Cy), 27.3 (d, *J* = 7.5 Hz, 1C, Cy), 27.1 (d, *J* = 10.8 Hz, 1C, Cy), 26.5 (dd, *J* = 8.2, 0.8 Hz, 1C, *C*HMeP), 17.7 (d, *J* = 2.39 Hz, 1C, CH*Me*P), 13.9 (s, 1C, Si–CH$_2$), −2.3 (s, 1C, Si–Me), −2.4 (s, 1C, Si–Me).

HRMS (ESI) found for [M+H]$^+$: 710.3146, calculated for $C_{41}H_{57}FeNP2Si$ [M+H]$^+$: 710.3159, (diff 1.76 ppm).

Synthesis of (R)-1-[(S$_p$)-2-(Diphenylphosphino)-1'-(dimethyl-3'-N-(cis-5-norbornene-2,3-dicarboximidopropylsilyl)-ferrocenyl]ethyl-di-cyclohexylphosphine (66)

Ligand **65** (1.30 g, 1.83 mmol) was weighed out into a 100.0 mL side-arm round-bottom flask with a 1" stir bar, and 5.0 mL of freshly distilled degassed toluene were added and stirred for 5 min. The solution was cannula transferred into a high-pressure reaction vessel, with an extra 3 X 5.0 mL of toluene used for washing purposes. *Cis*-5-norbornene-*endo*-2,3-dicarboxylic-anhydride (1.819 g, 10.99 mmol) was dissolved in 15.0 mL of toluene and added to the reaction flask, and an extra 2 X 15.0 mL of toluene was used for washing purposes. 1.52 mL of distilled degassed triethylamine (11.0 mmol) were added using a 1.0 mL gas-tight syringe. Finally, the volume was adjusted to ~65 mL by adding extra toluene. The reaction flask was sealed and heated to 90 °C while stirring at 1200 rpm. After 48 h, the flask was cooled to room temperature, and ~120 mL of saturated degassed sodium bicarbonate was added and stirred for 1 h. The product was extracted into 4 X ~20 mL of toluene, and the organic layer was cannula transferred into a 250.0 mL side-arm round-bottom flask containing anhydrous sodium sulfate. After stirring for 30 min, the solution was filtered into a clean 250.0 mL side-arm round-bottom flask, and the sodium sulfate was washed with 3 X ~20 mL toluene. The solvent was removed under high vacuum to obtain an orange gel-like product. Next, the crude mixture was purified using flash column chromatography (~35 g of silica, hexanes: ethyl acetate: NEt$_3$ = 10:1:0.01) to obtain an orange solid **66** (1.32 g, 84.2% yield).

¹H NMR (499.807 MHz, CD$_2$Cl$_2$, 27.0 °C): δ 7.67−7.60 (m, 2H, Ph−*H*), 7.41−7.35 (m, 3H, Ph−*H*), 7.16−7.11 (m, 5H, Ph−*H*), 5.99 (s, 2H, CH norbornyl alkene), 4.32−4.00 (m, 6H, Cp−*H*), 3.34−3.25 (m, 3H, C*H*MeP and C=CC−*H* from norbornyl), 3.22−3.16 (m, 4H, NCH$_2$ and COC−*H* norborynl group), 3.15 (m, 1H, Cp), 1.84−0.93 (m, 29H, PC*y$_2$*, CH$_2$C*H$_2$*CH$_2$, C*H$_3$*, C*H$_2$* bridge of norbornyl group), 0.42 (m, 2H, Si−CH$_2$), 0.11 (s, 3H, Si−Me), 0.04 (s, 3H, Si−Me).

¹³C{¹H} APT NMR (125.690 MHz, CD$_2$Cl$_2$, 27.0 °C): δ 177.8 (s, 2C, C=O), 142.6 (d, *J* = 8.0 Hz, PPh), 140.3 (dd, *J* = 10.3, 2.9 Hz, PPh), 136.3−127.1 (s, 12C, 10 C of PPh and 2 C of norbornyl alkene), 102.0 (dd, *J* = 27.7, 17.8 Hz, 1C, Cp), 74.6(s, 1C, Cp), 74.2 (dd, *J* = 12.2, 3.1 Hz, 1C, Cp), 74.1−73.4 (s, 4C, Cp), 71.7 (d, *J* = 5.15 Hz, 1C, Cp), 71.0−69.8 (s, 2C, Cp), 69.5 (dd, *J* = 4.9, 2.8 Hz, 1C, Cp), 52.5 (s, 1C, CH$_2$ norbornyl group), 46.0 (s, 2C, CH norbornyl group), 45.3 (s, 2C, CH norbornyl group), 41.5 (s, 1C, *C*H$_2$N), 33.4 (d, *J* = 21.6 Hz, 1C, Cy), 33.2 (d, *J* = 20.6 Hz, 1C, Cy), 31.7 (s, 1C, Cy), 31.5 (dd, *J$_1$* = 6.9 Hz, *J$_2$* = 1.5 1C, Cy), 30.4 (s, *J* = 5.9 Hz, 1C, Cy), 30.0 (d, *J* = 9.3 Hz, 1C, Cy), 28.1−27.2 (m, 6C, 5C from Cy and 1 *C*HMeP), 26.9 (d, *J* = 1.6 Hz, 1C, Cy), 22.9 (s, 1C, CH$_2$*C*H$_2$CH$_2$), 16.5 (s, 1C, CH$_3$), 14.5 (s, 1C, Si−CH$_2$), −2.4 (s,1C, Si−Me), −2.4 (s,1C, Si−Me).

³¹P{¹H} NMR (161.839 MHz, CD$_2$Cl$_2$, 26.1 °C): δ 15.6 (d, *^{4}J$_{PP}$* = 40.5 Hz, 1P, PCy), −26.3 (d, *^{4}J$_{PP}$* = 40.5 Hz, 1P, PPh).

HRMS (ESI) found for [M+H]$^+$: 856.3511, Calculated for C$_{50}$H$_{64}$FeNO$_2$P$_2$Si [M+H]$^+$ 855.3525 (diff -1.73 ppm)

EA: Calculated for C$_{50}$H$_{63}$FeNO$_2$P$_2$Si: C 70.16, H 7.42, N 1.64. Found: C 69.99, H 7.52, N 1.65.

Complexation of (R)-1-[(S_p)-2-(Diphenylphosphino)-1'-(dimethyl-3'-N-(cis-5-norbornene-2,3-dicarboximidopropylsilyl)-ferrocenyl]ethyl-di-cyclohexylphosphine with [Rh(COD)₂]BF₄ (67)

Ligand **66** (54.6 mg, 0.0638 mmol) and [Rh(COD)₂]BF₄ (25.5 mg, 0.0628 mmol) were weighed in separate NMR tubes inside the glovebox and septum sealed. The Rh precursor was dissolved in ~1 mL dichloromethane and cannula transferred into a 100.0 mL side-arm round-bottom flask containing a 1" stir bar, with an extra 2 X 1.0 mL of dichloromethane used for washing purposes. Ligand **66** was dissolved in 1.0 mL of dichloromethane and cannula transferred slowly into the rhodium precursor solution while stirring at 1200 rpm, with an extra 2 X 1.0 mL of dichloromethane used for washing purposes. The reaction mixture was stirred at room temperature for 1 h. Next, the solvent was removed, and the product was dried under high vacuum for 30 min. The solid was dissolved in 0.5 mL of dichloromethane, and 5.0 mL of ether were added slowly over the period of 5 h using a 5.0 mL gas-tight syringe yielding an oily red precipitate. The product was precipitated futher by adding 10.0 mL of ether. The solvent was removed using cannula filtration, and the precipitate was washed with 3 X 5.0 mL ether. The product was kept under vacuum overnight to obtain a reddish orange solid **67** (0.067g, 92% yield).

¹HNMR (499.807 MHz, CD₂Cl₂, 27.0 °C) δ 8.39−8.35 (m, 2H, Ph−H), 7.77−7.73 (m, 3H, Ph−H), 7.53−7.38 (m, 5H, Ph−H), 5.99 (s, 2H, CH norbornyl olefin), 5.54 (m, 1H, COD alkene), 5.27 (m, 1H, COD alkene), 4.64−3.45 (m, 7H, 6 Cp−*H* and 1 COD alkene), 3.30 (m, 3H, COD alkene and C=CC−*H* from norbornyl group), 3.19−3.16 (m, 4H, C*H₂*−N and COC−*H* norborynl group), 2.85 (m, 1H, C*H*MeP), 2.59−1.04 (m, 36H, P*Cy₂*, CH₂C*H₂*CH₂, C*H₃*, 7H of COD, C*H₂* bridge of

norbornyl group), 0.61 (m,1H, COD), 0.48 (m, 2H, Si–CH$_2$),0.16 (s, 3H, Si–Me),0.12 (s, 3H, Si–Me).

^{13}C{^{1}H} NMR (125.691 MHz, CD$_2$Cl$_2$, 27.0 °C): δ 177.9 (s, 2C, C=O), 137.1–137.0 (s, 2C, PPh), 134.7 (s, 2C, norbornyl alkene), 133.6 (d, J = 47.6 Hz, 1C, PPh), 133.2–128.8 (s, 8C, PPh), 128.7 (d, J = 49.1 Hz, 1C, PPh), 101.2–93.4 (s, 4C, COD alkene), 91.7 (d, J = 19.1, 1C, Cp), 75.8–69.2 (s, 9C, Cp rings), 52.5 (s, 1C, CH$_2$ norbornyl group), 46.0 (s, 2C, CH norbornyl group), 45.3 (s, 2C, CH norbornyl group), 41.3 (s, 1C, *C*H$_2$N), 40.6 (d, J = 15.3, 1C, PCy$_2$), 35.5 (d, J = 14.6 Hz, 1C, PCy$_2$), 34.0–32.5 (s, 3C, COD alkyl), 30.6 (m, 2C, *C*HMeP and COD alkyl), 28.7–26.4 (s, 10C, 10 PCy$_2$ carbons and *C*HMeP group), 22.7 (s, 1C, CH$_2$*C*H$_2$CH$_2$), 16.1 (d, J = 5.3 Hz, 1C, CH*Me*P), 14.3 (s, 1C, Si–CH$_2$), –2.4 (s, 1C, Si–Me), –2.5 (s, 1C, Si–Me).

^{31}P{^{1}H} NMR (161.8914 MHz, CD$_2$Cl$_2$, 27.0 °C) δ 52.8 (dd,$^1J_{RhP}$ = 144.2 Hz, $^4J_{PP}$ = 29.6 Hz, 1P, P*C*y), 20.7 (dd, $^1J_{RhP}$ = 144.7 Hz, $^4J_{PP}$ = 29.6 Hz, 1P, PPh).

HRMS (ESI) found for [M*]$^+$: 1066.3441, calculated for C$_{58}$H$_{75}$NO$_2$P$_2$RhSi [M*]$^+$: 1066.3447, (diff 0.02 ppm).

EA: Calculated for C$_{58}$H$_{75}$BF$_4$FeNO$_2$P$_2$RhSi: C 60.38, H 6.55, N 1.21. Found: C 59.97, H 6.65, N 1.22.

Polymerization of Rh JosiPhos Catalyst Monomer

The first-generation Grubbs' catalyst (2.4 mg, 2.92 x 10^{-6} mol) was measured inside the glovebox in an NMR tube and septum sealed. CD_2Cl_2 was added to the 4.7 cm mark in the NMR tube to create a standard solution of the Grubbs' catalyst.

Monomer **67** (14.2 mg, 1.23 x 10^{-5} mol) was weighed out inside the glovebox into an NMR tube, septum sealed, and dissolved with 0.3 mL of CD_2Cl_2. Next, 6.15 x 10^{-7} mol of the prepared standard Grubbs' catalyst solution were cannula transferred into the above monomer solution by measuring the meniscus height difference. The final volume of the reaction was adjusted to 0.6 mL by adding excess CD_2Cl_2, and the reaction mixture was shaken well. Next, 6.6 μL (5.07 x 10^{-5} mol) of COE solution were added to the reaction tube using a 10 μL syringe. Polymerization was set up in a 40 °C bath and went to completion in 17 h. Polymerization was confirmed by ^{1}H NMR analysis, which showed consumption of the cyclooctene and the monomer.
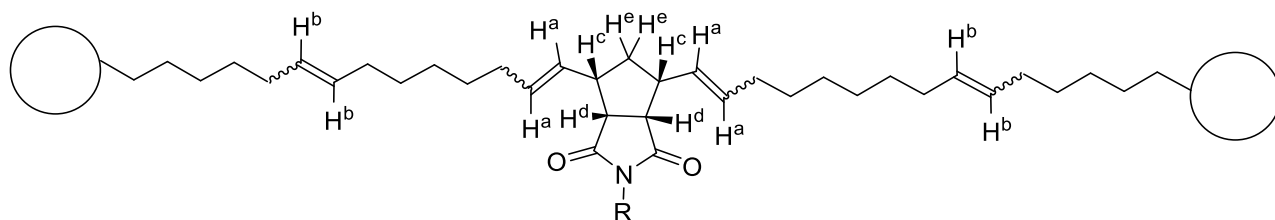
Figure 2.18 *Hydrogen label for the Alt-ROMP polymer of Rh JosiPhos derivative.*

^{1}H NMR (699.763 MHz, CD_2Cl_2, 27.0 °C): δ 8.42−8.34 (m, 2H, Ph−H), 7.80−7.70 (m, 3H, Ph−H), 7.55−7.38 (m, 5H, Ph−H), 5.56 (m, 1H, COD alkene), 5.53−5.44 (m, 4H, H^a), 5.44−5.34 (m, 6H, H^b), 5.28 (m, 1H, COD alkene), 4.65 (m, 1H, Cp), 4.41 (m, 1H, Cp), 4.35 (m, 1H, Cp),

4.29 (m, 1H, COD alkene), 4.00 (m, 1H, Cp), 3.99 (m, 1H, COD alkene), 3.46 (m, 1H, Cp), 3.44

(diethyl ether), 3.38–3.27 (m, 4H, 1 COD alkene, 1 Cp, 2 NCH_2), 3.18–3.02 (m, 2H, H^d),

2.90–2.76 (m, 3H, 1 CHMeP and 2 H^c)*, 2.58 (dd, $^2J_{HH}$ = 14.7 Hz, $^3J_{HH}$ = 4.9 Hz, 1H, COD alkyl),

2.48–0.99 (m, 83H, PCy_2, $NCH_2CH_2CH_2$, CH_3, 2 H^e, COD alkyl, polymer alkyl groups)*, 0.62 (m,

1H, COD alkyl), 0.51 (m, 2H, Si–CH_2), 0.19 (s, 3H, Si–Me), 0.15 (s, 3H, Si–Me).
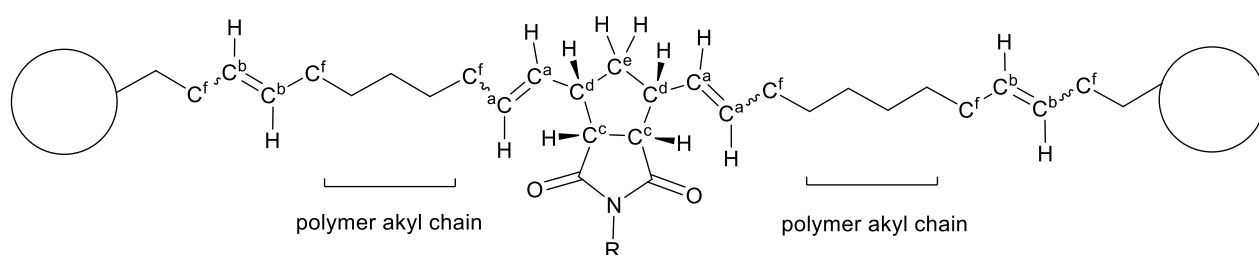
Figure 2.19 *Carbon label of alt-ROMP polymer of Rh JosiPhos derivative.*

^{13}C{^{1}H} NMR (175.975 MHz, CD_2Cl_2, 27.0 °C): δ 177.0–176.9 (m, 2C, C=O), 137.2 (s, 1C, Ph),

137.7 (s, 1C, Ph), 133.7 (d, J = 45.6 Hz, 1C, PPh), 133.2–132.8 (s, 3C, Ph), 132.2–131.9 (m, 2C,

C^a), 131.2 (s, 1C, Ph), 130.9–130.7 (m, 2C, C^b),130.4–130.1 (m, 2C, C^a), 129.5–128.9 (s,4C,

Ph), 128.7 (d, J = 45.6 Hz, 1C, PPh), 101.3–93.5 (s, 4C, COD alkene), 91.7 (m, 1C, Cp), 75.9–69.2

(s, 9C, Cp), 66.0 (diethyl ether), 49.5–49.0 (m, 2C, C^c), 46.0–45.5 (m, 2C, C^d), 41.7–41.4 (m,

1C, NCH_2), 40.6 (d, J = 15.1 Hz, 1C, PCy), 40.2–40.1 (m, unidentified), 37.9–37.7 (m, 1C, C^e),

35.5 (d, J = 13.9 Hz, 1C, PCy), 34.0 (s, 1C, COD alkyl), 33.6 (s, 1C, COD alkyl), 33.1–32.7 (m,

–CH_2CH_2C=C– polymer chain), 32.6 (s, 1C, COD alkyl), 30.6–30.3 (m, 2C, COD akyl and

CHMeP), 30.2–29.1 (m, polymer alkyl chain), 28.8–26.4 (PCy), 22.7 (s, 1C, NCH_2CH_2), 16.2 (s,

1C, CH_3), 15.5 (diethyl ether), 14.3 (s, 1C, SiCH_2), −2.3 (s, 1C, SiMe), −2.4 (s, 1C, SiMe).

³¹P{¹H} NMR (201.641 MHz, CD$_2$Cl$_2$, 27.0 °C) δ 52.9 (dd, $^1J_{RhP}$ = 145.2 Hz, $^4J_{PP}$ = 30.0 Hz, 1P, PCy), 29.2 (Grubbs Catalyst), 20.7 (dd, $^1J_{RhP}$ = 144.4 Hz, $^4J_{PP}$ = 30.0 Hz, 1P, PPh).
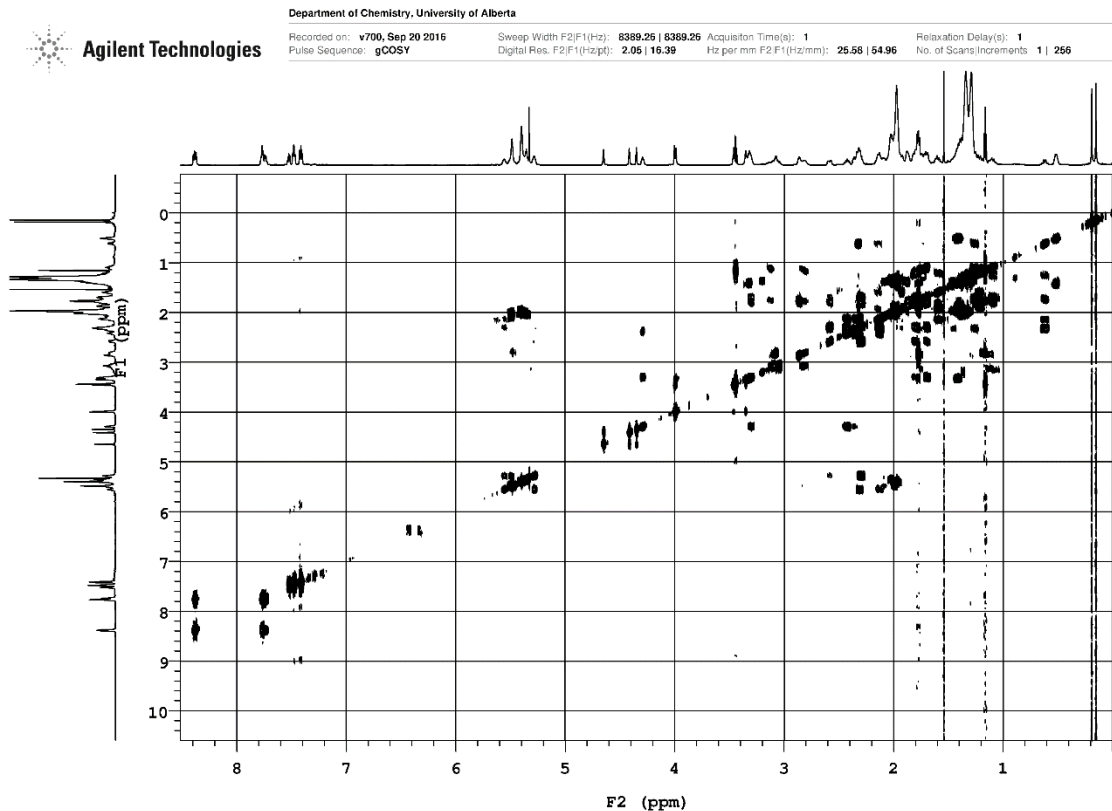
Figure 2.20 *2D-COSY NMR of the alt-ROMP polymer of Rh JosiPhos derivative.*

Kinetic Study of Polymerization of [Rh(66)(COD)]BF₄

Monomer **67** (19.8 mg, 1.72 x 10⁻⁵ mol) and first generation Grubbs' catalyst (1.8 mg, 2.19 x 10⁻⁶ mol) were weighed out inside the glovebox in separate NMR tubes and septum sealed. The Grubbs' catalyst was dissolved by adding CD$_2$Cl$_2$ to the 7.7 cm mark. A 3.05 cm difference of this solution (8.66 x 10⁻⁷ mol) was cannula transferred into the NMR tube containing **68** and shaken well. The reaction mixture was left to react at room temperature for 15 min, then

chilled in a NaCl ice bath. COE (7.6 mg, 6.70 x 10^{-5} mol) was measured out using a 10 μL syringe, obtained by the mass before and after delivery, into the chilled polymerization mixture. After shaking well, the mixture was brought to the Agilent/Varian VNMRS 600 MHz NMR spectrometer and warmed to 40 °C. The mixture was monitored by NMR at various time intervals.

Synthesis of Al_2O_3/PTA Acid Mixture (mole ratio Al_2O_3:PTA= 134:1)*

*Note: The Augustine procedure was used to prepare the Al_2O_3/PTA mixture.[50c]

28.0 mL of 95% ethanol were added to a 100.0 mL side-arm round-bottom flask charged with PTA (2.1154 g, 7.319 x 10^{-4} mol) and shaken gently. Ethanol pre-washed alumina (10.0 g, 9.808 x 10^{-2} mol) was weighed out into another 250.0 mL side-arm round-bottom flask containing a 1" stir bar inside the glovebox. A suspension of alumina was made by adding 80.0 mL of 95% ethanol (degassed). The PTA solution was cannula transferred slowly into the alumina suspension while stirring over a 4 h period. Next, the mixture was allowed to settle for 10–15 min, and the supernatant liquid (ethanol) was cannula filtered under $N_{2(g)}$ and discarded. The remaining alumina/PTA mixture was washed with 55.0 mL of anhydrous ethanol four times, after which the solid mixture was kept under high vacuum overnight and stored in the glovebox.

Deposition of Polymeric Rh JosiPhos Catalyst on Al_2O_3/PTA

Al_2O_3/PTA (9.851 g) was suspended in ~80 mL of CH_2Cl_2 in a 200 mL side-arm round-bottom flask containing 1" stir bar. Polymeric [Rh(**66**)(COD)]BF_4 was diluted using CH_2Cl_2 and cannula transferred dropwise into the Al_2O_3/PTA suspension while stirring rapidly at 1200 rpm. The volume was adjusted to 120 mL after washing the polymer containing NMR tubes with CH_2Cl_2. After letting the slurry stir overnight, the liquor was cannula filtered. The solid was washed further with CH_2Cl_2 (3 X 40 mL), and the washings were combined and concentrated using a rotatory evaporator. The $^{31}P\{^1H\}$ NMR and ^1H NMR of the residue indicated no catalyst leaching. The orange solid catalyst was dried further under high vacuum and stored in the glovebox.

XPS Studies on the Deposition of Polymeric Rh JosiPhos Catalyst on Al_2O_3/PTA

XPS experiments were performed at nanoFAB using Kratos Axis spectrometer with monochromatized Al K_α (hυ = 1486.71 eV). The spectrometer was calibrated by the binding energy (84.0 eV) of Au $4f_{7/2}$ with reference to Fermi level. Two samples, containing the Rh JosiPhos polymer deposited on Al_2O_3/PTA and the undeposited Al_2O_3/PTA, were prepared in two separate sample vials inside the glovebox. Then, the vials were sealed and bought into the spectrometer for measurement. The samples were quickly loaded into the spectrometer and kept under high vacuum. The pressure of analysis chamber during experiments was better than 5×10^{-10} Torr. A hemispherical electron-energy analyzer working at the pass energy of 20 eV was used to collect the core-level spectra, while survey spectrum within a range of binding energies from 0 to 1100 eV was collected at analyzer pass energy of 160 eV. Charge effects were corrected for the undeposited sample using C 1S peak at 284.6 eV and the resulting W $4f_{7/2}$ peak at 35.8 eV was matched with the deposited sample. Data was

processed using CasaXPS. Deconvolution was carried out for the Rh signal. A Shirley background was applied to subtract the inelastic background of core-level peaks. Non-linear optimization using the Marquardt Algorithm was used to determine the peak model parameters such as peak positions, widths and peak intensities. The model peak to describe XPS core-level lines for curve fitting was a product of Gaussian and Lorentzian functions.

Solvent Screening for Hydrogenation of MAC Ester

Eight different screening test tubes were weighed out inside the glovebox with methyl-(Z)-α-acetamidocinnamate (3.75×10^{-4} mol) and the immobilized catalyst (3.75×10^{-6} mol of Rh) (Table 2.3). The test tubes were septum sealed, brought out of the glovebox, connected to an Ar Schlenk line, and assembled in the screening hydrogenation reactor. The appropriate solvent was added to each test tube using a 5.0 mL gas-tight syringe. The test tubes were purged with H_2 for 10 min, and after the apparatus was closed, it was purged further with H_2 for 20 min. The reaction was pressurized to 15 psig and left stirring at 1200 rpm and room temperature for 4 h.

Table 2.3 *Mass measurement for solvent screening for asymmetric hydrogenation of MAC using Al$_2$O$_3$/PTA deposited polymeric Rh JosiPhos derivative*

Reaction	Substrate (mg)	Catalyst (mg)	Volume of Solvent (mL)	Solvent
A	86.7	254.2	1.5	Toluene
B	83.2	252.0	1.5	Tetrahydrofuran
C	80.2	253.5	1.5	Ethyl Acetate
D	85.4	256.7	1.5	Acetone
E	86.0	256.7	1.5	Ethanol
F	85.0	252.5	1.5	Methylene Chloride
G	85.4	253.2	1.5	Tertbutyl methyl ether
H	85.8	214.0	1.3	Methanol

Each sample was passed through the small Florisil plug to remove the catalyst. The solvent was removed using a rotatory evaporator and its NMR was obtained to determine the conversion. Next, the *ee* was determined using a literature method with the shift reagent europium tris[3-(trifluoromethylhydroxymethylene)-(+)-camphorate].[68]   For example, the shift reagent (45.2 mg, 5.06 x 10^{-5} mol) and hydrogenation product (11.2 mg, 5.06 x 10^{-5} mol) were weighed out in the NMR tube and dissolved in 0.69 mL of CDCl$_3$.

Table 2.4 *Results for solvent screening for asymmetric hydrogenation of MAC using* Al_2O_3/PTA

deposited polymeric Rh JosiPhos derivative

Label[a]	Solvent	Conversion[b]	% *ee*[c]
A	Toluene	74	21
B	Tetrahydrofuran	100	85
C	Ethyl Acetate	100	61
D	Acetone	100	87
E	Ethanol	100	56
F	Methylene Chloride	100	82
G	Tertbutyl methyl ether	85	32
H	Methanol	100	48

[a]Hydrogenation carried out at 2 bar H_2, rt, and 4 h. [b]Conversion determined via ^{1}H NMR. [c]*Ee* determined using shift reagent europium tris[3-(trifluoromethylhydroxymethylene)-(+)-camphorate].

Homogeneous Hydrogenation of MAC Using Complex 67

[Rh(COD)(**66**)]BF_4 (11.1mg, 10.0 µmol) was weighed out inside the glovebox in an NMR tube. MAC (930.7 mg, 5.00 mmol) was weighed out inside the glovebox in a glass bomb and parafilm covered. The glass bomb was assembled quickly into the hydrogenation apparatus and purged under Ar. Next, the Rh catalyst was dissolved in 1.0 mL of methanol and shaken

well (poor solubility). The resulting red solution was cannula transferred into the hydrogenation bomb. This step was repeated three more times. Even though the glass bomb was stirred, some of the substrate remained undissolved. Addition of an extra 3.0 mL of methanol via a 5.0 mL gas-tight syringe resulted in a homogeneous solution. Then, the reaction vessel was H_2 purged for 5 min to displace the Ar, the reaction was set at 15 psig, at 35 °C, and stirred at 1200 rpm. The reaction was stopped at 3 h, and the ^{1}H NMR of the aliquot showed complete conversion of the MAC to its hydrogenated product. The *ee* was determined using shift reagent as mentioned above.

General Reusable Batch Hydrogenation Procedure for DMI

A glass bomb was calibrated to the 1.0 mL and 4.0 mL marks. A standard dimethyl itaconate solution was prepared by dissolving dimethyl itaconate (15.873 g, 0.10037 mol) and 60.0 mL of methanol in a Schlenk tube. The immobilized catalyst (345.2 mg, 10.0 μmol of Rh) was weighed out in a glass bomb inside a glovebox with a $\frac{1}{2}^{"}$ stir bar, and the glass bomb was capped with parafilm. The glass bomb was removed from the glovebox and assembled quickly with the hydrogenation apparatus under positive N_2 pressure, and the setup was purged for 2 h with N_2. 1.0 mL of methanol was added to the glass bomb via a gas-tight 1.0 mL syringe, and 3.0 mL (5.02 mmol) of substrate solution, corresponding to 1:500 Rh:substrate ratio, were cannula transferred into the bomb. The bomb was purged for 30 min with H_2 (1 atm), the system was pressurized to 75 psig at rt, and stirred at 1200 rpm. After 4 h, the stirring was stopped for 1 h for the catalyst to settle, and during this period the bomb was depressurized slowly and then kept under a N_2 bubbler pressure. A cannula filter

(filter paper wired to the end of a flat cannula with copper wire) was connected to the inlet of the bomb through a septum and flushed with N_2. The outlet of the filter was connected to a degassed secondary collection flask that was kept under a bubbler. The cannula was purged for 30 min with N_2 to remove any air from the cannula filter system. Next, 3.0 mL of the reaction solution were cannula filtered, and fresh 3.0 mL of substrate solution was added to the bomb. The bomb was purged with H_2 under a bubbler pressure for 15 min, and the reaction was set up again. After 4 h, the above steps were repeated for a total of ten runs. The product was analyzed using GC-MS for *ee*. The product was confirmed further using NMR.

¹H NMR (498.118 MHz, CDCl₃, 27.0 °C): δ 3.71 (s, 3H, CH₃O-), 3.70 (s, 3H, CH₃O-), 2.94 (m, 1H, CH₃C*H*), 2.76 (dd, $^2J_{HH}$ = 16.4 Hz, $^3J_{HH}$ = 8.0 Hz, 1H, CH'H), 2.43 (dd, $^2J_{HH}$ = 16.4 Hz, $^3J_{HH}$ = 6.0 Hz, 1H, CH'H), 1.24 (d, $^3J_{HH}$ = 7.5 Hz, 3H, CH₃).

GCMS:
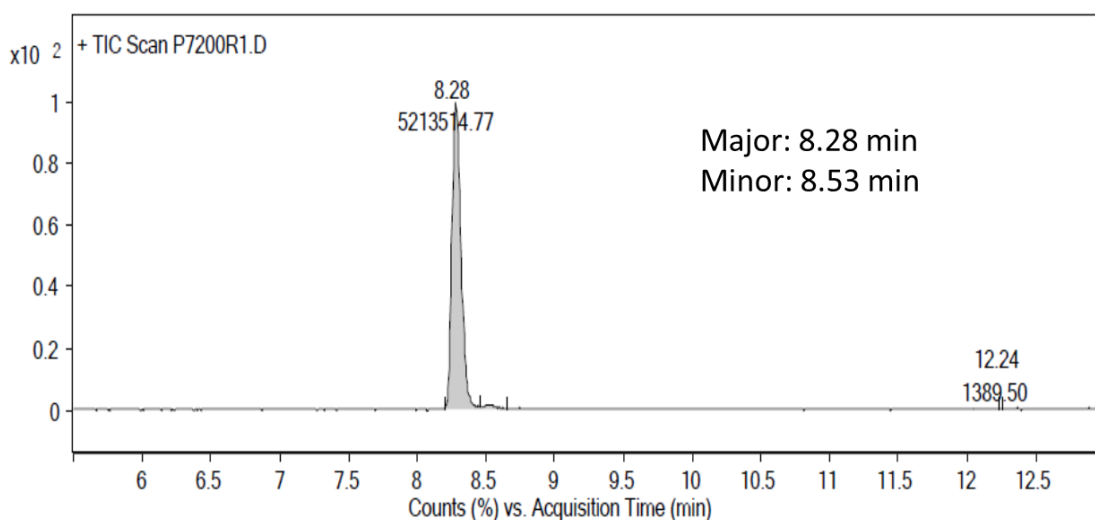
Figure 2.21 *GC-MS of the hydrogenation product of DMI*

Chapter 3 Conclusion

3.1 Overview

Heterogeneous asymmetric hydrogenation catalysis is an attractive technology, which incorporates the concept of catalyst recycling and reuse.[43] Despite the massive amount of techniques that have been explored over the past 50 years, immobilization of the molecular catalysts into various supports often has been plagued by common challenges. The immobilization of the soluble molecular catalyst onto a polymer or solid support often results in reduced mass transport, leading to lower TOF in comparison to the homogeneous analog. The modification carried out to immobilize the catalyst often results in changes in the steric and electronic environment of the active sites, resulting in poor selectivity, which is a key concern in the synthesis of chiral molecules. Further, the idea of reuses is only possible if the catalyst is stable and maintains good activity and selectivity over multiple reuses. Therefore, developing a heterogeneous asymmetric hydrogenation catalyst that retains the excellent catalytic activity of the homogeneous analog, gives high selectivity toward one chiral product, and maintains the catalytic performance for multiple reuses, is a challenging task. Hence, it is not surprising that, despite enormous scientific endeavours, very few successful systems have been reported in the literature.[55e]

The aim of our research was to address some of the issues outlined earlier with heterogeneous asymmetric hydrogenation, specifically with the catalyst based on the "privileged" JosiPhos type ligand. We explored our prior successful method of

polymerization, the alt-ROMP method, because it allows us to control the distribution of the metal centre precisely in the polymer.[59] We developed a high yielding versatile synthetic procedure to functionalize any derivative of a JosiPhos type ligand with an alt-ROMP active norimido group. This modified JosiPhos ligand was metallated with Rh to obtain the alt-ROMP active derivative. Alt-ROMP of the Rh complex and spacer *cis*-cyclooctene was carried out using the Grubbs metathesis catalyst to obtain the final polymer with precise control over the distribution of the metal sites within the polymer. Kinetic studies showed that the alternation of Rh diphosphine complex and the spacer *cis*-cyclooctene proceeded with a linear relation. This control over the distribution of catalytic sites within a polymer chain is an important feature that can allow better mass transport and an overall reliable performance of the obtained heterogeneous catalysts. The obtained polymer was deposited successfully onto a well known anionic support, Al_2O_3/PTA, held together via multiple electrostatic interactions between the cationic Rh centres in the polymer chain with an anionic PTA. The obtained heterogeneous catalyst was tested for catalytic asymmetric hydrogenation of prochiral olefins.

(3.1)
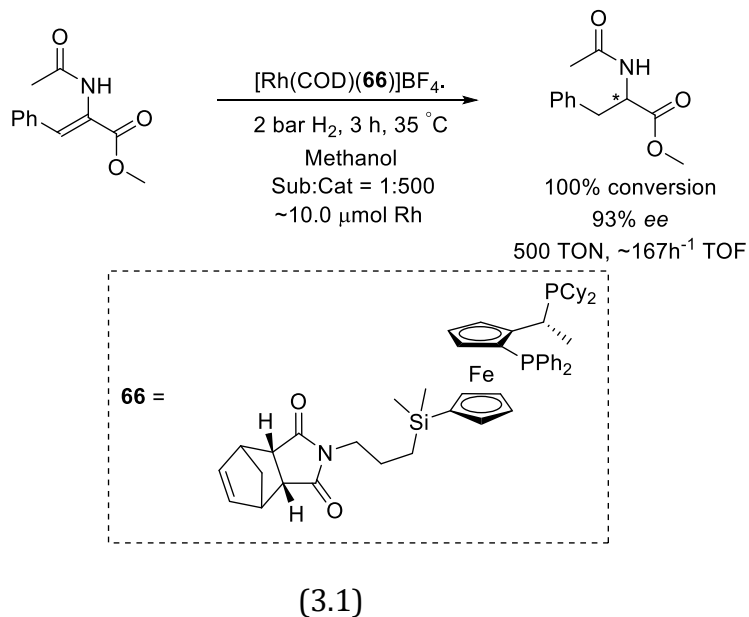
Homogeneous hydrogenation of methyl-(*Z*)-α-acetamidocinnamate ester carried out with alt-ROMP active Rh JosiPhos derivative gave an excellent selectivity and conversion (93% *ee*, 100% conversion, 500 TON, and ~167 h^{-1} TOF, eq 3.1). The synthetic modification carried out on the ligand had no significant effect on the catalytic activity. However, it was determined that the selectivity of the deposited catalyst was much lower, and the support did play a significant role in the catalytic performance. We carried out solvent screening in an effort to improve the selectivity of the heterogeneous catalyst, and the *ee* was improved from 48% in methanol to 87% in acetone (eq 3.2).

(3.2)
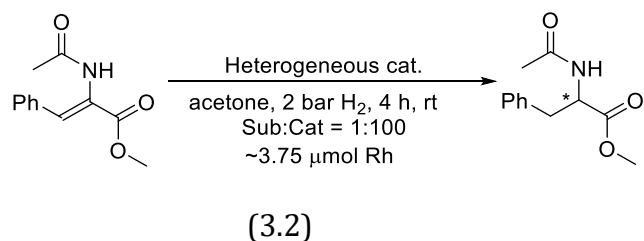
Next, we explored the catalyst reusability using dimethyl itaconate as the model substrate. Enantioselective hydrogenation of dimethyl itaconate was carried out with

119

excellent activity (100% conversion, 5000 TON) and selectivity (95–87% ee) with no significant metal leaching over 10 reuses (eq 3.3).

100% conversion

95–87% ee, 5000 TON

10 runs
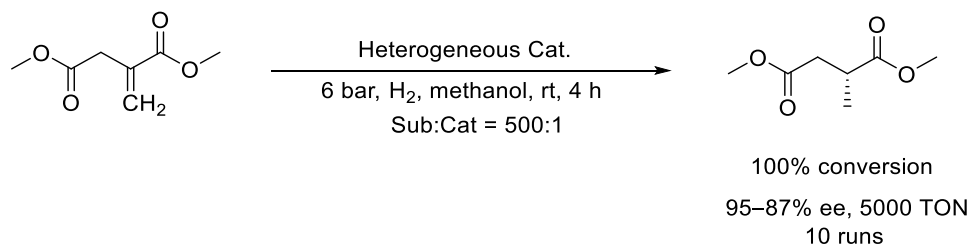
(3.3)

Next, we explored ways to stabilize the catalyst to maintain the selectivity during reuses. In an example, hydrogenation was carried out always in presence of some unreacted starting material. The catalyst gave a constant selectivity of 94–95% *ee* over a period of nine reuses, which maybe due to stabilization of the [Rh(diphosphine)(solvent)$_2$]anion by chelation from the starting material. Also, it was determined that overrunning the reaction in the presence of H$_2$ atmosphere led to a rapid drop in *ee* in the preceding run and that the handling of the catalyst during the resting period is essential to the catalyst stability. We explored various other solvents with different coordination ability, such as toluene, acetone, dimethoxyethane etc., to stabilize the catalyst intermediate. It was concluded that the catalyst undergoes slow deactivation into another species, which hydrogenates with much lower selectivity. This drop in *ee* over time is a common issue with an Al$_2$O$_3$/PTA support-based system, and no clear explanation exists in the literature.[50, 52, 54] The possible decomposition of Rh complex into metallic Rh after the end of hydrogenation has been proposed by Augustine and co-workers.[50f] If such is the case, metallic Rh could hydrogenate the olefin with no selectivity, leading to the drop in *ee* over the course of reuses. However, further mechanistic studies must be performed to confirm this.

120

3.2 Current Work and Future Directions

We have explored the application of heterogenous Rh JosiPhos derivatives for the hydrogenation of the model substrates methyl-(*Z*)-*α*-acetamidocinnamate and dimethyl itaconate. Currently, we are working on applying our method to "real world substrates". In particular, our group has synthesized a Rh alt-ROMP polymer using the tertbutyl derivative of JosiPhos **74**, which is used for the hydrogenation of dihydrositaglipin (refer Chapter 1 for the details).

Scheme 3.1

Heterogeneous catalyst

34.5 bar, methanol, 50 °C
overnight

76

Rh:Sub = 1:50

79.1% conversion
97.0% *ee*
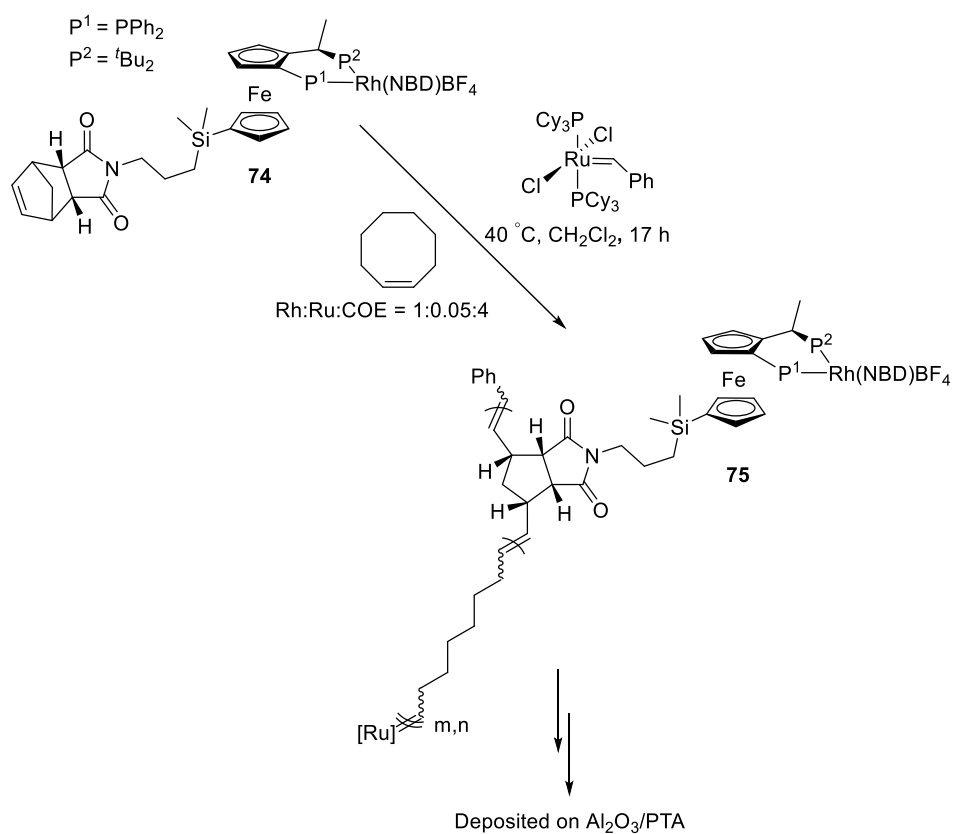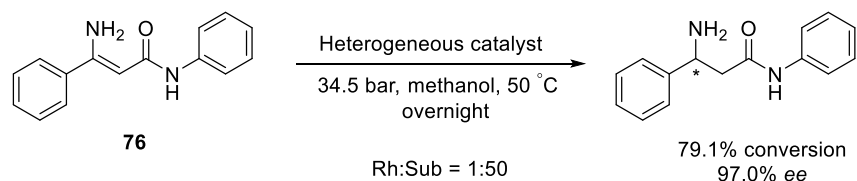
(3.4)

The resulting alt-ROMP polymer **75** was deposited on Al_2O_3/PTA successfully, and an

initial catalytic performance for the hydrogenation of the model enamine substrate of

sitagliptin **76** has been evaluated by Merck & Co.. In a preliminary example, immobilized alt-

ROMP polymer was tested for hydrogenation of a sitagliptin model substrate with 2 mol %

catalyst loading, 34.5 bar H_2, methanol as solvent, at 50 °C overnight. The catalyst gave an

excellent selectivity of 97.0% *ee*, and the reaction went to 79.1% conversion, as shown in

Scheme 3.1. However, the amine nature of the substrate must be considered when using an

acidic support. It is well known that the PTA decomposes in basic conditions, therefore, the

low conversion of the catalyst could due to the decomposition of the support itself. In fact,

the color of the liquor after hydrogenation was observed to be green, suggesting possible

decomposition of the support or the leaching of the Rh metal. However, this is a preliminary

result, and further work must be carried out to get a deeper insight. The limitations of using

acidic support Al_2O_3/PTA must be addressed. As shown in Scheme 3.2, we are planning to do

so by using crosslinkers to synthesize a 3D-polymer network, which could be self-supported

or deposited in a neutral support, like $BaSO_4$.

Scheme 3.2
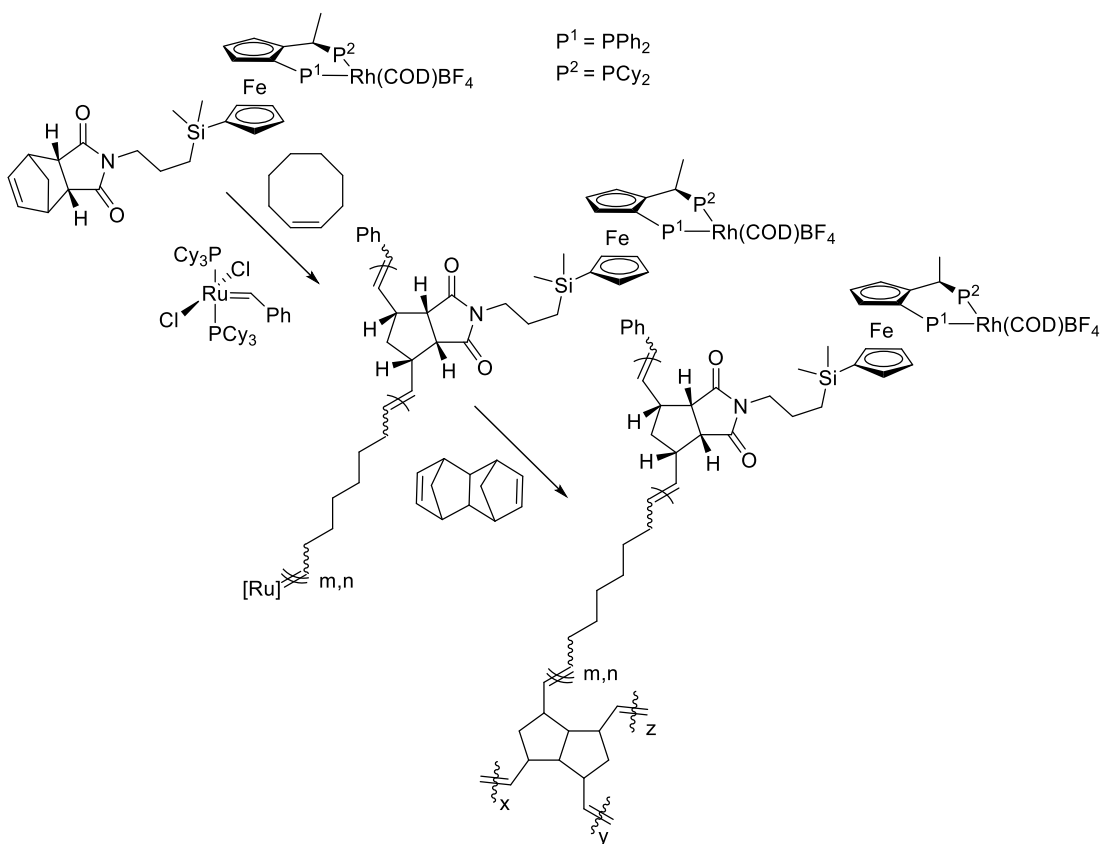
Further, designing a more robust homogeneous catalyst is essential for the long-term stability of its heterogeneous derivatives. Hence, one of our future steps would be to switch from an electron rich alkyl phosphine to a more electron defficient aryl phosphine (Figure 3.1), which is less prone to oxidation.
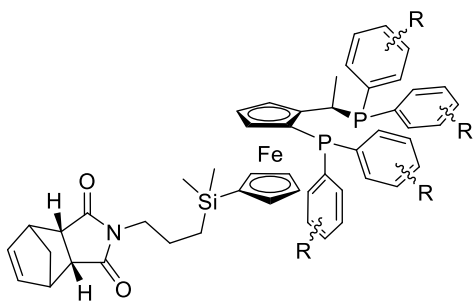
Figure 3.1 *Aryl JosiPhos derivatives.*

Bibiliography

1. Nguyen, L. A.; He, H.; Huy, C. P. *Int. J. Biomed. Sci.* **2006**, *2*, 85–100.

2. Noyori, R. *Angew. Chem., Int. Ed*. **2002**, *41*, 2008–2022.

3. Rachwalski, M.; Vermue, N.; Rutjes, F. P. J. T. *Chem. Soc. Rev.* **2013**, *42*, 9268–9282.

4. Matthews, S. J.; McCoy, C. *Clin. Ther*. **2003**, *25*, 342–395.

5. Blaschke, G.; Kraft, H. P.; Fickentscher, K.; Köhler, F. *Arzneim. Forsch.* **1979**, *29*, 1640–1642.

6. (a). Caldwell, J. *Chirality* **1989**, *1*, 249–250.

    (b). Hutt, A. J. *Chirality* **1991**, *3*, 161–164.

7. Stinson, S. C. *Chem. Eng. News* **1992**, *70* (39), 46–79.

8. Stinson, S. C. *Chem. Eng. News* **2001**, *79* (20), 45–56.

9. Rouhi, A. M. *Chem. Eng. News* **2002**, *80* (23), 43–50.

10. Sekhon, B. S. *J. Pestic. Sci.* **2009**, *34*, 1–12.

11. Ye, J.; Zhao, M.; Niu, L.; Liu, W. *Chem. Res. Toxicol.* **2015**, *28*, 325–338.

12. *Flavours and Fragrances: Chemistry, Bioprocessing and Sustainability*; Berger, R. G., Ed.; Springer-Verlag Berlin Heidelberg: Germany, 2007.

13. Etayo, P.; Vidal-Ferran, A. *Chem. Soc. Rev.* **2013**, *42*, 728–754.

14. Moss, G. P. *Pure Appl. Chem.* **1996**, *68*, 2193–2222.

15. McCague, R.; Casy, G. In *Progress in Medicinal Chemistry*; Ellis, G. P., Luscombe, D. K., Eds.; Elsevier Science Publishers, B. V.: Amsterdam, 1997; vol. 34, pp 203–261.

16. Sakai, K.; Hirayama, N.; Tamura, R. Novel Optical Resolution Technologies; Springer-Verlag Berlin, Heidelberg, 2007.

17. Faber, K. Biotransformations in Organic Chemistry, 6th ed.; Springer: Heidelberg, 2011; p 7.

18. Scott, J. W. Readily Available Chiral Carbon Fragments and their use in Synthesis. In *Asymmetric Synthesis*; Morrison, J. D., Ed.; Academic Press: New York, 1984; vol. 4, pp 1–226.

19. Sheldon, R. A. *Green Chem.* **2007**, *9*, 1273–1283.

20. Constable, D. J. C.; Curzons A. D.; Cunningham, V. L. *Green Chem.* **2002**, *4*, 521–527.

21. United States Environmental Protection Agency. Basics of Green Chemistry [Online]. https://www.epa.gov/greenchemistry/basics-green-chemistry (Accessed March 15, 2018).

22. *Asymmetric Catalysis on Industrial Scale: Challenges, Approaches and Solutions*; Blaser, H.-U., Schmidt, E., Eds.; Wiley-VCH Verlag GmbH & Co. KGaA: Weinheim, 2004.

23. Trost, B. M. *Proc. Natl. Acad. Sci. U. S. A.* **2004**, *101*, 5348–5355.

24. Knowles, W. S. *Angew. Chem., Int. Ed.* **2002**, *41*, 1999–2007.

25. Sharpless, K. B. *Angew. Chem., Int. Ed.* **2002**, *41*, 2024–2032.

26. (a). Xie, J.-H.; Zhu, S.-F.; Zhou. Q.-L. *Chem. Rev.* **2011**, *111*, 1713–1760.

    (b). Gopalaiah, K.; Kagan, H. B. *Chem. Rev.* **2011**, *111*, 4599–4657.

    (c). Wang, D.-S.; Chen, Q.-A.; Lu, S.-M.; Zhou, Y.-G. *Chem. Rev.* **2012**, *112*, 2557–2590.

    (d). Ager, D. J.; de Vries, A. H. M.; de Vries, J. G. *Chem. Soc. Rev.* **2012**, *41*, 3340–3380.

    (e). Xie, J.-H.; Zhu, S.-F.; Zhou. Q.-L.; *Chem. Soc. Rev.* **2012**, *41*, 4126–4139.

    (f). Yu, Z.; Jin, W.; Jiang, Q. *Angew. Chem., Int. Ed.* **2012**, *51*, 6060–6072.

(g). Rasu, L.; John, J. M.; Stephenson, E.; Endean, R.; Kalapugama, S.; Clement, R.; Bergens, S. H. *J. Am. Chem. Soc.* **2017**, *139*, 3065–3071.

27. (a). Zhu, S.; Zhou, Q. *Acc. Chem. Res.* **2017**, *50*, 988–1001.

    (b). Yang, X.; Yue, H.; Yu, N.; Li, Y.; Xie, J.; Zhou, Q. *Chem. Sci.* **2017**, *8*, 1811–1814.

28. Blaser, H.-U.; Pugin, B.; Spindler, F. *J. Mol. Catal. A: Chem.* **2005**, *231*, 1–20.

29. (a). Osborn, J. A.; Jardine, F. S.; Young, J. F.; Wilkinson, G. *J. Chem. Soc. A* **1966**, 1711–1732.

    (b). Knowles, W. S.; Sabacky, M. J. *Chem. Commun.* **1968**, 1445–1446.

    (c). Horner, L.; Siegel, H.; Buthe, H. *Angew. Chem., Int. Ed.* **1968**, *7*, 942.

    (d). Knowles, W. S.; Sabacky, M. J.; Vineyard, B. D. *Chem. Commun.* **1972**, 10–11.

    (e). Kagan, H. B.; Dang, T. P. *Chem. Commun.* **1971**, 481–482.

    (f). Kagan, H. B.; Dang, T. P. *J. Am. Chem. Soc.* **1972**, *94*, 6429–6433.

    (g). Knowles, W. S.; Sabacky, M. J.; Vineyard, B. D.; Weinkauff, D. J. *J. Am. Chem. Soc.* **1975**, *97*, 2567–2568.

30. (a). Knowles, W. S. Asymmetric Hydrogenations–The Monsanto L-Dopa Process. In *Asymmetric Catalysis on Industrial Scale: Challenges, Approaches and Solutions*; Blaser, H.-U., Schmidt, E., Eds.; Wiley-VCH Verlag GmbH & Co. KGaA: Weinheim, 2004; pp 21–38.

    (b). Selke, R. The Other L-Dopa Process. In *Asymmetric Catalysis on Industrial Scale: Challenges, Approaches and Solutions*; Blaser, H.-U., Schmidt, E., Eds.; Wiley-VCH Verlag GmbH & Co. KGaA: Weinheim, 2004; pp 39–53.

(c). Oro, L. A.; Carmona, D.; Fraile, J. M. Hydrogenation Reactions. In *Metal-catalysis in Industrial Organic Processes;* Chiusoli, G. P., Maitlis, P. M. Eds.; The Royal Society of Chemistry: Cambridge, U.K. 2006; pp 79–113.

(d). Min, K.; Park, K.; Park, D. H. *Appl. Microbiol. Biotechnol.* **2015**, *99*, 575–584.

31. (a). Fráter, G.; Bajgrowicz, J. A.; Kraft, P. *Tetrahedron* **1998**, *54*, 7633–7703.

(b). Chapuis, C. *Perfum. Flavor.* **2011**, 36 (*12*), 36–48.

(c). Dobbs, D. A.; Vanhessche, K. P. M.; Brazi, E.; Rautenstrauch, V.; Lenoir, J. -Y.; Genêt, J.-P.; Wiles, J.; Bergens, S. H. *Angew. Chem., Int. Ed.* **2000**, *39*, 1992–1995.

(d) Wiles, J. A.; Bergens, S. H.; Vanhessche, K. P. M.; Dobbs, D. A.; Rautenstrauch, V. *Angew. Chem., Int. Ed.* **2001**, *40*, 914–919.

(e). Teisserie, P. J.; Plattier, M. The preparation of methyl dihydrojasmonate. US Patent US3978108 A, December 17, 1971.

(f). Rautenstrauch, V.; Koenraad P. M.; Genêt, J.-P.; Lenoir, J.-V. US Patent US5874600A, February 23, 1999.

32. (a). Blaser, H.-U. Adv. Synth. Catal. **2002**, *344*, 17–31.

(b). H. Moser, G. Ryhs, Hp. Sauter, Z. *Naturforsch. B* **1982**, 37, 451–462.

(c). Blaser, H.-U.; Hanreich, R.; Schneider, H.-D.; Spindler, F.; Steinacher, B. The Chiral Switch of Metolachlor: The Development of a Large-Scale Enantioselective Catalytic Process. In *Asymmetric Catalysis on Industrial Scale: Challenges, Approaches and Solutions*; Blaser, H. -U., Schmidt, E., Eds.; Wiley-VCH Verlag GmbH & Co. KGaA: Weinheim, 2004; pp 55–70.

33. (a). Blaser, H.-U.; Pugin, B.; Spindler, F. *J. Mol. Catal. A: Chem.* **2005**, *231*, 1–20.

(b). Zweig, J. E.; Kim, D. E.; Newhouse, T. R. *Chem. Rev.* **2017**, *117*, 11680–11752.

(c). Chakraborty, S.; Bhattacharya, P.; Dai, H.; Guan, H. *Acc. Chem. Res.* **2015**, *48*, 1995–2003.

(d). Chirik, P.J. *Acc. Chem. Res.* **2015**, *48*, 1687–1695.

(e). Li, Y.-Y; Yu, S.-L.; Shen, W.-Y.; Gao, J.-X. *Acc. Chem. Res.* **2015**, *48*, 2587–2598.

34. (a). Beller, M.; Blaser, H.-U. *Platinum Met. Rev.* **2013**, *57*, 272–280.

(b). Blaser, H.-U. Industrial Asymmetric Hydrogenation. In *Applications of Transition Metal Catalysis in Drug Discovery and Development: An Industrial Perspective*; Crawley M.L., Trost, B.M., Eds.; John Wiley & Sons, Inc.: Hoboken, NJ, 2012; First edition, pp 315–341.

35. (a). Meißner, A.; Alberico, E.; Drexler, H.-J.; Baumann, W.; Heller, D. *Catal. Sci. Technol.* **2014**, *4*, 3409–3425.

(b). Landis, C. R.; Halpern, J. *J. Am. Chem. Soc.* **1987**, *109*, 1746–1754.

(c). Preetz, A.; Fischer, C.; Kohrt, C.; Drexler, H.-J.; Baumann, W.; Heller, D. *Organometallics* **2011**, *30*, 5155–5159.

(d). Seeman, J. I. *Chem. Rev.* **1983**, *83*, 83–134.

36. (a). Li, W.; Hou, G.; Sun, X.; Shang, G.; Zhang, W.; Zhang, X. *Pure Appl. Chem.* **2010**, *82*, 1429–1441.

(b). Teichert, J. F.; Feringa, B. L. *Angew. Chem., Int. Ed.* **2010**, *49*, 2486–2528.

(c). Gladiali, S.; Alberico, E.; Junge, K.; Beller, M. *Chem. Soc. Rev.* **2011**, *40*, 3744–3763.

(d). van Leeuwen, P. W. N. M.; Kamer, P. C. J.; Claver, C.; Pàmies, O.; Diéguez, M. *Chem. Rev.* **2011**, *111*, 2077–2118.

(e) Fernández-Pérez, H.; Etayo, P.; Panossian, A.; Vidal-Ferran, A. *Chem. Rev.* **2011**, *111*, 2119–2176.

37. Yoon, T.P.; Jacobsen, E.N. *Science* **2003**, *299*, 1691–1693.

38. (a). Blaser, H,-U.; Pugin,B.; Spindler, F.; Mejía,E.; Togni, A. Josiphos Ligands: From Discovery to Technical Applications. In *Privileged Chiral Ligands and Catalysts*; Zhou, Q.-L., Ed.; Wiley-VCH Verlag GmbH & Co. KGaA: Weinheim, 2011; pp 93–136.

39. (a). Marquarding, D.; Klusacek, H.; Gokel, G.; Hoffmann, P.; Ugi, I. K. *J. Am. Chem. Soc.* **1970**, *92*, 5389–5393.

    (b). Deng, W.-P; Snieckus, V.; Metallinos, C. Stereoselective Synthesis of Planar Chiral Ferrocenes. In *Chiral Ferrocenes in Asymmetric Catalysis: Synthesis and Applications*; Dai, L.-X., Hou, X.-L., Eds.; Wiley-VCH Verlag GmbH & Co. KGaA: Weinheim, 2010; pp 15–53.

    (c). Hayashi, T.; Yamamoto, K.; Kumada, M.; *Tetrahedron Lett.* **1974**, *15*, 4405–4408.

    (d) Gokel, G. W.; Marquarding, D.; Ugi, I. K. *J. Org. Chem.* **1972**, *37*, 3052–3058.

    (e). Togni, A.; Häusel, R. *Synlett* **1990**, 633–635.

    (f). Togni, A.; Breutel, C.; Schnyder, A.; Spindler, F.; Landert, H.; Tijani, A. *J. Am. Chem. Soc.* **1994**, *116*, 4062–4066.

40. (a). U.S. Food and Drug Administration. (Press Release) FDA Approves New Treatment for Diabetes First in a New Class of Diabetes Drugs [online], October 17, 2006.

    http://www.fda.gov/NewsEvents/Newsroom/PressAnnouncements/2006/ucm10 8770.htm

    (b). Hansen, K. B.; Hsiao, Y.; Xu, F.; Rivera, N.; Clausen, N.; Kubryk, M.; Krska, S.; Rosner, T.; Simmons, B.; Balsells, J.; Ikemoto, N.; Sun, Y.; Spindler, F.; Malan, C.; Grabowski, E. J. J.; Armstrong III, J. D. *J. Am. Chem. Soc.* **2009**, *131*, 8798–8804.

(c). Clausen, A. M.; Dziadul, B.; Cappuccio, K. L.; Kaba, M.; Starbuck, C.; Hsiao, Y.; Dowling, T. M. *Org. Process Res. Dev.* **2006**, *10*, 723–726.

(d). Hsiao, Y.; Rivera, N. R.; Rosner, T.; Krska, S. W.; Njolito, E.; Wang, F.; Sun, Y.; Armstrong, J. D., III.; Grabowski, E. J. J.; Tillyer, R. D.; Spindler, F.; Malan, C. *J. Am. Chem. Soc.* **2004**, *126*, 9918–9919.

(e). Jun-An, M. *Angew. Chem., Ind. Ed.* **2003**, *42*, 4290–4299.

41. (a). Garret, C. E.; Prasad, K. *Adv. Synth. Catal.* **2004**, *346*, 889–900.

(b). U.S. Department of Health and Human Services Food and Drug Administration. Guidance for Industry [Online]. February, 2012.

http://www.fda.gov/downloads/drugs/guidancecomplianceregulatoryinformation /guidances/ucm073395.pdf (Accessed Feb 04, 2018).

42. Market insider, commodities [Online]. http://markets.businessinsider.com/commodities/rhodium (accessed February 4th 2018)

43. *Recoverable and Recyclable catalysts*; Benaglia, M., Eds.; John Wiley & Sons, Ltd: UK, 2009.

44. Muhammad, I.; Toma, N. G.; C. Oliver. K. *ChemSusChem.* **2011**, *4*, 300−316.

45. (a). Fraile, J. M.; García, J. I.; Mayoral, J. A. *Chem. Rev.* **2009**, *109*, 360–417.

(b). Barbaro, P.; Liguori, F. *Chem. Rev.* **2009**, *109*, 515–529.

46. (a). Mazzei,M.; Marconi, W.; Riocci, M. *J. Mol. Catal.* **1980**, *9*, 381–387.

(b). Kleman, P.; Barbaro, P.; Pizzano, A. *Green Chem.* **2015**, *17*, 3826–3836.

(c). Barbaro, P.; Bianchini, C.; Liquori, F.; Pirovano, C.; Sawa, H. *Catal. Sci. Technol.* **2011**, *1*, 226–229.

(d). Feldman, R. A.; Fraile, J. M. *Catal. Commun.* **2016**, *83*, 74–77.

(e). Liao, H.; Chou, Y.; Wang, Y.; Zhang, H.; Cheng, T.; Liu, G. *ChemCatChem* **2017**, *9*, 3197–3202.

(f). Selke, R. *J. Mol. Catal.* **1986**, *37*, 227–234.

(g). Barbaro, P.; Bianchini, C.; Giambastiani, G.; Oberhauser, W.; Bonzi, L. M.; Rossi, F.; Dal Santo, V. *Dalton Trans.* **2004**, 1783–1784.

(h). Hems, W. P.; McMorn, P.; Riddel, S.; Watson, S.; Hancock, F. E.; Hutchings, G. *J. Org. Biomol. Chem.* **2005**, *3*, 1547–1550.

(i). Simons, C.; Hanefeld, U.; Arends, I. W. C. E. Sheldon, R. A.; Maschmeyer, T. *Chem. Eur. J.* **2004**, *10*, 5829–5835.

(j). Simons, C. Hanfeld, U.; Arends, I. W. C. E.; Maschmeyer. T.; Sheldon, R. A. *J. Catal.* **2006**, *239*, 212–219.

47. (a). Moya, J. F.; Rosales, C.; Fernández, I.; Khair, N. *Org. Biomol. Chem.* **2017**, *15*, 5772–5780.

(b). Xing, L.; Xie, J.-H.; Chen, Y.-S.; Wang, L.-X.; Zhou, Q.-L. *Adv. Synth. Catal.* **2008**, *350*, 1013–1016.

(c). Kumagai, N.; Shibasaki, M. *Isr. J. Chem.* **2017**, *57*, 270–278.

48. (a). Zhong, M.; Zhang, X.; Zhao, Y.; Li, C.; Yang, Q. *Green Chem.* **2015**, *17*, 1702–1709.

(c). Peng, J.; Wang, X.; Zhang, X.; Bai, S.; Zhao, Y.; Li, C.; Yang, Q. *Catal. Sci. Technol.* **2015**, *5*, 666–672.

(b). Wolfson, A.; Geresh, S.; Gottlieb, M.; Herskowitz, M. *Tetrahedron: Asymmetry* **2002**, *13*, 465–468.

49. Harmer, M. A.; Farneth, W. E.; Sun, Q. *J. Am. Chem. Soc.* **1996**, *118*, 7708–7715.

50. (a). Tanielyan, S.; Biunno, N.; Bhagat, R.; Augustine, R. L. *Top. Catal.* **2014**, *57*, 1564–1569.

    (b). Tanielyan, S. K.; Augustine, R. L.; Marin, N.; Alvez, G. *ACS Catal.* **2011**, *1*, 159–169.

    (c). Augustine, R. L.; Tanielyan, S. K.; Mahata, N.; Gao, Y.; Zsigmond, A.; Yang, H. *Appl. Catal., A* **2003**, *256*, 69–76.

    (d). Augustine, R. L.; Tanielyan, S. K.; Anderson, H.; Yang, H. *Chem. Commun.* **1999**, *10*, 1257–1258.

    (e). Madarász, J.; Nánási, B.; Kovács, J.; Balogh, S.; Farkas, G.; Bakos, J. *Monatsh. Chem.* **2018**, *149*, 19–25.

    (f) Augustine, R. L.; Goel, P.; Mahata, N.; Reyes, C.; Tanielyan, S. K. *J. Mol. Catal. A: Chem.* **2004**, *216*, 189–197.

51. Santacesaria, E.; Gelosa, D.; Carrà, S. *Ind. Eng. Chem. Prod. Res. Dev.* **1977**, *16*, 45–47.

52. Stephenson, P.; Kondor, B.; Licence, P.; Scovell, K.; Ross, S. K.; Poliakoff, M. *Adv. Synth. Catal.* **2006**, *348*, 1605–1610.

53. (a). Keggin, J. F. *Nature* **1933**, *131*, 908–909.

    (b). Zhu, Z.; Tain, R.; Rhodes, C. *Can. J. Chem.* **2003**, *81*, 1044–1050.

54. Duque, R.; Pogorzelec, P. J; Cole-Hamilton, D. J. *Angew. Chem., Int. Ed.* **2013**, *52*, 9805–9807.

55. (a). Ding, S. Y.; Wang, W. *Chem. Soc. Rev.* **2013**, *42*, 548–568.

    (b). Feng, X.; Ding, X. S.; Jiang, D. L.; *Chem. Soc. Rev.* **2012**, *41*, 6010–6022.

    (c). Pugin, B.; Blaser, H.-U. *Top. Catal.* **2010**, *53*, 953–962.

    (d). Liu, Y.; Xuan, W.; Cui, Y. *Adv. Mater.* **2010**, *22*, 4112–4135.

(e). Hübner, S.; de Vries, J. G.; Farina, V. *Adv. Synth. Catal.* **2016**, *358*, 3–25.

(f). Dioos, B. M. L.; Vankelecom, I. F. J.; Jacobs, P. A. *Adv.* **2006**, *348*, 1413–1446.

(g). Mastrorilli, P.; Nobile, C. F. *Coord. Chem. Rev.* **2004**, *248*, 377–395.

56. (a). Dumont, W.; Poulin, J.-C.; Dang, T.-P.; Kagan, H. B. *J. Am. Chem. Soc.* **1973**, *95*, 8295–8299.

(b). Frechet, J. M.; Schuerch, C. *J. Am. Chem. Soc.* **1971**, *93*, 492–496.

57. (a). Shi, L.; Wang, X.; Sandoval, C. A.; Wang, Z.; Li, H.; Wu, J.; Yu, L.; Ding, K. *Chem. Eur. J.* **2009**, *15*, 9855–9867.

(b). Wang, X.; Shi, L.; Li, M.; Ding, K. *Angew. Chem.,* **2005**, *117*, 6520–6524.

58. (a). Wang, T.; Lyu, Y.; Chen,X.; Li, C.; Jiang, M.; Song, X.; Ding, Y. *RSC Adv.* **2016**, *6*, 28447–28450.

(b). Sun, Qi.; Meng, X.; Liu, X.; Zhang, X.; Yang, Y.; Yang, Q.; Xiao, F.-S. *Chem. Commun.* **2012**, *48*, 10505–10507.

(c). Wang, T.; Lyu, Y.; Xiong, K.; Wang, W.; Zhang, H.; Zhan, Z.; Jiang, Z.; Ding, Y. *Chin. J. Catal.* **2017**, *38*, 890–898.

(d). Fan, Q.-H.; Ren, C.-Y.; Yeung, C.-H.; Hu, W.-H.; Chan, A. S. C. *J. Am. Chem. Soc.* **1999**, *121*, 7407–7408.

(e). Pugin, B.; Blaser, H.-U. *Adv. Synth. Catal.* **2006**, *348*, 1743–1751.

(f). Pu, L. *Chem. Eur. J.* **1999**, *5*, 2227–2232.

(g). Yu, H.-B.; Hu, Q. S.; Pu, L. *Tetrahedron Lett.* **2000**, *41*, 1681–1685.

(h). Wang, X.; Lu, S. M.; Li, J.; Liu, Y.; Li, C. *Catal. Sci. Technol.* **2015**, *5*, 2585–2589.

(i). den Heeten, R.; Swennemhuis, B. H. G.; van Leeuwen, P. W. N. M.; de Vries, J. G.; Kamer, P. C. J. *Angew. Chem., Int. Ed.* **2008**, *47*, 6602–6605.

j). Swennehuis, B. H. G.; Chen, R.; van Leeuwen, P. W. N. M.; de Vries, J. G.; Kamer, P. C. J. *Eur. J. Org. Chem.* **2009**, *33*, 5796–5803.

(k). Pugin, B.; Landert, H.; Spindler, F.; Blaser, H.-U. *Adv. Synth. Catal.* **2002**, *344*, 974–979.

(l). Ohkuma, T.; Takeno, H.; Honda, Y.; Noyori, R. *Adv. Synth. Catal.* **2001**, *343*, 369–375.

59. (a). Ralph, C. K.; Akotsi, O. M.; Bergens, S. H. *Organometallics.* **2004**, *23*, 1484–1486.

(b). Ralph, C. K.; Bergens, S. H. *Organometallics.* **2007**, *26*, 1571–1574.

(c). Corkum, E. G.; Hass, M. J.; Sullivan, A. D.; Bergens, S.H. *Org. Lett.* **2011**, *13*, 3522–3525.

(d). Corkum, E. G.; Kalapugama, S.; Hass, M. J.; Bergens, S. H. *RSC Adv*. **2012**, *2*, 3473–3476.

60. Noyori, R.; Takaya, H. *Acc. Chem. Res.* **1990**, *23*, 345–350.

61. (a). Jutz, F.; Andanson, J. M.; Baiker, A. *Chem. Rev.* **2011**, *111*, 322–353.

(b). Pugin, B.; Studer, M.; Kuesters, E.; Sedelmeier, G.; Feng, X. *Adv. Synth. Catal.* **2004**, *346*, 1481–1486.

(c). Theuerkauf, J.; Francio, G.; Leitner, W. *Adv. Synth. Catal.* **2013**, *355*, 209–219.

(d). Hintermair, U.; Franciò, G.; Leitner, W. *Chem. Eur. J.* **2013**, *19*, 4538–4547.

62. Köllner, C.; Pugin, B.; Togni, A. *J. Am. Chem. Soc.* **1998,** *120,* 10274–10275.

63. (a). Bergens, S. H.; Sullivan, A.D.; Hass, M. U.S. Patent US008962516B2, Feb 24, 2015.

(b). Bergens, S. H.; Kalapugama, S.; Nepal, P.; McGinitie, E. US Patent US20160175829A1, June 23, 2016.

64. (a). Varma, I. K.; Anand, R. C.; Madan, R. *Indian J. Chem. Technol.* **1998**, *5*, 74–80.

(b). Yoon, K.-H.; Kim, K. O.; Wang, C.; Park, I.; Yoon, D. Y. *J. Polym. Sci., Part A: Polym. Chem.* **2012**, *50*, 3914–3921.

(c). Alonso-Villanueva, J.; Cuevas, J. M.; Laza, J. M.; Vilas, J. L.; León, L. M. *J. Appl. Polym. Sci.* **2009**, *115*, 2440–2447.

65. (a) Furlani, C.; Mattogno, G.; Polzonetti, G.; Braca, G.; Valentini, G. *Inorg. Chim. Acta* **1983**, *69*, 199–205.

(b). Gheorghiu, C. C.; Machado, B. F.; Salinas-Martínez de Lecea, C.; Gouygou, M.; Román-Martínez, M. C.; Serp, P. *Dalton Trans.,* **2014**, *43*, 7455–7463.

(c). Solonin, Y. M.; Khyzhun, O. Y.; Graivoronskaya, E. A. *Cryst. Growth Des.* **2001**, *1*, 473–477.

66. Dyson, P. J.; Jessop, P. G. *Catal. Sci. Technol.* **2016**, *6*, 3302–3316.

67. Vineyard, B. D.; Knowles, W. S.; Sabacky, M. J.; Bachman, G. L.; Weinkauff, D. J. *J. Am. Chem. Soc.* **1977**, *99*, 5946–5952.

68. Wiles, J. A.; Bergens, S. H. *J. Am. Chem. Soc.* **1997**, *119*, 2940–2941.